



Study of fouling of ultrafiltration (UF) membranes by natural organic matter (MON): Characterizations of humic acid cakes formed on the surfaces of flat-sheet membranes for drinking water treatment

Anju Thekkedath

► To cite this version:

Anju Thekkedath. Study of fouling of ultrafiltration (UF) membranes by natural organic matter (MON): Characterizations of humic acid cakes formed on the surfaces of flat-sheet membranes for drinking water treatment. Chemical Sciences. Université d'Angers, 2007. English. NNT: . tel-00527504

HAL Id: tel-00527504

<https://theses.hal.science/tel-00527504>

Submitted on 19 Oct 2010

HAL is a multi-disciplinary open access archive for the deposit and dissemination of scientific research documents, whether they are published or not. The documents may come from teaching and research institutions in France or abroad, or from public or private research centers.

L'archive ouverte pluridisciplinaire **HAL**, est destinée au dépôt et à la diffusion de documents scientifiques de niveau recherche, publiés ou non, émanant des établissements d'enseignement et de recherche français ou étrangers, des laboratoires publics ou privés.

UNIVERSITE D'ANGERS

Année 2007

N° ordre : 819

THESE DE DOCTORAT

Pour obtenir le grade de

DOCTEUR DE L'UNIVERSITE D'ANGERS

Spécialité : CHIMIE ANALYTIQUE

ECOLE DOCTORALE D'ANGERS

**Etude du colmatage de membranes d'ultrafiltration
(UF) par les matières organiques naturelles (MON)**

Par

Anju THEKKEDATH

Soutenue le 7 Décembre 2007, devant le jury composé de :

Mme. RABILLER-BAUDRY Murielle
Professeur, Université de Rennes-I, France

Rapporteur

Mr. GHAFFOUR Noredine
Dr. HDR, MEDRC, Sultanat d'Oman

Rapporteur

Mr. JAOUEN Pascal
Professeur, Université de Nantes-St Nazaire, France

Examineur

Mr. LODE Thierry
Professeur, Université d'Angers, France

Examineur

Mr. PONTIE Maxime
Professeur, Université d'Angers, France

Directeur de thèse

UNIVERSITY OF ANGERS

Year 2007

Sl. No. : 819

DOCTORATE THESIS

To obtain the degree of

DOCTOR OF UNIVERSITY OF ANGERS

Speciality: ANALYTICAL CHEMISTRY

DOCTORAL SCHOOL OF ANGERS

**Study of fouling ultrafiltration (UF) membranes by
natural organic matters (NOM)**

by

Anju THEKKEDATH

Defended on 7 December 2007,

In front of the members of the jury:

Mme. RABILLER-BAUDRY Murielle
Professor, University of Rennes-I, France

Reporter

Mr. GHAFFOUR Noredine
Dr. HDR, MEDRC, Sultanate of Oman

Reporter

Mr. JAOUEN Pascal
Professor, University of Nantes-St Nazaire, France

Examinator

Mr. LODE Thierry
Professor, University of Angers, France

Examinator

Mr. PONTIE Maxime
Professor, University of Angers, France

Thesis director

ABSTRACT

Membrane fouling due to natural organic matter (NOM) is the major issue in drinking water treatment using low-pressure membrane processes (MF/UF). Fouling due to NOM is more pronounced in the form of humic acid fouling, which is a degradation product of plant and animal residues in the environment. According to previous studies it was reported that humic acid fouling is mainly governed by cake formation mechanism which increases the total hydraulic resistance and there by induces flux decline. We have analyzed humic acid cake, formed on regenerated cellulose flat sheet membranes in different operating conditions like pH, trans-membrane pressure, molecular weight cut-off (MWCO) of the membranes and humic acid concentration to understand the fouling mechanisms. Different parameters like hydraulic permeability and hydraulic resistance, percentage of flux decline, modified fouling index (MFI-UF), streaming potential coefficients, and fractal dimensions of the surface cake were determined in order to assess the nature and extent of fouling. Using a combination of these macroscopic, microscopic and *in situ* tools, we have developed a new method for the analysis of humic acid cake and there by to assess the nature, mechanisms, and consequences of fouling due to NOM in low-pressure membrane processes. This method was applied to hollow fibers (virgin and fouled by natural surface water), combined with membrane autopsy. We have also conducted a pretreatment method for the removal of NOM using bentonite (mont-Al-CTAB). Pre-treatment method using bentonite was effective by reducing the total hydraulic resistance of the fouling layer.

Key words: low-pressure membranes, fouling, ultrafiltration, natural organic matter (NOM), humic acid, cake formation, bentonite, fractal dimension.

RESUME

Les technologies à membranes sont en plein développement ; toutefois, les problèmes de colmatage limitent cette expansion. Les acides humiques présents dans les eaux naturelles induisent des chutes de production des membranes et sont à l'origine de fortes diminutions des durées de vie des matériaux filtrants. L'objectif principal de ce travail a été de développer une approche originale du colmatage de membranes basses pression d'ultrafiltration (UF) en cellulose régénérée. L'originalité de ce travail est de proposer plusieurs outils d'autopsie de membranes à deux échelles, l'une macroscopique (par des mesures de perméabilité hydraulique, dont sont déduites les résistances de colmatage et l'indice de colmatage MFI-UF) et microscopique (par la détermination de la dimension fractale des particules d'acides humiques et leurs agrégats déposés à la surface de la membrane). En utilisant une combinaison de ces outils macroscopiques, microscopiques et *in situ*, nous avons développé une nouvelle méthode pour l'analyse un gâteau d'acide humique et pour évaluer la nature, les mécanismes, et les conséquences du colmatage de membranes basses pression. Cette méthode a été appliquée aux fibres creuses (vierge et colmaté par l'eau de surface naturelle), combinées avec l'autopsie de membrane. De plus, un nouvel appareillage semi-automatique de la mesure du potentiel d'écoulement permet également de réaliser des investigations à l'intérieur de la structure de la membrane afin d'y déceler le cas échéant la présence de matière organiques naturelles. La dernière partie est consacrée à une étude de prétraitement réalisée avec .bentonite (mont-Al-CTAB) à limiter le colmatage par MON. La méthode de prétraitement employant la bentonite était efficace en réduisant la résistance totale du gâteau d'acides humiques.

Mots-clé: membranes à basse pression, colmatage, matière organique naturelle (MON), acide humique, formation du gâteau, bentonite, dimension fractale.

Acknowledgements

This thesis is the result of work done at Group Analysis and Processes ((GA&P): at UFR Sciences, University of Angers from December 2004 to December 2007

I would like to express my sincere gratitude to my thesis supervisor Maxime PONTIE, without whom this work would not be possible. I acknowledge him for introducing me to the various concepts in membrane technology and experimental techniques. He has been not only a guide but also a good friend for these years. He has been very kind and always ready to hear and help me.

I am indebted to Prof. Murielle RABILLER-BAUDRY and Dr. Noredine GHAFFOUR for accepting to be the 'rapporteurs' of the thesis for reading the manuscript patiently, and giving their intelligent suggestions and comments. I would also like to thank Prof. Pascal JAOUEN and Prof. Thierry LODE for accepting to be in the jury. I would like to thank them for their useful remarks and suggestions with regard to the thesis which indeed helped in improving the quality of the thesis.

I am grateful to Mr. H. Suty and Ms. K. Kecili for allowing us to work in their laboratory at VEOLIA WATER, Anjou Recherche, France, and help with the analyses. I am thankful to Mr. Daniel Lemordant for their help with the measurements of contact angle in their laboratory at University of Tours. I would also like to thank Mr. Wahib Mohammed Naceur of University of Blida (Algeria) for providing us with the samples of modified bentonite. I would like to acknowledge the help offered by Laurent AURET (NEOSENS, Toulouse, France) for the development of software profluid.

I take this opportunity to express my sincere thanks to Mr. Robert FILMON (SCIAM, University of Angers) for the Scanning electron microscopic analyses. I cannot forget the help offered to me by Romain and Sonia (SCIAM), with the numerous beautiful SEM images.

I would like to acknowledge the help of Prof. Jean Duchesne (INH, Angers) for us with the principles and measurements of fractal dimensions.

I would like to thank the American Water Works Association Research fundation (AWWARF- University of Poitiers, especially Jean Philippe Croué) and GA&P for the fellowship which has supported me during the two years of my research.

I also thank sincerely all the members of GA&P for being kind to me at all the times.

And special acknowledgements to the people of IT section of the University (Olivier) for keeping my PC in good working condition.

I would like to seize this opportunity to say a huge thanks to all my friends, who have made Angers a very special place: Hanane, Karima, Valerie, Fred, Jean, Nadjib, Mohammed Sbai, Barry, Eric, Mallé, Tony, Anita, and all others who passed through.. I will always remember the support and kindness offered by each and every one of them through out the good and the bad times.

I am grateful to all my family members and relatives, especially to my brother Anumod Jathavedan Thekkedath and to my brother-in-law Sasikumar Cherukulappurath for their concern, encouragements and support.

To my Parents, I have no words to express my sincere love and thanks, to them I dedicate this work.

And to my husband and my best friend, Sudhir, I just don't know how to express my thanks to you...without your love, encouragement, constant and unconditional support; I would not have finished this thesis.

Contents

<i>List of Figures</i>	8
<i>List of Tables</i>	11
<i>List of abbreviations</i>	12
<i>List of symbols</i>	14
A- GENERAL INTRODUCTION	15
B- BIBLIOGRAPHIC STUDY	21
A general overview of membrane processes for water treatment	22
Membrane fouling	23
Mechanisms of membrane fouling	24
Natural Organic Matter (NOM)	26
Pre-treatment methods to limit NOM fouling	31
Membrane autopsy tools	34
Some analytical tools and their applications	36
Fractal Dimension theory and application	36
MFI theory and application	38
Streaming potential theory and application	39
C-MATERIALS AND METHODS	43
Membranes and modules	44
pH and conductivity measurements	45
Elimination of chemicals	45
Streaming potential and IEP measurements	45
Humic acid (HA) solutions and fouling experiments	46
FESEM analysis	47
Fractal dimension determination	47
C- FUNDAMENTAL STUDIES CONDUCTED WITH FLAT-SHEET MEMBRANES IN DEAD-END ULTRAFILTRATION	49
Preliminary studies	50
Role of solution pH on fouling	60
Role of membrane molecular weight cut-off (MWCO) on fouling	68
Role of trans-membrane pressure on fouling	75
Role of humic acid concentration on fouling	82
D- PERSPECTIVES	88
Pre-treatment to minimize NOM fouling	89
AWWARF project (CONFIDENTIAL RESULTS)	93
E-ABSTRACTS OF PUBLISHED WORKS	103
F- GENERAL CONCLUSION	106
G- REFERENCES	110
APPENDIXES	115
List of publications and communications	116
Referees REPORTS	117

List of Figures

Figure 1 A schematic drawing illustrating a membrane process.....	16
Figure 2 Distribution of dissolved organic carbon (DOC) in natural waters.	27
Figure 3 Model structure of humic acid.....	28
Figure 4 SEM image of fouled membrane surface and the threshold image.....	37
Figure 5 plot of log (count) with log (box size) illustrating the box counting method	37
Figure 6 t/V vs V graph for the determination of MFI, a cake formed on a polysulfone UF membrane for the filtration of NOM.....	38
Figure 7 Schematic representation of the double layer and potential drop across the double layer; surface charge, Stern layer, and diffuse layer of counter ions.....	40
Figure 8 Schematic diagram of UF system for filtration with flat-sheet membranes	44
Figure 9 A schematic representation and Photography of the system of streaming potential and IEP measurements.....	45
Figure 10 Evolution of flux vs. time during the filtration of 5 mg/ L HA at a constant pressure of 2 bars for RC 100 kDa membrane	50
Figure 11 Variations of pure water permeability values of the virgin clean membrane, after adsorption with Aldrich humic acid (5 mg/L, pH 6.5) and at the end of filtration with the HA cake	51
Figure 12 SEM images showing (a) the clean membrane surface, (b) fouled membrane surface, (c) a cross section of a humic acid cake and (d) the magnification of the cake	52
Figure 13 A double logarithmic plot showing the evolution of log N with log ϵ . The absolute value of the slope gave the fractal dimension FD	53
Figure 14 A theoretical three dimensional model showing particle–cluster aggregation comes under diffusion-limited aggregation	54
Figure 15 Evolution of t/V vs. V for RC 100 kDa membrane during the filtration of Aldrich humic acid 5 mg/L, pH 6.7	55
Figure 16 Evolution of potential difference vs. pressure for a membrane of RC 100 kDa before and after filtration with HA 5 mg/ L, pH 6.7; $KCl = 0.001$ M.....	56
Figure 17 The distribution of mean particle size (nm) and zeta potential for Aldrich humic acid (5 mg/L) in different pH (zetasizer Malvern Co. Inc.).	57
Figure 18 Evolution of SP vs. pH for the determination of IEP for clean RC 100 kDa membrane and that fouled by HA (Aldrich 5 mg/L, pH 6.7, filtration at constant $\Delta P = 2$ bars), $[KCl] = 10^{-3}M$	58

Figure 19 Normalized flux vs. time and Normalized flux with volume for humic acid 5 mg/L solutions at pH 3, pH 6.7 and at pH 9.5. $\Delta P = 2$ bar, $T = 20^\circ \text{C}$	61
Figure 20 pH titration graph of Acrôs humic acid. The particle size (nm) and the zeta potential (mV) values for different pH ranges from zetasizer Malvern Co. Inc.	62
Figure 21 Streaming potential (SP) values for YM 100 membranes, virgin membrane, after filtration with humic acid solutions at pH 3, pH 6.7, and pH 9.5. $[\text{KCl}] = 0.001 \text{ M}$, pH 6.5 for SP measurements.	62
Figure 22 SEM images showing the membrane surfaces of YM 100 membranes fouled by humic acid solutions at (a) pH 6.7, (b) pH 3 and (c). pH 9.5.....	65
Figure 23 Schematic description of the effect of pH on the conformation of HA macromolecules in solution and on the membrane surface.	66
Figure 24 Normalized flux with filtration volume for the filtration of 5 mg/L humic acid solution at pH 6.7, $\Delta P = 2$ bars, $T = 20^\circ \text{C}$ for 100 kDa, 30 kDa and 10 kDa regenerated cellulose membranes.	69
Figure 25 Evolution of flux with time for YM 100, YM 30 and YM 10 membranes during the filtration of Acrôs humic acid in a concentration of 5mg/L at a pH 6.7. $\Delta P = 2$ bars, $T = 20^\circ \text{C}$	70
Figure 26 Evolution of fractal dimension values with fouled (membranes fouled by HA 5 mg/L at pH 6.7, $\Delta P = 2$ bars, $T = 20^\circ \text{C}$) membrane permeability values and fractal dimension variation with MWCO.	73
Figure 27 Evolution of pure water flux with trans-membrane pressure for membranes fouled with humic acid Acrôs 5mg/L, at pH 6.7(a) after filtration with HA at constant pressure of 2 bar (b) after filtration with HA at constant pressure of 1 bar (c) after filtration with HA at constant pressure of 4 bar	76
Figure 28 Evolution of normalized flux with filtration volume during humic acid filtration through YM 30 membranes at constant pressure of 1bar, 2 bars and 4 bars. $[\text{HA}] = 5 \text{ mg/L}$; $\text{pH} = 6.7$; $T = 20^\circ \text{C}$	77
Figure 29 Evolution of fractal dimension with cake layer resistance. Membranes fouled with 5 mg/L solution of Acrôs humic acid at pH 6.7. Filtration was carried out in three different trans-membrane pressure, 1 bar, 2 bars and 4 bars at 20°C	80
Figure 30 Variation of pure water flux with trans-membrane pressure for 30 kDa YM 30 membranes, after filtration with different concentration of Acrôs humic acid (5 mg/L, 10 mg/L, 50 mg/L) at pH 6.7, $\Delta P = 2$ bar, $T = 20^\circ \text{C}$	83
Figure 31 Normalized flux with filtration volume during the filtration of 5 mg/L, 10 mg/L and 50 mg/L concentrations of Acrôs humic acid solutions at pH 6.7, $\Delta P = 2$ bars, $T = 20^\circ \text{C}$ for 30 kDa regenerated cellulose membranes.	84
Figure 32 Evolution of t/V vs. V during the filtration of Acros humic acid solutions at pH 6.7 in different concentrations (a) 50 mg/L, (b) 10 mg/L and (c) 5 mg/L ; $\Delta P = 2$ bar, $T = 20^\circ$	85
Figure 33 Evolution of flux vs. time and normalized flux with filtration volume during the filtration of humic acid and humic acid+ bentonite suspension. pH of humic acid 6.7, $\Delta P = 2$ bar, $T = 20^\circ \text{C}$	89

Figure 34 Evolution of pure water flux with trans-membrane pressure for virgin RC 100 membrane, membrane fouled by HA (Acros 5mg/L, pH 6.7, $\Delta P = 2$ bar $T = 20^{\circ}\text{C}$) and HA+bentonite(mont-Al-CTAB 2g/L) suspension.....	90
Figure 35 Evolution of potential difference (mV) vs. trans-membrane pressure (bar) for virgin membrane, membrane fouled by HA (Acros 5 mg/L, pH 6.7, $\Delta P = 2$ bar, $T = 20^{\circ}\text{C}$) and HA+ bentonite (mont-Al ₁₃ -CTAB 2g/L) Electrolyte KCL 0.001M, pH 6.5.....	90
Figure 36 Evolution of t/V vs. V for the determination of MFI –UF. $[\text{HA}] = 5\text{mg/L}$, $\text{pH} = 6.7$, $\Delta P = 2$ bar, $[\text{mont-Al}_{13} \text{CTAB}] = 2\text{g/L}$	91
Figure 37 Pieces of one fibre cut in order to see the exterior and interior surfaces and the circular transverse section of the membranes inside SEM chamber	93
Figure 38 External surface of A- Hydranautics (PES) and C- Norit (PES) membrane in the clean state.	94
Figure 39 Internal surfaces of both A-Hydranautics and C-Norit membranes.....	94
Figure 40 FESEM image of cross section of membranes A, B & C	95
Figure 41 Evolution of SP with pH for the determination of IEP of clean Hydranautics PES membrane.[KCl].....	96
Figure 42 Pyrrochromatogram of virgin C-Norit (PES) membrane.....	97
Figure 43 Pyrochromatogram of virgin A-Hydranautics (PES) membrane.	98
Figure 44 Pyrochromatogram of virgin Zenon (PVDF) membrane.....	98
Figure 45 External surfaces of clean and fouled Zenon (PVDF) showing NOM	99
Figure 46 FESEM image of the Inner side of the fouled Zenon (PVDF) membrane.....	100
Figure 47 Evolution of SP with pH for Zenon (PVDF) membrane, before and after fouling.....	101

List of Tables

Table 1 Characteristics of membrane processes.....	17
Table 2 Membrane pore size and particles/solutes to be eliminated	22
Table 3 Constant pressure filtration laws for unstirred dead-end filtration.....	24
Table 4 Characteristics of flat-sheet membranes.....	44
Table 5 Properties of hollow fibre membranes	48
Table 6 Resistance values of the YM 100 membrane before and after filtration with humics	52
Table 7 Permeability, resistance values and MFI values obtained during the filtration of humic acid solutions at different pH, pH 3, pH 6.7 and pH 9.5. Acros [HA] = 5 mg/L, $\Delta P = 2$ bars, $T = 20^\circ C$, YM 100 membranes.	60
Table 8 Permeability, resistance values, MFI values obtained during the filtration of Acros humic acid 5 mg/L at pH 6.7 with different MWCO (100 kDa, 30 kDa and 10 kDa) RC membranes.....	68
Table 9 Experimental results of streaming potential measurements of clean and fouled membranes of YM 100, YM30 and YM 10 membranes $KCl\ 10^{-3}$ M, pH 6.5, $T = 20^\circ C$	72
Table 10 Permeability, resistance values and MFI values obtained during Acros humic acid filtration at different trans-membrane pressure HA Acros 5 mg/L, pH 6.7	75
Table 11 Experimental results of streaming potential measurements of clean and fouled membranes of YM30 membranes.....	79
Table 12 Permeability, resistance values and MFI values obtained during the filtration of humic acid solutions at pH 6.7, different concentrations, 5 mg/L, 10 mg/L and 50 mg/L. $\Delta P = 2$ bars, 30k Da Regenerated cellulose membranes (YM 30)	82
Table 13 Streaming potential values for clean and fouled (by 5 mg/L, 10 mg/L and 50 mg/L solutions of Ha at pH 6.7) YM 30 membranes. $KCl = 0.001$ M, pH 6.5, $T = 20^\circ C$	86
Table 14 Membrane characteristics from FESEM observations	95
Table 15 Average roughness (Ra) of samples A, B and C	96
Table 16 IEP/Membrane charge values for clean membranes	97

List of abbreviations

AFM	Atomic Force Microscopy
ATR-FTIR	Attenuated Total Reflection Fourier Transform spectroscopy
C _b	Concentration of particles
CTAB	Cetyltrimethylammonium bromide
DBP	Disinfection by-products
DOC	Dissolved organic carbon
DLCA	Diffusion-limited cluster aggregation
DOM	Dissolved organic matter
FA	Fulvic acid
FD	Fractal dimension
FESEM	Field emission scanning electron Microscopy
HA	Humic acid
IEP	Isoelectric point
kDa	Kilo Daltons
MBR	Membrane bioreactor
MF	Microfiltration
MFI -UF	Modified fouling index for Ultrafiltration
MWCO	Molecular weight cut-off
NF	Nanofiltration
NBW	Natural brown water
NOM	Natural organic matter
OM	Optical microscopy
PAC	Powdered activated carbon
PES	Polyethersulfone
POC	Particulate organic carbon
POM	Particulate organic matter
PVDF	Polyvinylidenefluoride
Ra	Average roughness
RC	Regenerated cellulose
RO	Reverse osmosis
SDI	Silt density index
SEM	Scanning electron microscopy

SP	Streaming potential
TEM	Transmission electron microscopy
TOC	Total organic carbon
UF	Ultrafiltration

List of symbols

		Unit
L_p	Hydraulic permeability	$L \cdot m^{-2} \cdot h^{-1} \cdot bar^{-1}$
V	Volume	L
J	Flux	$L \cdot m^{-2} \cdot h^{-1}$
J_0	Initial flux	$L \cdot m^{-2} \cdot h^{-1}$
T	Time	s
T	Temperature	°C
α	Specific cake resistance	$m \cdot (kg)^{-1}$
χ	Conductivity	$\mu S \cdot (cm)^{-1}$
ϵ	Dielectric constant	Debye units
μ	Viscosity of the permeate	Pa. s
θ	Contact angle	Degree (θ)
ζ	Zeta potential	mV
$\Delta\phi$	Potential difference	mV
ΔP	Trans-membrane pressure	bar
R_a	Adsorption resistance	m^{-1}
R_c	Cake resistance	m^{-1}
R_m	Membrane resistance	m^{-1}
R_t	Total hydraulic resistance	m^{-1}

A- GENERAL INTRODUCTION

To say that water is a very precious resource may well be an understatement: water is the most precious resource of all, on our earth. Availability of good quality drinking water is extremely vital to mankind. During the last three decades, membrane filtration has emerged as a separation technology for water treatment which is competitive in many ways with conventional separation techniques, such as distillation, adsorption, absorption and extraction etc. The key component in all membrane separation processes is the membrane itself. A membrane can be described as a thin barrier between two bulk phases that permits the transport of some components but retain others. A driving force is necessary to allow mass transport across the membrane. A schematic drawing illustrating a membrane process is given in Fig 1.

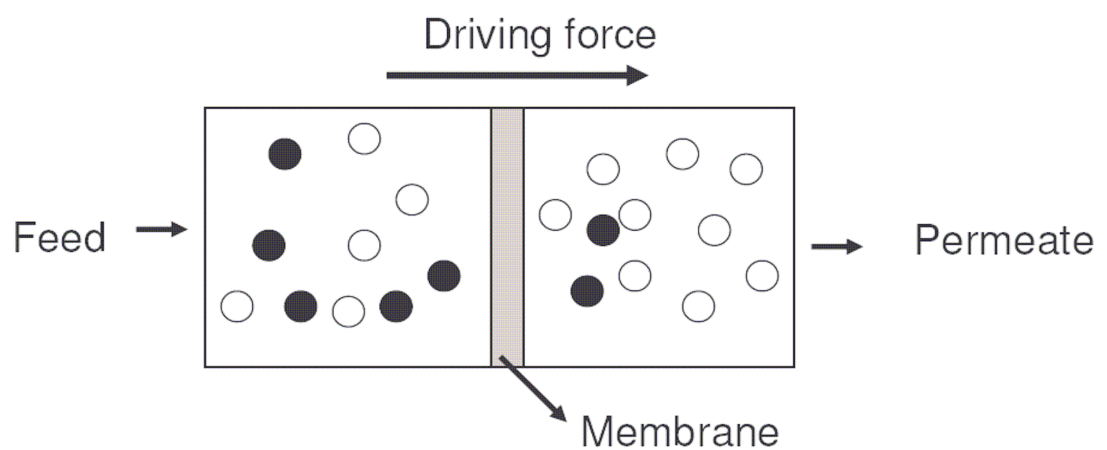


Figure 1 A schematic drawing illustrating a membrane process

Fig1 provides a general illustration of all types of membrane separation processes. The actual separation mechanism can be based on the differences in the sizes of the permeating components (sieving effect), or in the membrane affinity towards the feed solution constituents (chemical effect). The solute chemical nature or electrical charges, as well as the vapour pressure of the different components in a mixture often play an important role in membrane separation processes. The two phases separated by the membrane, i.e., feed and permeate can be present in the liquid or in the gaseous state. The driving force necessary for the transport is a trans-membrane pressure gradient ΔP , a concentration or activity gradient (or chemical

potential) Δc or Δa , respectively, an electrical potential gradient ΔE , or a temperature gradient ΔT . Membrane separation processes can be classified as shown in Table 1.

Table 1: Characteristics of membrane processes

membrane process	driving force	feed state	permeate state	separation mechanism
microfiltration (MF)	ΔP	liq	liq	size
ultrafiltration (UF)	ΔP	liq	liq	size
nanofiltration (NF)	ΔP	liq	liq	size/affinity
reverse osmosis (RO)	ΔP	liq	liq	size/affinity
piezodialysis (PD)	ΔP	liq	liq	affinity
gas separation (GS)	ΔP	gas	gas	affinity/size
pervaporation (PV)	ΔP	liq	gas	affinity
dialysis (D)	Δc	liq	liq	size
osmosis (O)	Δc	liq	liq	affinity
liquid membranes (LM)	Δc	liq	liq	chemical nature
electrodialysis (ED)	ΔE	liq	liq	charge
thermo-osmosis (TO)	$\Delta T, \Delta p$	liq	liq	vapour pressure
membr. distillation (MD)	$\Delta T, \Delta p$	liq	liq	vapour pressure

Low pressure membrane processes, namely ultrafiltration (UF) and microfiltration (MF), play a major role in the production of drinking water, free of health hazards. These processes have been increasingly used in drinking water treatment as an alternative technology to conventional filtration and clarification in order to remove particles, turbidity, and microorganisms from surface and ground water to meet stricter regulations established in drinking water quality (Cheryan, 1998). Moreover, during the last decade these membrane processes (due to the development of immersed hollow fiber design, (Habarou , Ph D Thesis 2004 and references there in)), have found increased applications in the treatment of domestic and industrial effluents (Membrane Bio Reactors-MBR) and in the production of water suitable for reuse (Sridang *et al.* 2006)

One of the critical issues in the successful application of membrane systems for water treatment is membrane fouling, which leads to increased operational and maintenance costs,

increased energy consumption and ultimately affects the water quality output. Surface water sources used for drinking water purposes always contain dissolved natural organic matter (NOM), a complex mixture of organic compounds derived from the decay of plant and animal material. NOM can be divided into humic and non-humic fractions. The heterogeneous mixture of aquatic humic substances contains various aromatic and aliphatic components and carboxylic and phenolic functional groups that determine the intensity of the charge of these macromolecules.

NOM can adversely affect water treatment, the distribution and can cause several drinking water quality problems. NOM challenges the water treatment process by transporting metals and hydrophobic organic chemicals, thus making their removal difficult, as well as by reacting with disinfectants and thus increasing their demand. The major water quality concern, however, relates to residual NOM reacting with chlorine forming toxic, carcinogenic, and/or mutagenic disinfection by-products (DBPs) (Kwon *et al.* 2005)

Another major concern with residual NOM in drinking water is its ability to support bacterial growth in the drinking water distribution network. Bacterial growth may lead to pathogen multiplication, can cause undesirable taste, colour and odour and contributes to corrosion of pipe materials. The ability of residual NOM to support bacterial growth is connected to the biodegradable fraction of NOM. Biodegradable NOM is generally measured either as biodegradable dissolved organic carbon or as assimilable organic carbon (AOC). In natural waters biodegradable dissolved organic carbon forming compounds typically consist of large organic macromolecules such as humic and fulvic acids as well as of small organic carbon compounds (Hong and Elimelech, 1997). Recently, NOM isolates/fractions; organic colloids and hydrophobic, transphilic and hydrophilic fractions, polysaccharides and proteins were investigated in low pressure membrane filtration (Laabs *et al.*, 2006, Lee *et al.*, 2006 and Jarusutthirak *et al.*, 2007)

Because of the complexity of NOM and the diversity of the species, it is very difficult to predict the fouling caused by NOM. One of the methods to assess fouling is by membrane autopsy (Pontie *et al.* 2005). Characterization of the membrane before and after fouling helps to estimate the extent of fouling. Actually, there is a need to develop *in situ* tools to assess fouling.

This thesis deals with the problem of fouling due to NOM, especially fouling caused by humic acid of UF membranes in drinking water treatment. According to earlier studies, membrane fouling by humic substances is influenced by the characteristics of humic substances and that of the membrane, hydrodynamic conditions, and the chemical composition of the feed water. Despite the myriad of studies on membrane fouling due to NOM and related phenomena, the fundamental mechanisms involved are still not fully understood. It is reported that humic acid fouling is mainly governed by cake formation mechanism, which plays a major role in flux decline (Nyström, 1996). We have conducted different fouling experiments by varying different operating parameters like trans-membrane pressure, pH, molecular weight cut-off (MWCO) of the membranes and humic acid concentration, on flat sheet regenerated cellulose UF membranes to understand the fouling mechanisms. Different parameters like hydraulic permeability and hydraulic resistance, Modified Fouling Index for Ultrafiltration (MFI-UF) and streaming potential coefficients (SP) were determined in order to assess the extent and consequences of humic acid fouling on UF membranes. Scanning electron microscopic (SEM) images of the clean and fouled membranes were taken to understand the morphological changes and it was found that the humic acid cake was organized in *fractal* forms. Fractal dimensions of the images were determined from SEM images. Thus, fractal geometry was used *as a new tool* to analyze the microstructure of the cake. The originality of our work is based on a double approach on cake analysis on both macroscopic and microscopic scales. As a macroscopic approach, the parameters like hydraulic permeability, percentage of flux decline at constant pressure, modified fouling index (MFI-UF), resistance in series model

were taken into account. Microscopic tools like SEM and fractal dimension helped us to analyze the microstructure of the cake more effectively. Thus we have developed a new approach in cake analysis to search solutions for humic acid fouling in drinking water treatment. To complete this approach, trans-membrane streaming potential measurements was carried out with a new home made apparatus developed in our laboratory which works with a software namely *profluid. 3.0*.

We have also studied the effectiveness of a pre-treatment method for UF to decrease NOM fouling. Pre-treatment was done with a modified bentonite,-a type of clay which occurs naturally. We found that these naturally occurring materials can effectively decrease the fouling to some extent.

We also carried out the membrane autopsy of virgin and fouled hollow fiber membranes (fouled by real water NOM) which were subjected to morphological (SEM), topographical (AFM) and chemical (Pyrolysis GC-MS) analyses along with charge related modifications (Streaming potential and isoelectric point determination) and contact angle analysis.

This thesis is divided into the following sections:

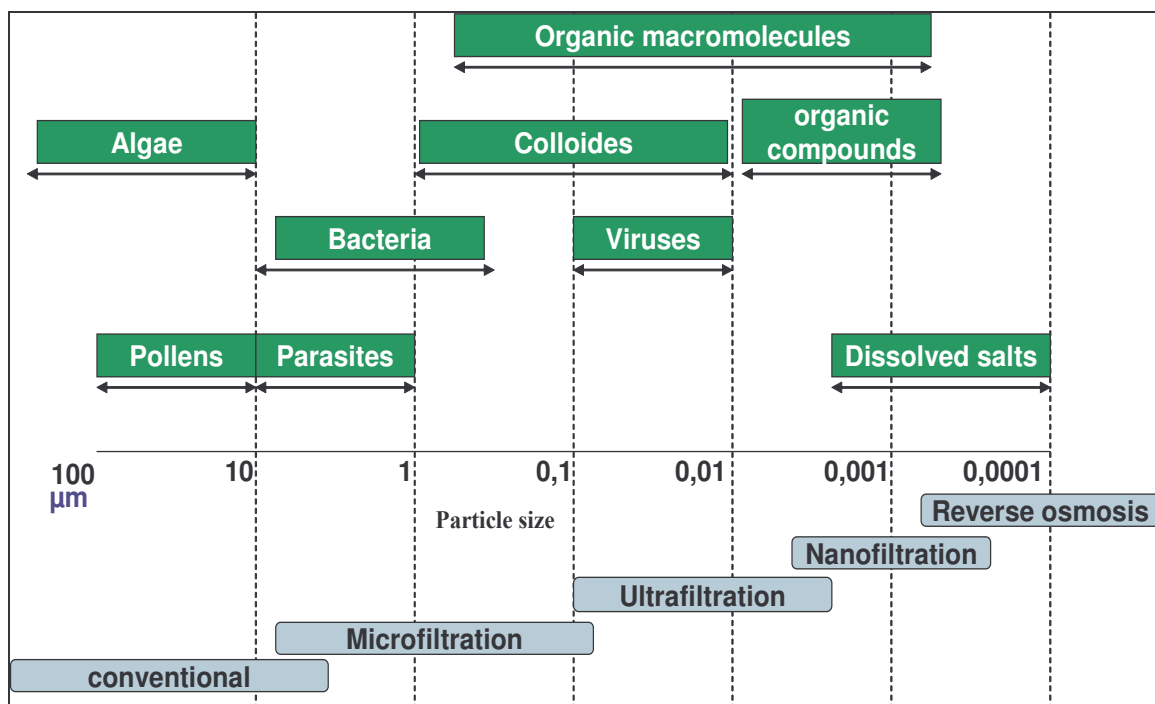
- The first section is dedicated to state-of-the-art of the studied domain: bibliographic references which illustrate our work were cited.
- The second one is dedicated to the experimental results followed by discussion.
- and the third section is about perspectives of our work followed by conclusions.

B- BIBLIOGRAPHIC STUDY

A general overview of membrane processes for water treatment

There are many processes available for water treatment. The selection of a treatment process is dependent on the water quality output, and therefore which solutes or particles to be retained. Conventional treatment consists of different processes like clarification, coagulation, flocculation, sand filtration, adsorption, distillation etc in order to attain the required water quality. In water treatment processes, membrane technology has gained importance because a membrane can remove contaminants - depending on the membrane, from bacteria, viruses, suspended particles, macromolecules to dissolved organics and salts - and helps to provide high quality drinking waters. The major pressure-driven membrane processes in the water treatment industry are MF, UF, NF and RO.

Table 2 Membrane pore size and particles/solutes to be eliminated



As can be seen in Table 2, membrane separation processes cover the entire size range from suspended solids to mineral salts and organics.

Of the process options considered, MF is the process with the largest pore size. It is generally used to remove turbidity and suspended solids. MF can retain major pathogens (cryptosporidium, giardia) and bacteria from feed water. A typical MF membrane pore size ranges from 0.1-10 μm . It is also common to be used as a pre-treatment method for RO and NF.

UF is becoming increasingly popular in water treatment industry and can provide good quality drinking water, because of its ability to remove turbidity, micro organisms including viruses and macromolecules UF membranes are having a pore size range of 0.01-0.10 μm . It can remove macromolecules of nominal molecular weight cut-off (NMWCO) 1 k Da to 100 k Da. MF membranes have been used for reducing turbidity/particles and larger micro organisms (protozoa, bacteria) from natural waters while UF membranes have been applied for removing inorganic and organic particles/colloids, and smaller microbes like viruses (Jacangelo and Buckley, 1996). Similar to MF, UF also can be used as a pre-treatment method either to NF or to RO.

RO and NF are mainly used in desalination applications of sea water or brackish water. RO is primarily used in desalination or for waters where micro pollutants are difficult to remove by other processes. However, in surface water treatment, full demineralisation is not required, NF can also be used. NF is also attractive in the treatment of surface waters because of its ability in softening and high rejection of organics and micro pollutants. Compared to RO and NF, UF and MF are operated in low pressures and hence consume lower amount of energy.

Membrane fouling

A major challenge in membrane filtration is the contamination of membranes, which greatly limits its performance. Contamination of membranes causes a higher energy use, a higher cleaning frequency and a shorter life span of the membrane. Membrane contamination is usually called fouling. According to Koros *et al.* (1996), the term **fouling** describes the

“process resulting in loss of performance of a membrane due to the deposition of suspended or dissolved substances on its external surface, at its pores openings or within its pores”.

Mechanisms of membrane fouling

There are different mechanisms to explain fouling in dead-end filtration. Depending on the particle size and pore size of the membrane, fouling can be classified as shown in Table 3

Table 3 Constant pressure filtration laws for unstirred dead-end filtration (Cheryan, 1998)

Law	Equation	Description
Complete blocking (pore blocking)	$V = (J_0/k_{CB}) (1 - e^{-k_{CB}t})$	Particles do not accumulate on each other and particles arriving at the membrane will seal the pore $d_{\text{particle}} \cong d_{\text{pore}}$
Intermediate blocking (long term adsorption)	$V = (J_0/k_{IB}) \ln (1 + k_{IB} t)$	Particles do accumulate on each other and seal membrane pores, $d_{\text{particle}} \cong d_{\text{pore}}$
Standard blocking (pore constriction)	$t/V = (1/J_0) + (k_{SB}/J_0) t$	Particles deposit on internal pore walls, decreasing the pore diameter, $d_{\text{particle}} \ll d_{\text{pore}}$
Cake filtration (boundary layer resistance)	$t/V = (k_{CF}/4 J_0^2) V + 1/J_0$	Particles are retained due to sieving and form a cake on the surface, $d_{\text{particle}} > d_{\text{pore}}$

MF and UF membranes are porous membranes and they separate solutes mainly by size (steric) exclusion. The accumulated molecules (in, on and/or near a membrane pore) cause flux decline through the increased resistance of the fouled membrane. These filtration models are valid for unstirred, dead-end filtration and complete rejection of solute by the membrane (but obviously allowing pore penetration).

The **complete blocking** (pore blocking) model is valid for particles which are having very similar size to the pores. Particles seal the pores and do not accumulate on each other.

The **standard blocking** (pore constriction) model describes pore blocking for particles

which are much smaller than the pores. Particles pass through the pores and deposit on the surface of the pores. The internal pore volume will decrease proportionally with the filtrate volume. The **intermediate blocking** describes long term adsorption. Every particle reaching a pore will contribute to blockage and particles accumulate on each other. The **cake filtration** model describes the filtration of particles which are much larger than the pores and will be retained, without entering the pores. The deposition of particles on the membrane surface contributes to the boundary layer resistance. Included in this model is deposition due to concentration polarisation.

Bowen *et al.* (1995) elucidated consecutive steps of membrane blocking in flux decline during protein microfiltration- the smallest pores were blocked by all particles arriving at the membrane for the initial blocking process, then the inner surfaces of bigger pores were covered, and afterwards, some particles covered other pre-existing particles while others directly blocked some of the pores, and finally, a cake layer started to build. Ho and Zydney (2000) developed a mathematical model for elucidating initial fouling due to pore blockage and subsequent fouling due to the growth of a protein cake or deposit over the initially blocked area in MF membrane filtration. Continuous membrane filtration leads to flux decline by pore blockage or cake/gel layer formation.

Pure water flux of a clean membrane under laminar conditions can be described by Darcy's law (Eqn. 1).

$$J = \frac{\Delta P}{\mu \cdot R_m} \quad (1)$$

Where, J: Permeate flux (m/sec), ΔP : Trans-membrane pressure drop (kg/m²), μ : The absolute viscosity of the permeate (kg/m·sec) and R_m : The hydraulic resistance of the clean membrane (m⁻¹)

The **resistance in series model** describes the flux of a fouled membrane (Eqn. 2). R_a is resistance due to adsorption, R_c the cake resistance, and R_t the total hydraulic resistance.

$$J = \frac{\Delta P}{\mu(R_m + R_a + R_c)} = \frac{\Delta P}{\mu R_t} \quad (2)$$

An empirical relationship often applied to account for trans-membrane pressure is Eqn (3) which relates specific cake resistance, α to trans-membrane pressure to the power of a compressibility coefficient (n) and a constant α_0 .

$$\alpha = \alpha_0 P^n \quad (3)$$

Natural Organic Matter (NOM)

Natural organic matter (NOM) is a heterogeneous mixture with wide ranges in molecular weight (size) and functional groups and is formed by allochthonous input such as terrestrial, vegetative debris and autochthonous input such as algae. NOM has been shown to be aesthetically undesirable and imparts potential health impacts such as forming carcinogenic compounds. In particular, the humic substances fraction of NOM with high aromaticity affects disinfection-by-product (DBP) formation (Singer, 1999).

NOM is difficult to quantify due to its complexity. For practical purposes, organic matter is quantified by measuring organic carbon concentrations as total organic carbon (TOC), particulate organic carbon (POC), and dissolved organic carbon (DOC). In general, total organic matter (TOM), particulate organic matter (POM), and dissolved organic matter (DOM) constitute approximately twice the mass of TOC, POC, and DOC. The boundary between POC and DOC is 0.45 μm ; DOC is operationally defined as organic carbon passing through 0.45 μm filtration (Thurman *et al.*, 1978).

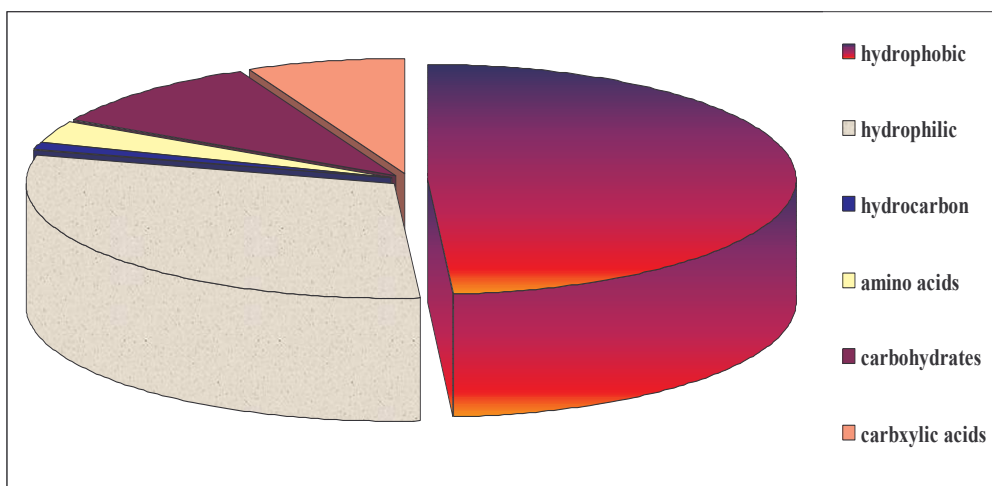


Figure 2 Distribution of dissolved organic carbon (DOC) in natural waters (Thurman, 1985).

As shown in Fig.2, 49% of total DOC is hydrophobic humic substances, mainly humic acids. Twenty one percentage of the total DOC is hydrophilic humic substances (fulvic acids). The rest are hydrocarbons, amino acids, carbohydrates and carboxylic acids (Thurman, 1985).

Humic and fulvic acids represent the major fraction of dissolved natural organic matter in aquatic environments. They are responsible for natural water colour and for initiating photochemical transformations of both organic compounds and trace metals (Schnitzer M., 1978). Humic substances are typically characterized by physical and chemical heterogeneous nature which derives from: (a) the absence of a discrete structural and supra-molecular level; (b) the wide variety of sizes and shapes assumed in the solid and colloidal states; (c) the occurrence of complex aggregation and dispersion phenomena in aqueous media and (d) the various degrees of roughness and irregularity of exposed surfaces. These properties have an important role in determining the physical, chemical and biological reactivity of humic substances towards mineral surfaces, metal ions, organic chemicals, plant roots, and micro organisms in soil.

Humic acids are thought to be complex aromatic macromolecules with amino acids, amino sugars, peptides, aliphatic compounds involved in linkages between the aromatic groups. The hypothetical structure for humic acid, shown in Fig.3, contains free and bound phenolic OH

groups, quinone structures, nitrogen and oxygen as bridge units and COOH groups variously placed on aromatic rings.

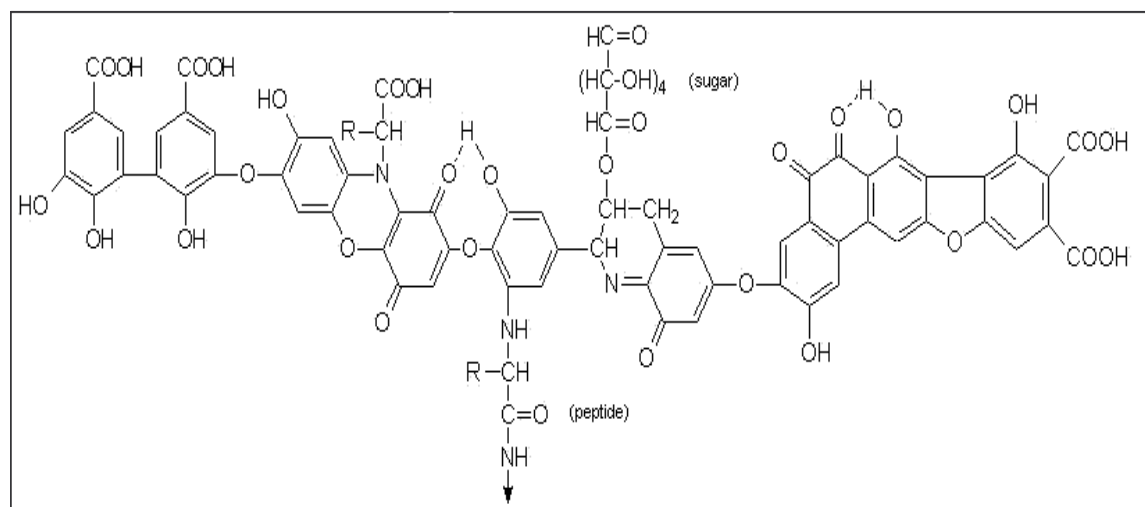


Figure 3 Model structure of humic acid (Stevenson, 1982)

Many researchers suggest that humic substances might play a role in irreversible fouling of membranes (Combe *et al.*, 1999, Jones and O'Melia, 2000, Yuan and Zydney, 1999). Several previous studies have demonstrated that NOM, and in particular humic acids, have a major influence on the flux decline (Nyström, 1996). Svinko *et al.*, (1986) reported that when a cellulose acetate membrane was filtered with humus water in a study with UF and RO, membranes were fouled.

Membrane fouling by humic substances is influenced by the properties of humic substances and the characteristics of membrane, the hydrodynamic conditions, and the composition of the feed solution. A better comprehension of these factors is important to control fouling by natural organic matter. Membrane pore size, charge and hydrophilic/hydrophobic character will also affect membrane fouling. pH and ionic strength will also have an important role to play. Hydrophobic interactions between the hydrophobic NOM fraction and a hydrophobic membrane may cause more flux decline than that of hydrophilic membrane associated with adsorptive fouling. However, recent studies suggest that neutrals and hydrophilic materials

contribute more significant membrane flux decline. (Cho. *et al.*, 1999, Amy, 1999, Lin *et al.*, 2000), and that low-aromatic hydrophilic neutral compounds determined the rate and extent of flux decline (Fan *et al.*, 2001, Carroll *et al.*, 2000).

Many authors have described the properties of natural organic matter. For example, D.Violleau *et al.* (2005) characterized two natural organic matter fractions, one hydrophobic and other hydrophilic humic acid fraction to study the fouling properties of a polyamide nanofiltration membrane. The authors discussed that the major differences in properties between the hydrophobic and hydrophilic NOM arise due to the differences in their molecular structure in terms of aromaticity. The authors also discussed about the effects of NOM on the membrane surface charge. Besides hydrophobic/hydrophilic effects the electrostatic forces are also to be taken into account in order to explain the fouling phenomena. It has been shown that the irreversible fouling of a hydrophobic membrane (e.g. polysulfone, polypropylene) is more significant due to chemical bonds with higher energy (Wiesner *et al.*, 1996). The different organic fractions have different hydrophobicities, molecular weights/sizes, and charge densities. Thus, different interactions in membrane filtration are expected.

Bian *et al.* (1999) reported that UF membranes having 50 kDa to 200 kDa molecular weight remove only large size of humic substances and pre-coagulation enhanced the removal efficiency of humic substances. Maartens *et al.* (1999) also suggested pre-treatment of feed water to reduce fouling of polysulfone UF membranes caused by natural brown water. Wiesner and Aptel (1996) reported that hydrophobic interactions might increase the accumulation of NOM on membranes with adsorptive fouling. Previous researchers (Comb *et al.*, 1998, Jones and O'Melia, 1999) have indicated that NOM is responsible for membrane fouling by interacting with the membrane surface and structure. Yuan and Zydney (1999) have found that NOM adsorbed both inside the pores and on the membrane surface, and formed a gel layer. The physical and chemical characteristics of humic acid can affect MF membrane fouling. For example, Aldrich humic acid with less functional group (i.e. carboxylic acids) content caused

more significant flux decline than Suwannee River humic acid, which is more negatively charged and hydrophilic. The aromaticity of NOM can be an important factor in flux decline of UF membranes while it affects NF membranes less (Cho *et al.*, 1999). Her *et al.* (2000) reported that significant flux decline is dependent on high DOC, high divalent cations (i.e., Fe and Al), high alkalinity and low temperature in natural water for NF membranes.

Braghetta and co-authors (1997) described the relationship between ionic strength, pH and flux decline. Low pH and high ionic strength caused compaction of membrane pores with a concomitant reduction of pure water permeability, allowing the molecules to accumulate more densely at the membrane surface by charge neutralization, and shifting macromolecules to a smaller apparent macromolecular size range. These trends have been demonstrated for protein fouling of hydrophobic UF membranes.

Metal ions affect flux decline during membrane filtration of humic substances. Hong and Elimelech (1997) studied chemical and physical aspects of NOM fouling in nanofiltration. Membrane fouling was increased with increasing electrolyte (NaCl), decreasing solution pH, and addition of Ca^{2+} ; the rate of fouling is controlled by interplay between permeation drag and electrostatic double layer repulsion in nanofiltration. The influence of calcium presence was investigated by many researchers as well. Calcium induced charge neutralization by the divalent cation interacting with the carboxylic functional groups of humic substances, increasing deposition of NOM on membrane surface (Maartens *et al.*, 1999, Cho *et al.*, 2000, Fan *et al.*, 2001).

Her *et al.* (2002) investigated high performance liquid chromatography (HPLC), size exclusion chromatography (SEC) with ultraviolet absorbance (UVA) and on-line dissolved organic carbon (DOC) detectors. The on-line DOC detector is capable of providing molecular weight distribution of non-aromatic carbon compounds as well as aromatic carbon compounds. Huber *et al.* (1998) identified molecules (i.e. polysaccharides, humics, acids and amphiphilics) contained in feed water for RO membrane treatment with liquid chromatography with high-

sensitivity organic carbon detection. Lee *et al.* (2002) found that macromolecules (i.e. polysaccharides and proteins) which have large size or molecular weight and low UV response corresponded to the first peak of HPSEC-DOC/UV response were attributable to significant low pressure membrane (MF/UF) fouling.

Colloidal substances and proteins also cause MF and UF membrane fouling by deposition or forming of a cake/gel layer (Schafer *et al.*, 2000, Ho, 2001). Waite *et al.* (1998) suggested that the Carmen-Kozeny equation appeared to provide a reasonable description of the proportional differences in specific resistances that might be expected for cakes formed from aggregates of differing sizes and fractal dimensions in colloidal fouling. Jonsson *et al.* (1995) calculated electrostatic interaction by the Poisson-Boltzmann equation, dispersion forces and solid sphere interaction by the Carnahan-Starling equation in order to explain the interaction between the particles and the concentration polarization phenomena in ultrafiltration of colloidal dispersions.

Pre-treatment methods to limit NOM fouling

In MF or UF, organic matter may cause fouling by forming a cake on the membrane surface, while dissolved material may cause fouling by adsorbing within the membrane pore space. In both of the cases the total filtration resistance is related to the permeability of the surface cake. The amount of material that adsorbed on the membrane surface or inside the pores can be minimized by a number of ways. Chemical cleaning agents can remove the deposited foulant and retrieve the membrane permeability. However, these are expensive, can influence the retention properties of the membranes and, after lengthy use can cause severe membrane damage and changes in membrane permeabilities (Maartense *et al.* 1998, 1999). Backwash technique is used to remove a weakly adhered cake layer. Another option is to prevent or minimise the foulant adsorption by pre-treatment of feed water. In this section

different modes of pre-treatments to control fouling due to NOM for low pressure membrane processes are presented.

There are many pre-treatment methods used to minimize the effect of NOM fouling in MF and UF. Some of them are coagulation, activated carbon adsorption, ozonation, etc. The pre-treatment method employed is very much related to the raw water quality. Carroll *et al.* (2000) found that coagulation can be used to improve NOM removal and minimize fouling in MF of surface water. The authors also compared two different pre-treatment methods, coagulation with alum and powdered activated carbon (PAC) adsorption. They remarked that coagulation pre-treatment helped to reduce membrane fouling and also NOM removal. The authors explained that coagulation pre-treatment selectively removed some fraction of NOM. They attributed the fouling due to NOM after coagulation to fouling by neutral hydrophilic substances. The reduction in the rate of fouling after coagulation could be caused by aggregation of fine particles, incorporation of particles into flocs, or adsorption or precipitation of dissolved materials into flocs (Weisner and Lainé, 1996). The extent to which the rate of fouling is determined by colloidal or dissolved NOM will depend on the characteristics of both the raw water and the coagulant used in any pre-treatment.

Maartense *et al.* (1999) suggested alteration of pH and application of metal ions as pre-treatment techniques of feed water to reduce fouling of polysulfone UF membranes caused by natural brown water (NBW). NBW with pH 7 was sustained at 69% of its original flux after 300 min of filtration whereas NBW with pH 2 was only 33%. The authors hypothesised that the presence of Al^{3+} and Ca^{2+} in the NBW would help to block the functional groups of NOM by forming large precipitated organic materials of metal ions and hence influenced the potential of adsorptive behaviour of NOM on membrane. However, the results of their experiments indicated that coagulation with metal ions could not prevent membrane fouling, on the contrary caused more extensive fouling than the untreated solutions. They explained that the increased

fouling was due to the greater adsorption of NOM onto the UF membrane caused by metal ion complexes.

Schaffer et al. (2001) reported that coagulation can be used to increase NOM rejection. In their experiment, FeCl_3 was used as the coagulant before microfiltration. The organics which were retained by the membrane as precipitate of ferric oxyhydroxide caused membrane fouling by pore blocking or by cake deposition.

Another chemical addition such as Powdered Activated Carbon (PAC) has been found to reduce both cake deposition and dissolved organic carbon (DOC) adsorption. PAC helps to improve hydraulic properties of the cake by increasing its permeability and reducing compressibility. But some authors had reported that the presence of PAC particles increased the fouling problems and caused severe flux decline (Lin *et al.* 2000).

Lin *et al.* (2000) reported that the use of PAC as pre-treatment of humic substances or in combination with different UF operating systems to reduce membrane fouling had a negative effect. The PAC used in their study was not only effective in removing the molecular weight fractions of humic acids but also caused worse fouling than the PAC non-treated solution. Similar results were reported by Li *et al.* (2004). In their study, a solution containing both NOM and PAC induced a higher degree of fouling than a solution without PAC. The authors remarked that the fraction of NOM that is not removed by PAC caused as much as or even worse fouling than caused by solution without treated by PAC. PAC alone has not imposed significant fouling on the membrane. Thus PAC pre-treatment would enhance the organic removal but at the same time increased fouling.

Another chemical addition is the addition of naturally occurring clays such as montmorillonite or bentonite. Zermane et al. (2005) used a pillared bentonite (mont- Al_{13} -CTAB) for adsorption of humic acid in synthetic seawater. The crude bentonite was extracted from the Russel site in Algeria and pillared with an Al_{13} polymer (PCBA) and a surface active agent (cetyl trimethyl ammonium bromide - CTAB). A kinetic study at pH 3 revealed a 60%

elimination of humic substances within 30 minutes. Afterwards, it reached a maximum value of 70% for an equilibrium time of 3 hours. The authors remarked that the presence of the surface active agent CTAB helped to better adsorb the organic matter.

M. W. Naceur *et al.* (2004) used the same clay (mont-Al₁₃-CTAB) for NOM adsorption coupled with tangential flow microfiltration using mineral membranes. The authors found that the retention of NOM obtained with the bentonite adsorption and microfiltration was much higher than that obtained by the MF membrane alone. For MF alone they got retention of 60% while with bentonite adsorption and MF the value of retention increased to 98%. It also should be noted that the membrane fouling with bentonite adsorption was slightly higher than the fouling caused by the solution of NOM alone. Thus this method of pre-treatment also provides a rejection of NOM, and at the same time cause more membrane fouling due to the direct adsorption of the NOM-metal-clay complex.

X. Peng *et al.* (2005) also used an aluminium polycation pillared bentonite for humic acid adsorption from water. They reported that the adsorbent is very effective in removing humic acid. The authors also noted that the zeta potential of the bentonite particles and the solution chemistry of natural water also play a very important role in the adsorption of humic acid.

Membrane autopsy tools

Fouling can lead to increase in operational and maintenance costs, increase in energy consumption and ultimately affects the water quality output. To better understand the reason for deteriorating membrane performance, operating conditions, feed water quality, pre-treatment design and the chemicals in use must be considered. Even then, this information alone may not be sufficient to resolve the problem. The only reliable method to understand the true identity of a foulant is membrane autopsy (Pontié *et. al*, 2005). Membrane autopsy is a destructive procedure including physical, chemical, microbiological and microscopic

examinations. Membrane autopsy can be used to identify, diagnose and predict fouling and even prevent further consequences. Microscopy represents a powerful technique to visualize directly the structural appearance of MF and UF. Optical microscopy (OM), transmission electron microscopy (TEM), scanning electron microscopy (SEM), and atomic force microscopy (AFM) have been used for membrane characterization.

SEM has been widely used for surface analysis. It produces topographical images of the membrane surface, and direct, practical and instant structural membrane information (Zemane and Zydney, 1996). Madaeni (1997) employed field emission scanning electronic microscopy (FESEM) to provide better understand of critical flux mechanism in MF membrane filtration. Lee *et al.* (2003) provided morphological analysis with SEM and AFM for low pressure (MF/UF) membranes fouled by NOM. They addressed that membrane fouling was caused by pore blockage and cake/gel layer formation with NOM and is affected by the roughness and structure of membrane. Kim *et al.* (1999) employed AFM for analyzing pore size with comparison of SEM analysis. The pore diameters obtained from AFM were larger than those obtained from SEM and AFM analysis is considered to be more accurate due to its non-coating preparation of samples. Zeng *et al.* (2003) investigated surface morphology and nodule formation mechanism of cellulose acetate membranes with AFM and found that temperature and variation of the solvent environment are major factors for nodule formation on the membrane. AFM was used to investigate surface pore structures of MF and UF membranes and provided quantitative information on surface pore structure such as pore size, pore density and porosity (Dietz, 1992, Bowen, 1996).

The measurement of contact angle explains the hydrophobicity/hydrophilicity of the membrane surface. Previous research has shown that a hydrophobic membrane can be changed in its hydrophobicity/hydrophilicity due to adsorption of foulants on the surface (Cho, 1998). Esparza-soto *et al.* (2001) used fluorescence spectroscopy to study the behaviour of humic substances in bio mass. Attenuated Total Reflection-Fourier Transform Infrared Spectroscopy

(ATR-FTIR) analysis provides valuable information related to the chemical structure of foulants and membrane surface by reading functional groups of molecules. Jarusutthirak (2002) and Her (2002) provided that the functional groups such as alcohol, amide which came from polysaccharides and proteins, on fouled membranes by FTIR and those macromolecules cause significant NF membrane fouling. Belfer *et al.* (2000) also investigated functional group of modified polyethersulfone (PES) ultrafiltration membranes and adsorption of albumin on the surface of membrane.

In our study we used different tools for membrane autopsy. A membrane was analysed before and after fouling. Tools for membrane autopsy include physical, physio-chemical and chemical tools. Physical tools include hydraulic permeability determination, scanning electron microscopic (SEM) analysis and atomic force microscopic (AFM) analysis. Streaming potential (SP) measurements and contact angle measurements come under physico-chemical tools. One of the chemical tools we used was pyrolysis. This was done by a gas chromatography/mass spectrometry system at 400° C.

Some analytical tools and their applications

Fractal Dimension theory and application

Euclidian geometry describes regular objects such as points, curves, surfaces and cubes using integer dimensions 0, 1, 2 and 3 respectively. Associated with each dimension is a measure of the object such as the length of a line, area of a surface and volume of a cube. However, numerous natural objects, such as coast lines, rivers, lakes, and porous media are disordered and irregular, which cannot be described by Euclidian geometry due to the scale-dependent measure of length, area and volume. These objects are called fractals and their dimensions are non integral and defined as fractal dimensions. A fractal object can be divided into parts, each of which is similar with the whole. However, self-similarity in a global sense is

seldom observed in actual applications. Numerous objects found in nature are not exactly self-similarity, but statistical self-similarity, which implies that these objects exhibit the self-similarity in some average sense. SEM images of the fouled surface cake were analyzed using an image analyzer called *Image J*. From the original SEM image, a threshold (binary) image is generated with the help of the software as shown in Fig 4.

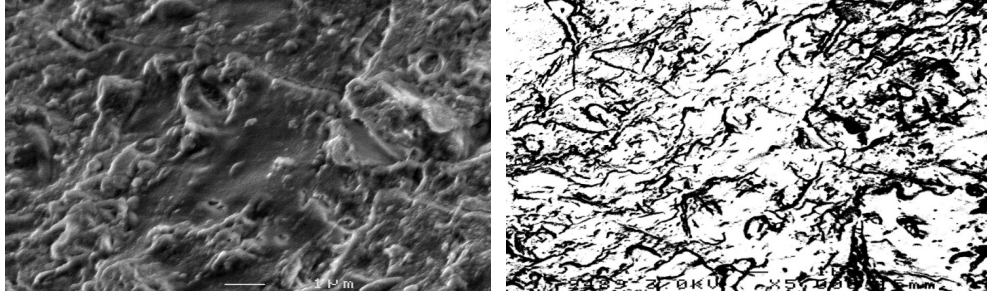


Figure 4 SEM image of fouled membrane surface and the threshold image

Box counting method

One of the most common methods for calculating the fractal dimension of a self-similar fractal is the box counting method (Fig. 5). By covering a structure with boxes of length ϵ the fractal dimension, FD is given by

$$\ln N = -(\text{FD}) \cdot \ln \epsilon \quad (4),$$

where N is the number or count of boxes. The absolute value of the slope is taken as the fractal dimension; FD (B. B. Mandelbrot, 1982)

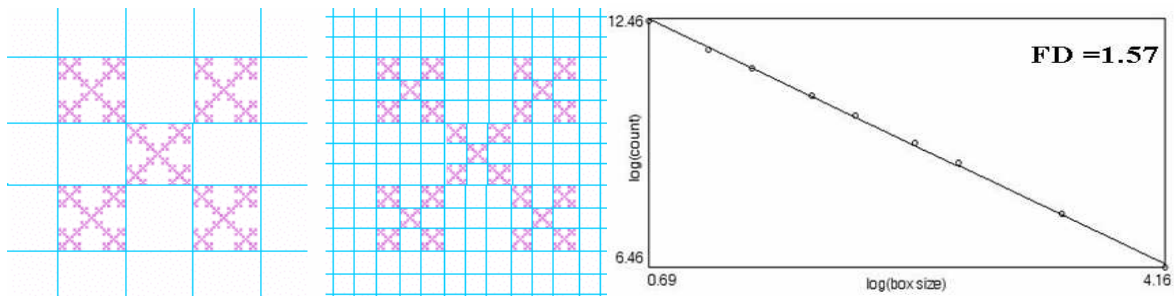


Figure 5 plot of log (count) with log (box size) illustrating the box counting method

MFI theory and application

MFI parameter gives an idea of the fouling potential of the feed. It is based on cake filtration mechanism, as reported by Schippers *et al.* (1980).

The equation is given as,

$$\frac{t}{V} = \frac{\mu.R_m}{\Delta P.S} + \frac{\mu.I}{2\Delta P.S^2}.V = A + MFI.V \quad (5)$$

Where, t is the filtration time, μ is the water viscosity, ΔP is the trans-membrane pressure, S is the surface area and I is the fouling index which depends upon the specific resistance of the cake α and the particle concentration C_b (Eqn. 6).

$$I = \alpha C_b. \quad (6)$$

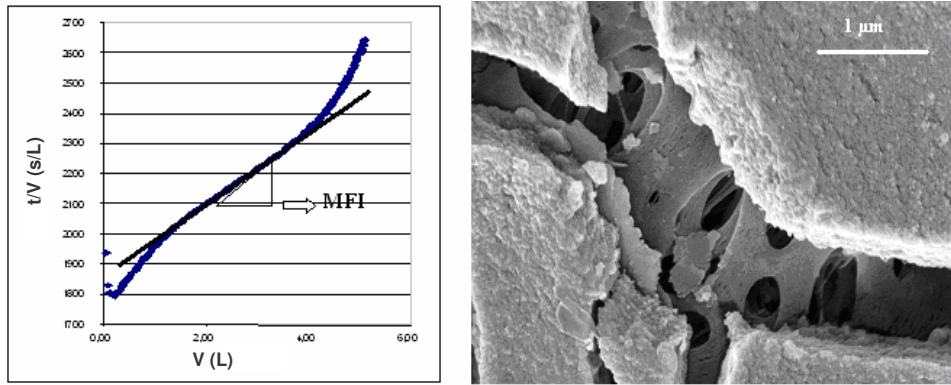


Figure 6 t/V vs V graph for the determination of MFI, a cake formed on a polysulfone UF membrane for the filtration of NOM (K. Kecili Thesis, 2006).

As shown in Fig. 6, filtration occurs usually in three stages: (i) the first part is the blocking of the pores, (ii) the second part is the gradual formation of the cake and (iii) the third part is the compression of the cake. When there is a formation of an incompressible cake, the relation between t/V and V is showed to be linear and the slope of the linear relation will give the indicator MFI which corresponds specifically to the fouling potential of the feed solution. The results of the test are thus a series of measurements of time with cumulated permeate volumes.

The classical Silt Density Index (SDI) is not based on a distinction between filtration mechanisms occurring during the test and therefore cannot model flux decline in membrane systems. Moreover, there is no linear relationship between the index and particle concentration. Conversely, MFI is based on cake filtration and can be used to model flux decline in membrane systems. In addition, MFI index is linear with the concentration of particles in feed water (Schipper *et al.*, 1980).

Streaming potential theory and application

Commonly, to describe mass transfer in UF, the size exclusion model is used. Nevertheless, in certain conditions (low molecular weight cut-off membranes) the property of the electrical double layer near the pore walls is an important part of the pore volume. Therefore, the membrane electro-kinetic properties (i.e. streaming potential and surface conductivity) play an important role. When an electrolyte solution is forced to flow through a capillary, an electrical potential is generated which is known as streaming potential (SP). SP measurement gives information about the charge related modifications on the surface/ inside the pores of a membrane.

Electrical double layer and streaming potential

The electrical double layer model was first introduced by Stern (1924), by combining the Helmholtz and the Gouy-Chapman models. According to Stern about one molecule distance the presence of a layer, Stern layer, is considered. The oppositely charged ions in this layer can decrease the surface potential linearly. Besides, there is another layer which consists of the other scattered ions. Here, the potential decrease is not linear, but approaches to zero as shown in Fig. 7, which means that the ion concentration decreases with the increase in distance and reaches to the normal concentration of the solution.

The electrical charge on the solid surface (S_s) is the electrical charge in the Stern layer. The effect of electrolyte concentration on the double layer thickness and can be best understood

in terms of the zeta potential. Zeta potential (ξ) is the electric potential that exists at the "slip plane" (order streaming plane) - the interface between the hydrated particle and the bulk solution. It is the measurable potential of a solid surface and also called electro-kinetic potential.

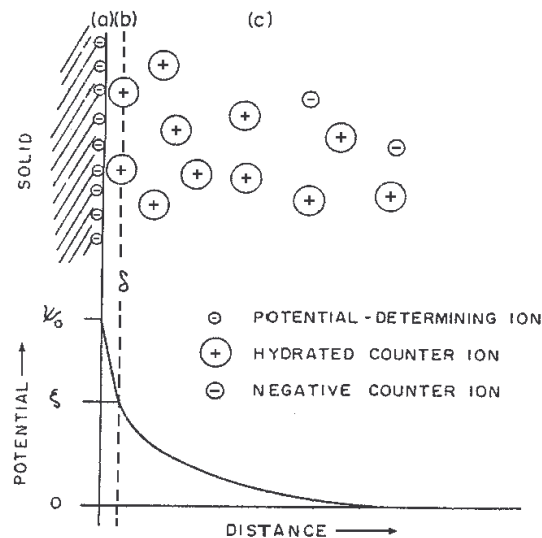


Figure 7 Schematic representation of the double layer and potential drop across the double layer; surface charge, Stern layer, and diffuse layer of counter ions

There are four basic types of electro-kinetics effects. Theoretically, each can be utilized to evaluate the zeta potential for a given set of conditions.

1. *Electrophoresis*: dealing with mobility of a charged colloidal particle suspended in an electrolyte in which a potential gradient is set up.
2. *Electro-osmosis*: denoting a movement of liquid in a capillary or in a system of capillaries (porous plug) under an applied potential.
3. *Sedimentation potential*: determining the magnitude of the potential developed by a dispersion of particles settling under the influence of gravity.
4. *Streaming potential*: concerned with the magnitude of induced electric potential, generated by a flow of liquid in a single capillary or in a system of capillaries.

According to Helmholtz-Smoluchovsky equation (Eqn. 7), the streaming potential can be linked to the zeta potential by the equation:

$$\Delta\phi = \frac{\epsilon\zeta}{\mu\chi} \Delta P \quad (7)$$

Where $\Delta\phi$ is the trans-membrane potential difference, ΔP is the trans-membrane pressure, ϵ , the permittivity, ζ , the zeta potential; μ , the dynamic viscosity; χ , the ionic conductivity of KCl (0,001 M, pH=6,5), the electrolyte solution; and $\Delta\phi/\Delta P$, the coefficient of streaming potential.

From the measurements of variations of potential differences between two Ag/AgCl electrodes vs. trans-membrane pressure, it is possible to follow the charge evolution of pore walls of the membrane, because the trans-membrane potential difference per unit pressure is directly proportional to the zeta potential of the filtration medium. SP is the more simple way to determine the charge carried by a porous material, as reported recently (K. Kecili, 2006, Patent (2006) Pontié *et al.*).

The use of Helmholtz-Smoluchovski equation is restricted to high ionic strengths (Debye length, κ^{-1} should be less than 3 nm) in large capillaries (pore radius, r_p higher than 1.5 nm). If such SP measurements are made across the surface of a membrane, calculation of the zeta potential from the basic experimental data is generally unambiguous. However, the calculation requires more care if measurements are made with a flow through a membrane. In this case, an electrical double layer is formed in between the charged membrane pore walls and the adjacent electrolyte solution. It was shown that Eqn. 7 can be used to the limit of the ratio κ^{-1}/r_p around 10 in the case of high charge density. Thus a correction should be made to Helmholtz-Smoluchovsky equation with regard to narrow capillaries which takes into account of the double layer thickness on the interface. In the case of MWCO under 100 kDa with a concentration of electrolyte 0.001M, κ^{-1} will be double the size (9.7 nm) of the pore radius and overlapping of double layers will occur. Then Eqn (7) will not be valid for the calculation of

absolute zeta potential but permits a qualitative measurement of the charge. So, we have to specify that our study was focalized on streaming potential (SP) measurements.

Summary

In this bibliographic chapter, a general overview of membranes used for the production of drinking water was presented. The problem of membrane fouling, and mechanisms of membrane fouling were reviewed. Importance of low pressure membrane processes and fouling of MF/UF membranes due to NOM were also mentioned. Factors which affect fouling due to humic substances, like the properties of humic substances (size and charge of the particles, pH, hydrophobic/hydrophilic nature and combination with metals) as well as the properties of the membrane (pore size, zeta potential, hydrophobic/hydrophilic nature) were also reviewed. Membrane autopsy tools -which help to diagnose the true identity of the foulants-, were incorporated. Finally some pre-treatment methods to limit NOM fouling were also presented.

C-MATERIALS AND METHODS

Membranes and modules

Flat-sheet membranes used in our study are listed in the table given below (Table 4).

Table 4 Characteristics of flat-sheet membranes

Membrane	Material	Type	MWCO
YM 100	Regenerated cellulose	Flat-sheet UF	100 kDa
YM 30	Regenerated cellulose	Flat-sheet UF	30 kDa
YM 10	Regenerated cellulose	Flat-sheet UF	10 kDa

Amicon 8200 model filtration cell which operated in dead-end mode, without stirring was used. The system used for filtration is shown in Fig. 8. The filtration cell was connected to a N₂ gas source to induce pressure. Permeate was collected and the flux was measured. The effective surface area of all the membranes was 29 cm². All experiments were carried out at room temperature (20 °C).

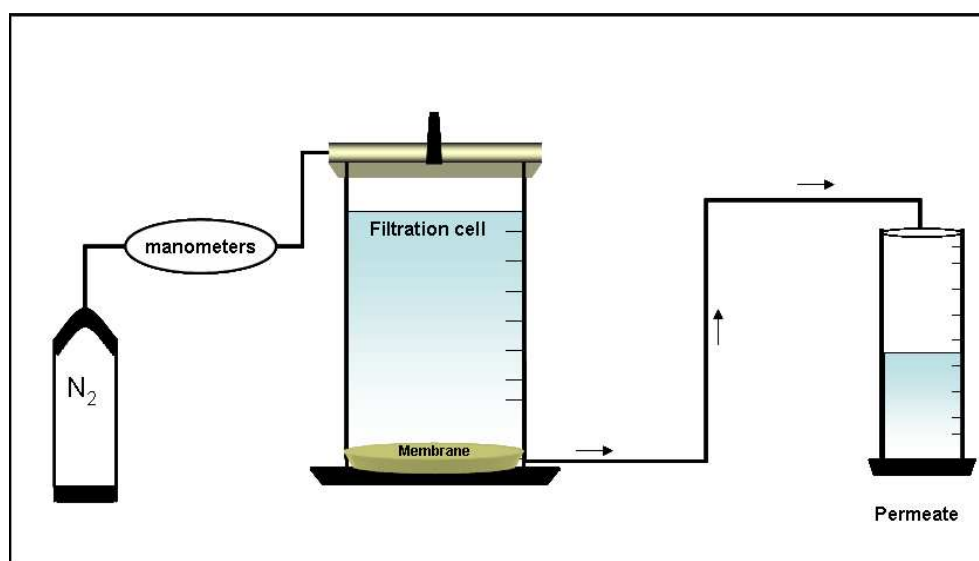


Figure 8 Schematic diagram of UF system for filtration with flat-sheet membranes

pH and conductivity measurements

The pH and conductivity of the solutions were determined using a pH meter (PHG301) and conductimeter (CDC866T), which were purchased from Radiometer analytical.

Elimination of chemicals

The virgin membranes were subjected to washing with ultra pure water prior to filtration to eliminate chemicals, like glycerine and sodium azide. These chemicals were added by the membrane manufacturers to prevent drying of the membranes during transportation.

The procedure used for washing of membranes is as follows. Membrane disc was kept in a Petri dish containing ultra pure water with glossy side (active layer) downward. Water in the Petri dish was changed four times, each every half an hour. Then it was mounted on the filtration cell and filtered with ultra pure water at a pressure of 2 bars. Conductivity of permeate was checked each time. Filtration with ultra pure water was continued until the permeate conductivity was the same as that of the feed solution ($\sim 0.7 \mu\text{S}/\text{cm}$).

After the elimination of unwanted chemicals, hydraulic permeability coefficient (L_p) and Streaming potential (SP) of the virgin membrane were determined. The trans-membrane pressure range used for our study was from 0.5 to 3.0 bars.

Streaming potential and IEP measurements

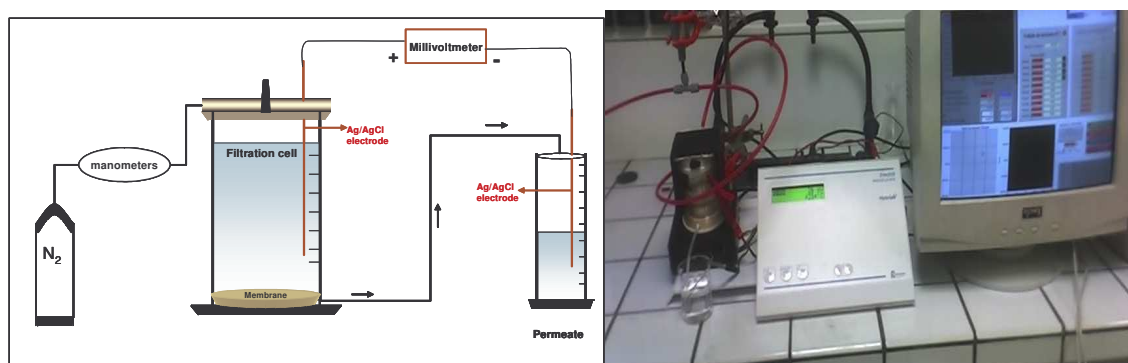


Figure 9 A schematic representation and Photography of the system of streaming potential and IEP measurements

Fig. 8 shows the general filtration system for UF using flat-sheet membranes. To this system two Ag/AgCl electrodes were introduced (as shown in Fig. 9) which in turn connected

to a millivoltmeter (PHM250 from *Radiometer Analytical*, France). Fig. 9 shows a photograph of the system used for SP and IEP measurement using software denoted as *profluid 3.0*.

This millivoltmeter with high impedance was connected to a PC, via a RS232. The software (denoted as *proFluid 3.0*) was developed in University of Angers in collaboration with NEOSSENS (Toulouse, France). For each trans-membrane pressure value a corresponding potential difference was indicated on the milli-voltmeter and also on the PC. The same experiment was conducted under different pressures (from 0.5 to 3 bars, with 0.5 bar increment). SP and the correlation coefficient R^2 were automatically generated. A mean average value of 1 mV/bar is attached to each SP measurement.

The sign of the SP directly gave the sign of the net charge of the membrane, i.e., the global charge behind the shear plane. We connected the positive potential to the feed and the negative to the permeate, then from the slope we obtained directly the sign of the membrane pore walls and consequently the charge density of the membrane pore walls. SP measurements under different pH were carried out to measure the isoelectric point (IEP).

Humic acid (HA) solutions and fouling experiments

HA solutions of different concentrations (5 mg/L, 10 mg/L, 50 mg/L) were prepared by dissolving humic acid (purchased Sigma Aldrich, Acrôs Organics) in ultra pure water (Milli Q Water System, Millipore, France). No purification or pre-filtration of the HA samples were conducted prior to filtration through membranes. NaOH 0.1 M and HCl 0.1 M solutions were used to adjust the pH of the humic acid solution. All the reagents used were of analytical grade. Pure water permeability and charge (SP) of the virgin membranes were measured prior to the fouling experiments. Two liters of HA solution was filtered through a membrane under constant pressure in one batch of filtration experiment. Permeate Flux was followed with time during the entire batch of experiment. At the end of the experiment, fouled membrane

permeability with ultra pure water and the SP were determined to assess the extent of fouling. Modified fouling index (MFI) was also calculated from the flux vs. time data.

FESEM analysis

Virgin and fouled membranes were subjected to FESEM analysis to understand the morphological variations with fouling. The apparatus used was JSM-6301F from JEOL. Images obtained were from secondary electrons under 3-5 keV with magnifications situated between 100 and 20000. Membranes were dissected and glued to a carbon support. Finally carbon of 2 nm thickness was deposited by evaporation under vacuum (BAL-TEC MED 020 Balzers Lichtenstein apparatus).

Fractal dimension determination

Two dimensional Fractal dimensions (FD) were determined using *Image J* software from the SEM images. From the original SEM images, a threshold image is generated with the help of the software and using the box counting method, fractal dimension is determined. Two dimensional Fractal dimensions will be having values in between 1 and 2. The method to determine fractal dimension is explained in figures 4 and 5.

We have also studied some virgin and fouled hollow fibre membranes. The fibres were fouled by real water NOM (Tampa bay water, USA). Hollow fibre membranes used in our study are detailed in Table 5.

Table 5 Properties of hollow fiber membranes

Membrane	Material	Type	Pore size (μm)
A- Hydranautics	PES	UF In-- Out	0.015
B - Zenon	PVDF	UF Out--In	0.035
C- Norit	PES	UF In--Out	0.015

All the hollow fibres were ultrafiltration membranes. The membranes, A-Hydranautics and C-Norit was of the same material, polyethersulfone (PES). Both of these membranes were of in-out configuration. The membrane, B-Zenon was made of polyvinylidene fluoride (PVDF) with out-in configuration.

**C- FUNDAMENTAL STUDIES CONDUCTED
WITH FLAT-SHEET MEMBRANES IN DEAD-
END ULTRAFILTRATION**

Preliminary studies

Ultrafiltration can effectively remove macromolecules, suspended matter, micro organisms and provide good quality drinking water. The problem of fouling due to humic substances is the main issue that limit the application of UF in drinking water treatment. Each component of the feed stream will react differently with the membrane: conformation, charge, zeta potential, pH of the solution, hydrophobic/hydrophilic interactions and other factors will have a significant role in fouling of membranes. So it is very important to understand the role of membrane material properties, the role of solute properties and the role of operating parameters (like pH, trans-membrane pressure, MWCO, solute concentration etc.) to limit and control fouling.

In this study we used regenerated cellulose YM 100 membranes which are very hydrophilic and quite ideal for water treatment. YM 100 membranes were subjected to Aldrich humic acid filtration of 5 mg/L, at a pH of 6.7. The system used for filtration is given in the Fig. 8.

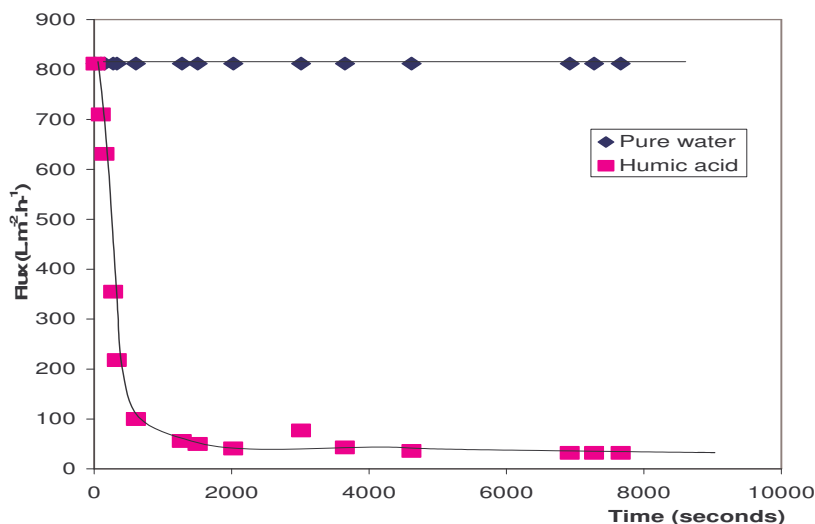


Figure 10 Evolution of flux with time during the filtration of 5 mg/ L HA at a constant pressure of 2 bars for RC 100 kDa membrane

Permeate flux at constant pressure was plotted with filtration time as given in Fig. 10. At constant pressure, the flux of pure water remained the same and that of humic acid declined so quickly in the first few seconds of filtration, then became gradual and reached a steady state. At the end of the experiment, the decrease of the flux from the initial value was 90%. The flux decline was attributed to the deposition of HA particles on the membrane surface which gradually formed a cake.

Fig 11 shows the variations of pure water permeability values of the virgin membrane, after adsorption with humic acid (in contact with the solution for 2 hrs) and after filtration with humic acid at a constant trans-membrane pressure of 2 bar. The pure water permeability obtained was $390 \text{ L. m}^{-2} \cdot \text{h}^{-1} \cdot \text{bar}^{-1}$. After adsorption, permeability value decreased to $380 \text{ L. m}^{-2} \cdot \text{h}^{-1} \cdot \text{bar}^{-1}$ and after fouling, it was decreased to $122 \text{ L. m}^{-2} \cdot \text{h}^{-1} \cdot \text{bar}^{-1}$ as shown in Fig. 10.

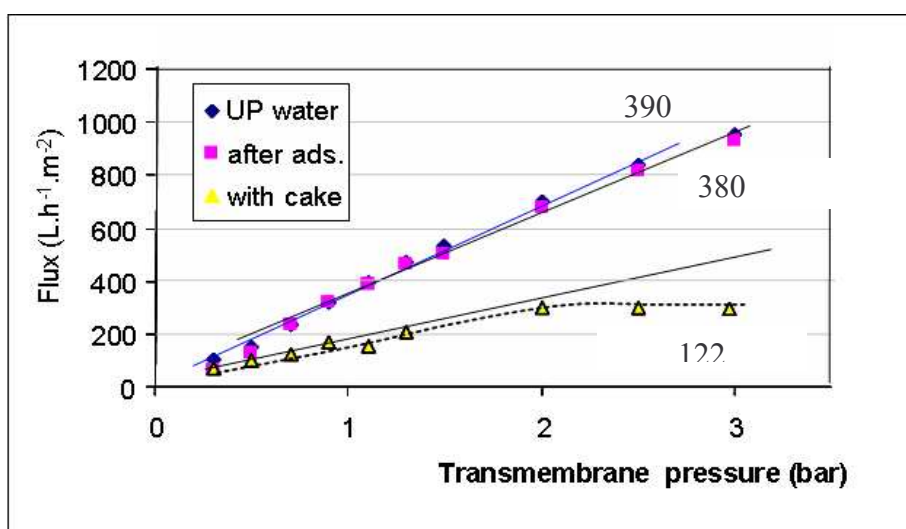


Figure 11 Variations of pure water permeability values of the virgin clean membrane, after adsorption with Aldrich humic acid (5 mg/L, pH 6.5) and at the end of filtration with the HA cake

From the clean permeability value, intrinsic membrane resistance, R_m , was calculated as $0.92 \times 10^{12} \text{ m}^{-1}$. Following the resistance in series model (Eqn 2) adsorption resistance (R_a) and resistance due to fouling (R_c) was also determined. The R_a value was determined as $0.02 \times 10^{12} \text{ m}^{-1}$ and fouling layer resistance was determined as 2.01

$\times 10^{12} \text{ m}^{-1}$ (Table 3). The fouling layer was analyzed with the help of SEM images (fig. 11) and found that it was formed a cake on the membrane surface, which increased the total hydraulic resistance, R_t , as reported elsewhere. (Nyström *et al.* 1998).

Table 6 Resistance values of the YM 100 membrane before and after filtration with humics

Resistance values ($\times 10^{-12} \text{ m}^{-1}$)	Membrane resistance (R_m)	Adsorption resistance (R_a)	Cake resistance (R_c)	Total resistance (R_t)
100 k Da	0.92 ± 0.05	0.020 ± 0.001	2.01 ± 0.1	2.95 ± 0.15

From Table 6, cake resistance contributed 68% to the total resistance which further explains that cake formation was the cause of the fouling.

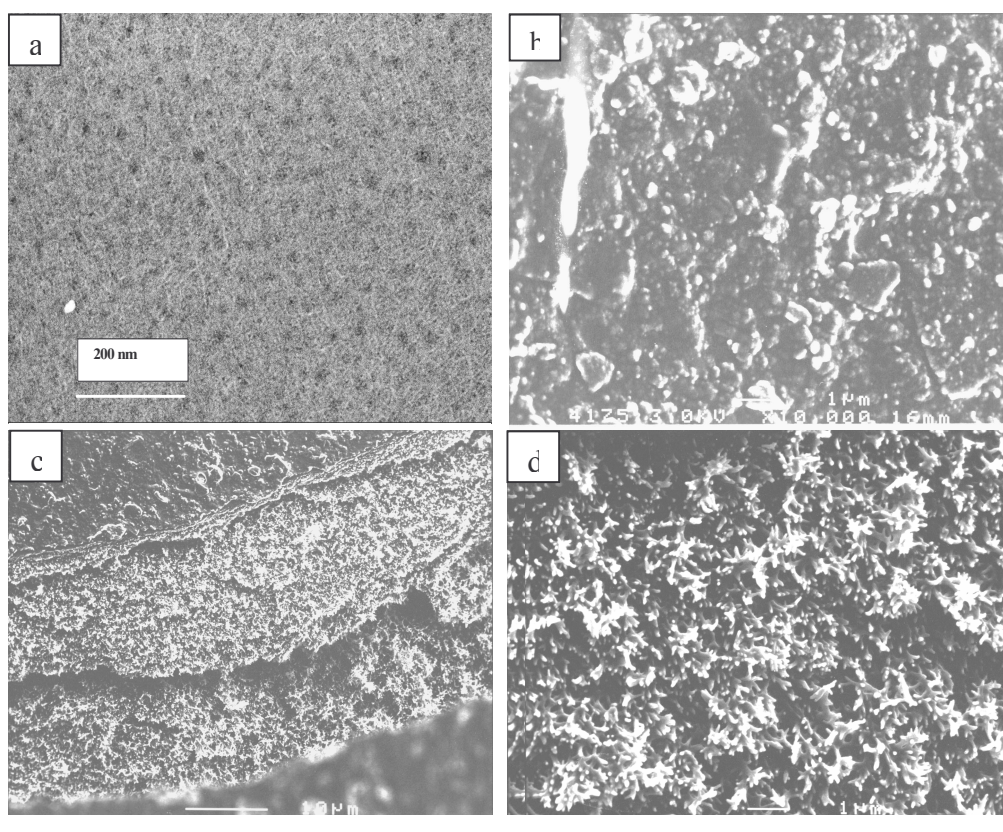


Figure 12 SEM images showing (a) the clean membrane surface, (b) fouled membrane surface, (c) a cross section of a humic acid cake and (d) the magnification of the cake

Fig 12 demonstrates the SEM images of YM100 membrane in the virgin and fouled states. The fouled membranes showed the presence of humic acid deposit which was the cause of flux reduction. The image (Fig 12 (c)) also shows a cross section of the humic acid cake.

When the microstructure of the humic acid cake was analyzed, it showed *fractal* structures, as shown in Fig. 12 (d). Waite *et al.* (1999) reported the fractal nature of the aggregates formed on the surface of a membrane. Meng *et al.* (2005) also reported that fouling layer formed on an MBR is having a fractal nature and fractal dimension can be used to analyze cake formation.

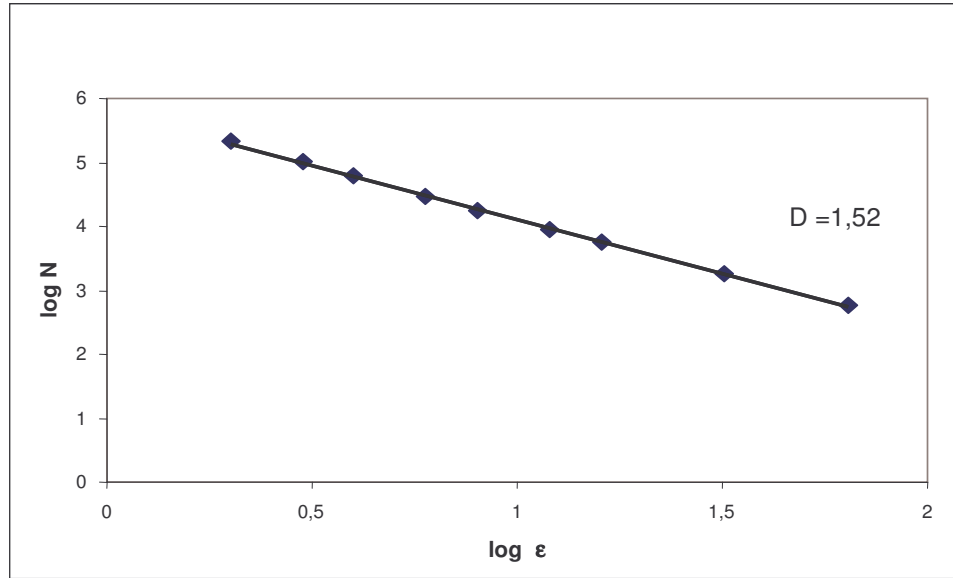


Figure 13 A double logarithmic plot showing the evolution of $\log N$ with $\log \epsilon$. The absolute value of the slope gave the fractal dimension FD

We have determined the fractal dimension of humic acid cake surface and that of the magnified structures (Fig 12 (b) and 12(d)). FD was calculated using the box counting method as explained in the previous chapter. The slope of the double-logarithmic graph (Fig.13) gave the FD of the image in two dimensions as 1.52.

Two and three dimensional fractal dimensions of YM 100 fouled surface and the humic acid cake were determined as 1.52 ± 0.02 and 2.52 ± 0.02 , respectively. These values corresponds to a mechanism of deposition, namely particle-cluster aggregation underlying diffusion limited cluster aggregation (DLCA) (Witten *et al.*, (1983), Meakin, 1983). Typical Fractal dimension of DLCA is 1.75 in two dimension and 2.51 (Fig. 14) in three dimension which is in agreement with our results. Witten et al. reported that particle cluster aggregation has been shown to lead to flocs with a well defined fractal dimensionality of 2.51 in three

dimensions and 1.51 in two dimensions. N. Senesi *et al.* (1997) reported that humic acid suspensions in aqueous medium are susceptible to exhibit fractal structures. The authors also found that the value of FD can also change according to different operating conditions like humic acid solution concentration, pH and ionic strength. That work was also based on SEM observations.

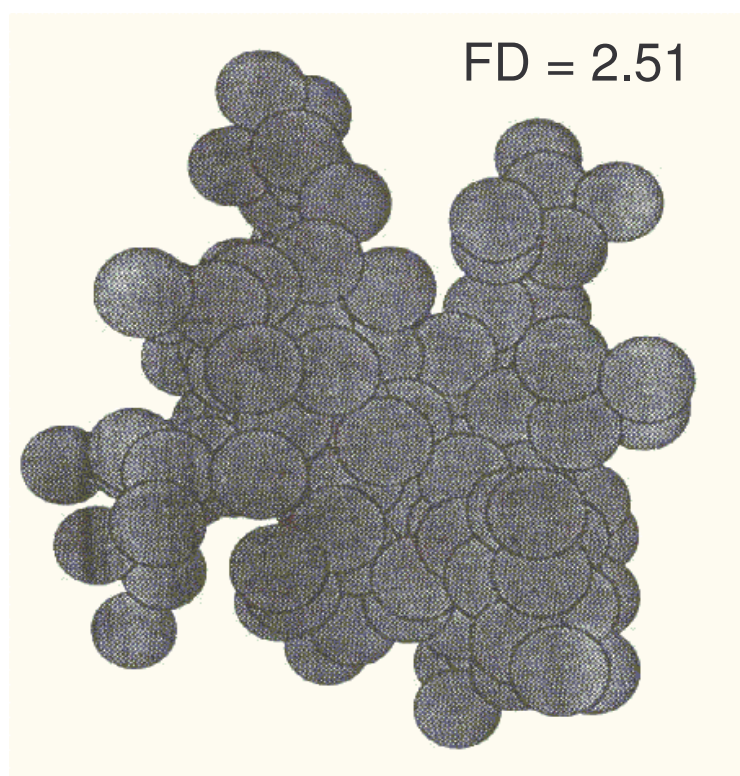


Figure 14 A theoretical three dimensional model showing particle-cluster aggregation comes under diffusion-limited aggregation

In our study, the aggregates formed are having a complicated multi-branched structure. Paul Meakin reported that diffusion limited deposition on fibres and surfaces may also result in open dendrite structures with a “fractal” nature. Meng *et al.* (2005) studied the microstructure of a cake formed during microfiltration and found that the porosity of the cake and the FD values obtained were inversely proportional. Thus as a microscopic approach, fractal dimension can be used as a parameter to describe cake formation and there by flux decline, as described later.

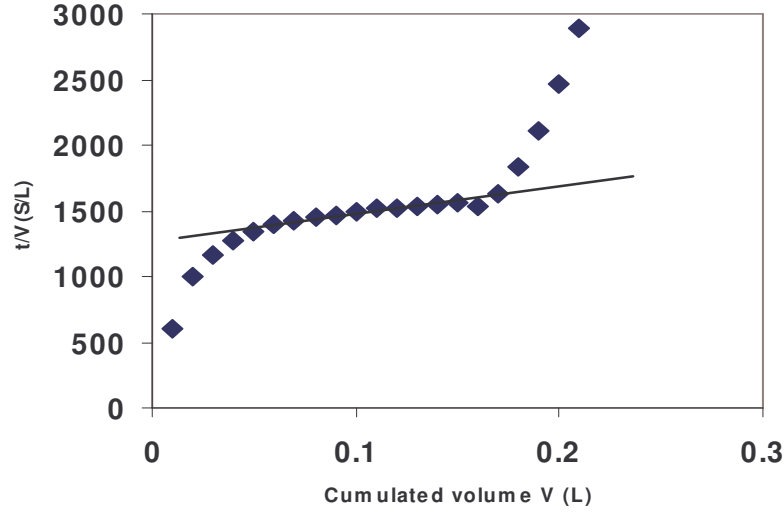


Figure 15 Evolution of t/V with V for RC 100 k Da membrane during the filtration of Aldrich humic acid 5 mg/L, pH 6.7

Modified fouling index (MFI –UF) is a parameter which purely depends on cake formation mechanism. MFI value was calculated from the slope of the linear portion of the t/V with V plot (Fig. 14) as reported by Schippers *et al.* (2003). MFI value was determined as 1650 s/L^2 in our study.

To understand the effect of charge on NOM membrane fouling mechanisms we developed a new home made streaming potential apparatus (Thekkedath *et al.* 2007). The SP of the virgin and fouled RC 100 k Da membrane are determined as indicated in Figures 16. It is found that the $\Delta\phi/\Delta P$ is linear according to Helmholtz Smoluchovsky equation (Eqn. 7). It is found that the clean membrane posses a SP value -27 mV/bar which further indicate that the membrane is negatively charged, as reported elsewhere (Pontie *et al.* 1999).

We have determined the streaming potential of the membrane before and after filtration with humic acid under fixed pH conditions (Fig. 16) (pH=6.5). Figure 16 illustrates the variation of potential difference (mV) vs. trans-membrane pressure (bar) obtained using the homemade SP measurements design. SP values obtained both for clean and fouled membranes are compared.

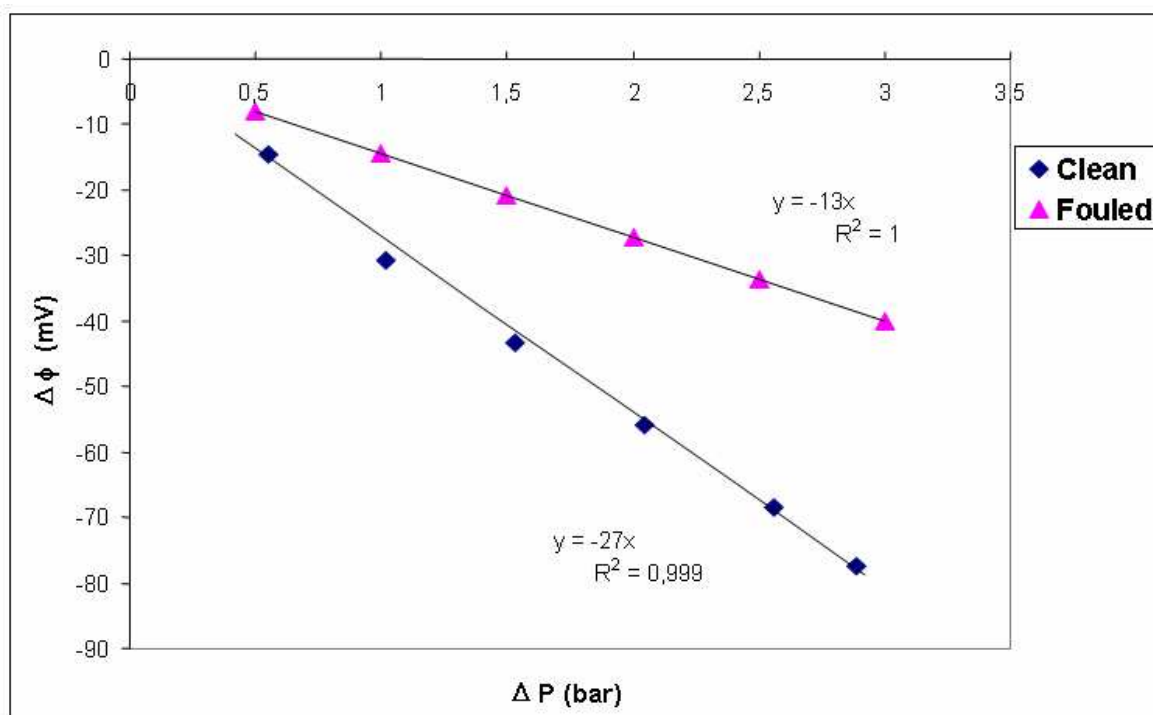


Figure 16 Evolution of potential difference with pressure for a membrane of RC 100 k Da before and after filtration with HA 5 mg/L, pH 6.7; KCl = 0.001 M.

Indeed, the sign of the streaming potential directly yields the sign of the net charge of the membrane, i.e., the global charge behind the shear plane. The charge of the clean RC 100 k Da membrane was -27 mV/bar and that for the fouled membrane was shown to be -13 mV/bar. From these values, we can conclude that after the cake elaboration on the surface of the membrane, the charges carried by the membrane pore walls have drastically reduced.

This modification of internal pore charge is attributed to the penetration of lower sized (lower than the minimum average size) humic acid fractions into the membrane pores which caused fouling inside the membrane, as reported recently by Violleau *et al.* (2005). The authors characterized the molecular weight of humic acid fractions and found that humic acids in their study were having molecular weights 1570 and 1040 Da, which is very low. Further experiments have demonstrated that NOM fractions are capable to penetrate inside NF membrane pores and can change their internal charges.

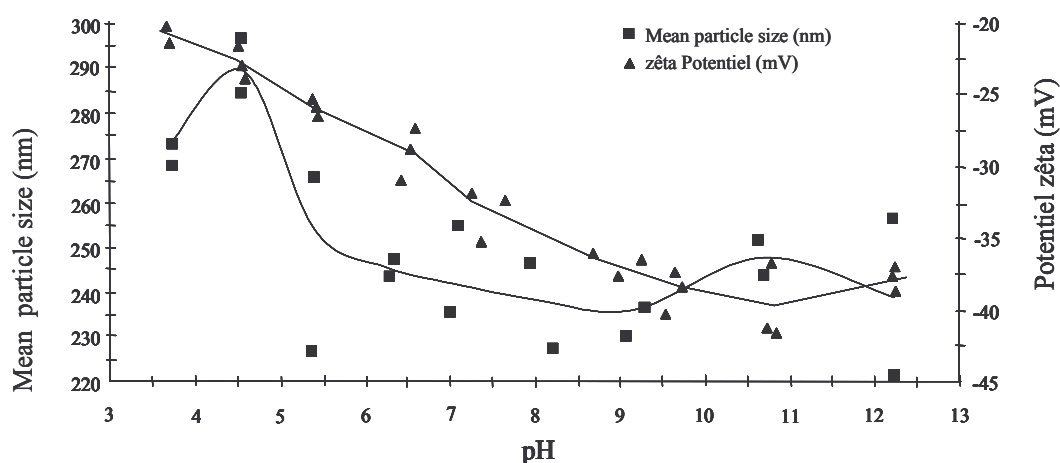


Figure 17 The distribution of mean particle size (nm) and zeta potential for Aldrich humic acid (5 mg/L) in different pH (zetasizer Malvern Co. Inc.).

Fig 17 shows the mean particle size distribution and zeta potentials for different pH values for Aldrich humic acid. As the size of the humic acid particles at pH 6.7 in our study is 240 nm and the average pore size of the membrane is 10 nm, it should be impossible to have fouling inside the pores. But from our SP results it is proved that one portion of humic acid particles which are having particle sizes less than 10 nm (or lower MW fractions) have entered into the membrane pores and changed the charge of the membrane.

We also determined the Isoelectric point (IEP) of the clean membrane and fouled membrane (Fig. 18). This represents the pH dependence of streaming potentials ($\Delta\phi/\Delta P$) for clean and fouled membranes. The electrolyte used was 0.001 M KCl solution. The streaming potentials appear to be sensitive to pH shifting as expected. The isoelectric point (IEP), i.e., the particular pH for which the net charge on the membrane surface (and also, the streaming potential) is zero, is found to be close to 2.3 for the clean membrane and 1.8 for the fouled membrane. The IEP value of the clean membrane was different with that found by Pontié *et al.* (1999). The authors found an IEP value of 3.4 for virgin RC 100 kDa membrane. This difference can be explained by lot-to lot membrane variability.

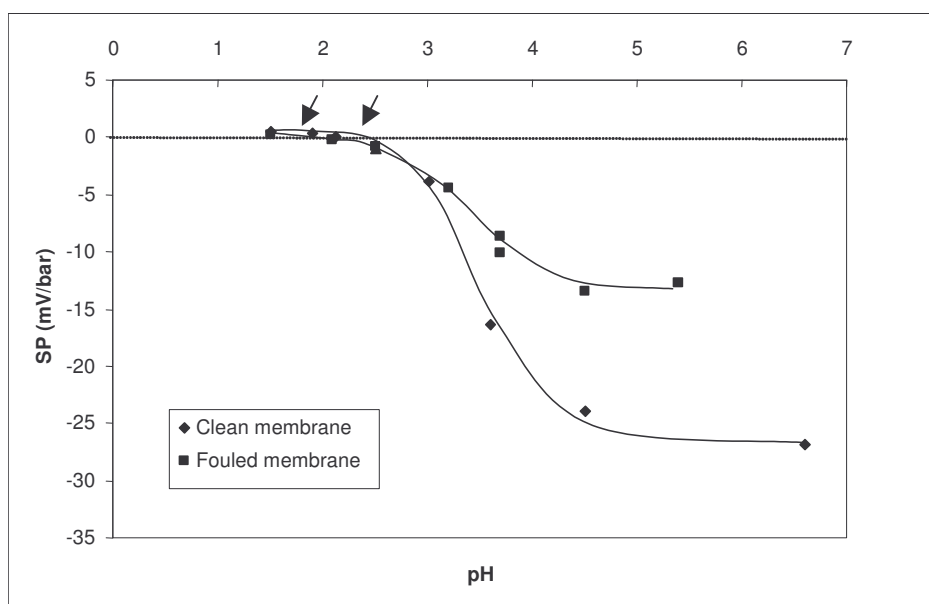


Figure 18 Evolution of SP with pH for the determination of IEP for clean RC 100 kDa membrane and that fouled by HA (Aldrich 5 mg/L, pH 6.7, filtration at constant $\Delta P = 2$ bars), $[KCl] = 10^{-3}M$.

Fig. 18 shows the variation of SP with different pH. The SP curves are not symmetric with respect to the pH range due to the ionic strength effect. In general, the SP decreases as the ionic strength of the treated solution increases due to the phenomenon of double layer compression (Sbai *et al.* 2003)]. In fact, as the protons concentration can be neglected with respect to that of K^+ ions at pH greater than 3.5. The ionic strength of the solution is fixed by concentration of KCl solution. Between pH 2.0 and 3.5 the ionic strength of the solution is fixed by both KCl solution and by protons (H^+) concentrations. At pH less than 2.0 the ionic strength of the solution is fixed only by the concentration of protons. By comparing the streaming potential values of the clean membrane and those of the fouled one (Fig.17) we can see that the membrane charge decreases with the formation of the HA cake. Thus, the decrease of membrane charge can be attributed to penetration of low molecular weight fractions of HA inside the pores.

Partial conclusion 1

Humic acid particles, aggregated on the RC-UF membrane and analysed by SEM demonstrated that the fouling layer appears to have a fractal nature with a fractal dimension of

$D = 2.51$. Then, as a microscopic approach, fractal dimension can be used as a new parameter to describe cake layer formation. As macroscopic tools MFI-UF value and cake resistance value (R_c) can be used to explain cake formation mechanism. SP measurements helped to understand the charge related modification on/inside the pores. These results suggest that this microscopic tool, fractal dimension, should be linked to any of the macroscopic parameters (flux decline with time, MFI, cake resistance) associated with cake formation. The variations of operating parameters like solution pH, molecular weight cut-off of the membranes, concentration of humic acids as well as trans-membrane pressure can be helpful to deduce the relation between these macroscopic and microscopic parameters.

Role of solution pH on fouling

Regenerated cellulose YM 100 membranes were subjected to humic acid filtration at constant pressures of 2 bars, at different solution pH. Acrôs humic acid solutions, at a concentration of 5 mg/L, in three different pH values (pH 6.7, pH 3 and pH 9.5) were used for the experiment. The results obtained are summarized in Table 7.

Table 7 Permeability, resistance values and MFI values obtained during the filtration of humic acid solutions at different pH, pH 3, pH 6.7 and pH 9.5. Acros [HA] = 5 mg/L, ΔP = 2 bars, T = 20° C, YM 100 membranes.

Parameters	pH 3	PH 6.7	pH 9.5
L_p clean ($L \cdot m^{-2} \cdot h^{-1} \cdot bar^{-1}$)	597 ± 100	597 ± 50	597 ± 50
L_p fouled ($L \cdot m^{-2} \cdot h^{-1} \cdot bar^{-1}$)	210 ± 20	155 ± 25	297 ± 30
Flux decline at the end of filtration (%)	68	88	53
$R_m \times 10^{12} m^{-1}$	0.60 ± 0.03	0.60 ± 0.03	0.60 ± 0.03
$R_c \times 10^{12} m^{-1}$	1.12 ± 0.05	1.72 ± 0.05	0.62 ± 0.03
$R_t \times 10^{12} m^{-1}$	1.72 ± 0.05	2.32 ± 0.05	1.22 ± 0.05
MFI (s/L^2)	544 ± 55	1358 ± 100	490 ± 50

It shows that all the three initial clean membranes have same the hydraulic permeability values ($597 L \cdot m^{-2} \cdot h^{-1} \cdot bar^{-1}$) and thus the same membrane resistance values ($0.60 \times 10^{-12} m^{-1}$). Regarding the fouling layer resistance or cake layer resistance, R_c , the highest value is determined for the membrane fouled with humic acid at pH 6.7 and the lowest for the

membrane fouled with humic acid at pH 9.5. In the case of pH 6.7 filtration, R_c contributed 74% to the total hydraulic resistance, R_t .

In acidic pH, (pH 3) R_c contributed 65% to R_t , which is also a considerable amount. In basic pH, (pH 9.5) R_c contributed only 51% to R_t .

Figure 19 shows the evolution of normalized flux with filtration time and filtered volume during constant pressure filtration of humic acids. Greatest amount of flux decline is occurred for humic acid filtration at pH 6.7 (88%) and the lowest for filtration at pH 9.5 (53%). Many authors (Nyström *et. al*, 1998) described that the highest degree of fouling during humic acid filtration was occurred at acidic pH. Surprisingly, in our case, we found that the greatest flux decline was occurred at neutral pH (pH 6.7) and the lowest amount of fouling at pH 9.5. At acidic pH, (pH 3) the flux decline was intermediate (68%).

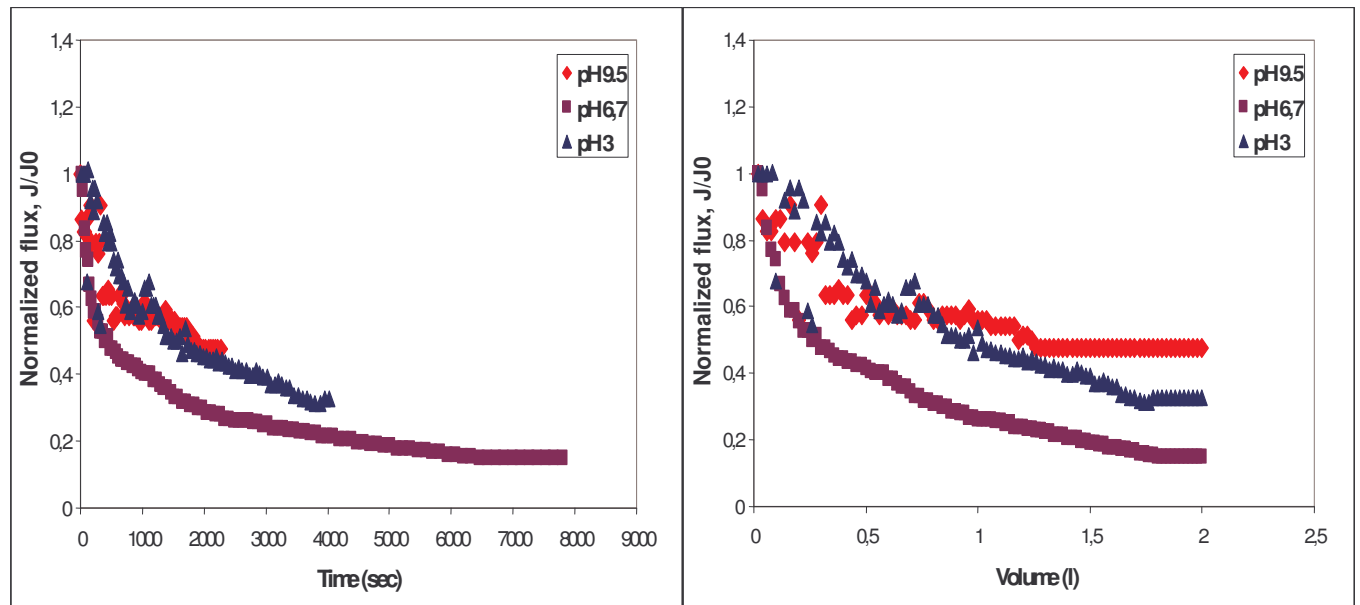


Figure 19 Normalized flux with time and Normalized flux with volume for humic acid 5 mg/L solutions at pH 3, pH 6.7 and at pH 9.5. $\Delta P = 2$ bar, $T = 20^\circ C$.

Foulant sizes may strongly affect fouling mechanisms in membrane filtration systems. If foulants have comparable or smaller sizes than the membrane pores, pore blocking may

occur. However, if the foulants are generally much larger than the membrane pores, they cannot enter the pores and a cake layer may be formed on the membrane surface.

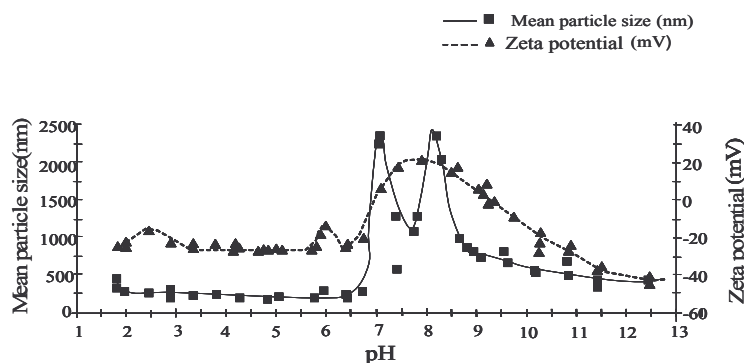


Figure 20 pH titration graph of Acros humic acid. The particle size(nm) and the zeta potential(mV) values for different pH ranges from zetasizer Malvern Co. Inc.

The YM 100 membrane is having an approximate pore diameter of 10 nm, and Acros humic acid particles are having a minimum average size of 250 nm and a maximum average size of 2500 nm (Fig.20) as determined from zetasizer experiment (Malvern corporation). Conventionally, a particle cannot pass through the pores of 100 kDa membrane in the above-mentioned pH ranges. From that an assumption is made that, the only mechanism that can increase the fouling layer resistance is cake layer formation. But to completely understand the fouling mechanisms during humic acid fouling the charge related modifications were also be taken into account.

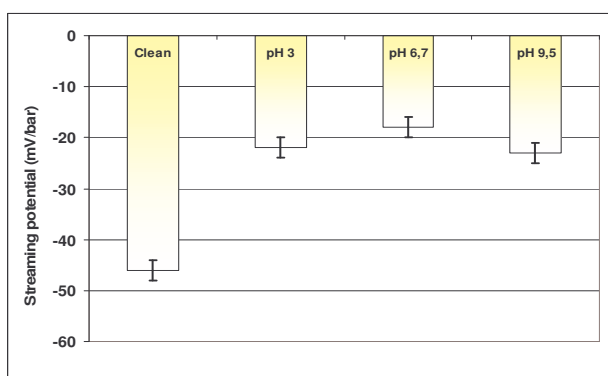


Figure 21 Streaming potential (SP) values for YM 100 membranes, before filtration with humic acid, after filtration with humic acid solutions at pH 3, pH 6.7, and pH 9.5. $[KCl] = 0.001\text{ M}$, pH 6.5 for SP measurements.

SP measurements were carried out according to Helmholtz-Smoluchovsky equation (Eqn. 7). Potential difference (mV) values with corresponding ΔP values were plotted and the slope of the curve gave directly the SP value or charge of the membrane in mV/bar. Clean regenerated cellulose membrane was having a charge of -46 mV/bar (Fig. 21). The IEP of the clean membrane was determined as 1.8 (Fig. 17). At 6.99 and 9.26 pH values, the Acrôs HA particles are having no apparent physical charge, or they are in the isoelectric point.

For a protein, flux is the lowest at the IEP and is higher as the pH is moved away from the IEP. Changes in the pH affect the solubility and confirmation of the feed components (Cheryan, 1998). In our case, greatest amount of fouling occurred at neutral pH, which can be explained by the fact that, humic acid particles were very close to their isoelectric point and hence the deposition of the humic acid particles on the surface/inside the pores were intensified due to lack of electrostatic repulsion. The charge of the membrane after fouling with humic acid at pH 6.7 became less negative (-18 mV/bar) (Fig. 21) which can also be explained by the same phenomenon. Another possible reason is that the cake layer, which formed on the active layer of the membrane, itself acted as another membrane; the global charge exerted by the electrical double layer was screened and appeared apparently less negative.

Even though we assumed that the HA particles could not enter the pores of the membrane due to steric hindrance, from the SP values we can see that lower sized fractions of humic acid particles (which are lower than the minimum average particle size) did enter the pores as reported else where (Violleau *et al.*, 2005). Hong and Elimelech, (1997) reported that the initial permeate flux decline on an NF membrane was due to the pore penetration of Suwannee River humic acid, which was further confirmed by a decrease in TOC rejection at low pH.

Modified fouling index for ultrafiltration (MFI-UF) is a parameter to analyze the particulate fouling potential of the feed solution. MFI-UF is determined from the slope of the linear portion of the t/V vs. V curve and is expressed in s/L^2 . MFI-UF is a parameter based on

cake formation mechanism. From Table 7, MFI values are the highest for pH 6.7 which is in agreement with the percentage of flux decline at the end of filtration. Thus MFI-UF parameter also underlines the fouling capacity of the humic acid solution at a pH 6.7.

The shape and conformation of the particles also change according to change in pH. At higher pH, the humic acid macromolecules are having a smaller macromolecular configuration due to the reduced inter chain electrostatic repulsion and thus they can pass easily through the membrane pores (Hong *et al.* 1997). The authors also attributed this to a lower rejection of NOM by the studied NF membrane. This phenomenon can be attributed to the 68 % flux decline at the end of the filtration at pH 3 of YM 100 membranes. With decreasing pH, more carboxylic groups of NOM become protonated, resulting in a reduction in the charge of the humic macromolecules. And as a result, the humic acid particles were increasingly adsorbed to the pores of the membrane and also caused pore plugging, which is obvious from the fouled membrane SP values.

Several studies have focused on identifying which fraction of NOM contributed the most to membrane fouling (Jucker and Clark, 1997). The general census was that the hydrophobic fraction of NOM tends to adsorb favourably on to the membrane surfaces than hydrophilic fraction. Typically, the hydrophobic nature of NOM increases with increasing molecular weight and decreasing acidity. Nilson and Digiano (1996) observed increased fouling with increased molecular weight of particles. So, in our study at pH 3, the more hydrophobic macromolecules of HA aggregates were readily adsorbed to the hydrophobic cake layer, already formed on the membrane surface, and resulted in a more compact and dense fouling layer.

All these parameters used in our study like hydraulic permeability or hydraulic resistance and flux decline with time are macroscopic parameters to describe the properties of the cake layer. For a clearer and more accurate picture, we were focused towards some microscopic parameters like fractal dimension (FD) of the surface cake from SEM images.

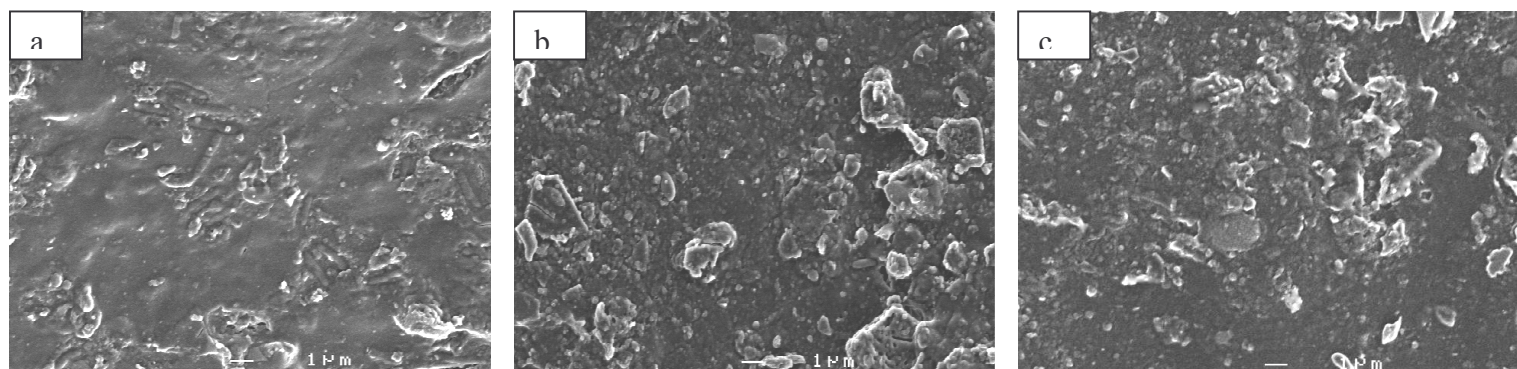


Figure 22 SEM images showing the membrane surfaces of YM 100 membranes fouled by humic acid solutions at (a) pH 6.7, (b) pH 3 and (c). pH 9.5

From the SEM images (Fig. 22), FD values of the humic acid cake formed at different pH were determined. FD values for membranes fouled by HA at pH 6.7, HA at pH 3 and HA at pH 9.5 were determined as 1.57 ± 0.01 , 1.62 ± 0.01 and 1.52 ± 0.01 respectively. A highest FD value was reported for membrane fouled by HA at pH 3 and the lowest for the membrane fouled by HA at pH 9.5. A higher value of fractal dimension indicates a lower value of permeability in the fouled state (or a dense and compact cake layer) (Aimar *et al.* 2005) and a lower value of FD indicates lower flux decline (or a loose and thin fouling layer). Meng *et al.* (2005) used fractal analysis to analyze the cake layer formed in membrane bioreactors (MBR). The authors found that a lower value of fractal dimension corresponds to a lower value of porosity or higher value of permeability which was also coherent with our results.

Most recently, a study (Li *et al.* 2008) was conducted on membrane bio-reactor (MBR) fouling and the authors concluded that biological constituents and the morphological properties of activated sludge contributed to the fouling layer resistance. They also concluded that membrane fouling resistance increased exponentially with fractal dimension values of the fouled membrane surface which is also coherent with our results.

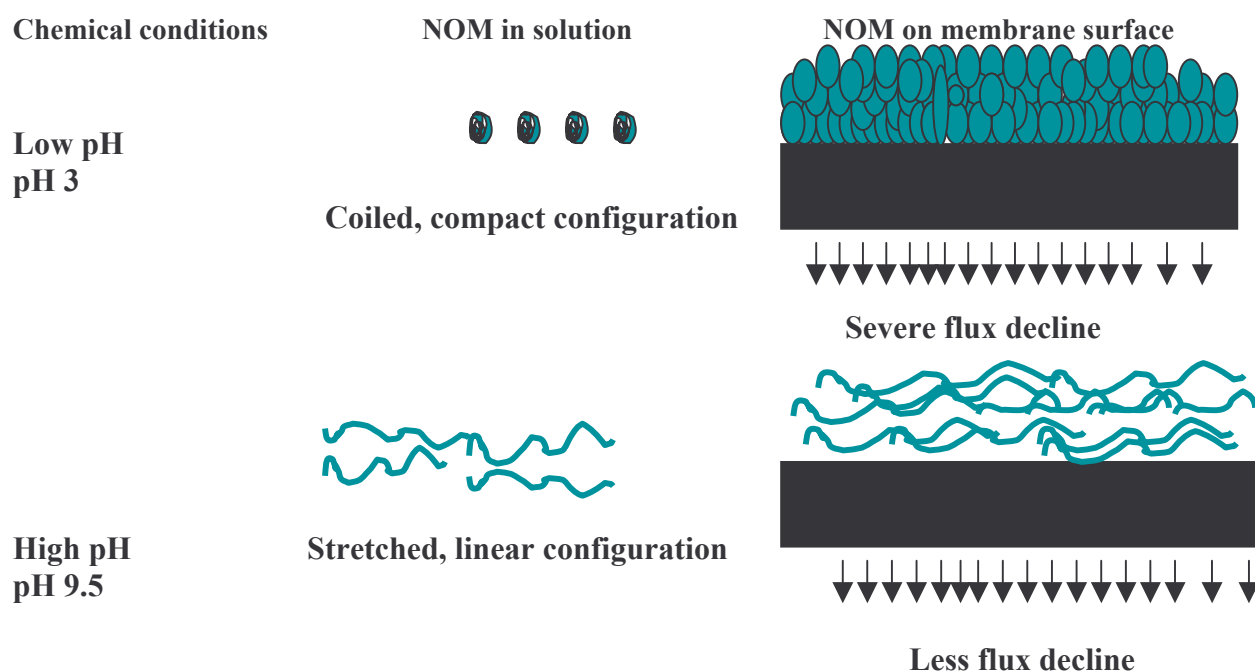


Figure 23 Schematic description of the effect of pH on the conformation of HA macromolecules in solution and on the membrane surface.

As described in Fig. 23, basic pH is favourable to minimize NOM fouling because of the presence of a thin and loosely packed fouling layer. A lower value of fractal dimension was observed for the cake formed at pH 9.5 (1.52) and a higher value of FD (1.62) was found for cake formed at pH 3 which indicated a dense cake layer. Thus fractal dimension was considered as a microscopic parameter to estimate membrane fouling.

Partial conclusion 2

Our results demonstrated that the feed solution pH greatly influences the fouling phenomena due to NOM. The highest amount of humic acid fouling on regenerated cellulose YM 100 membranes has occurred at neutral pH, then on acidic pH and the lowest amount of fouling at basic pH. Streaming potential measurements (*in situ* tool) helped us to show that humic acid particles had entered the membrane pores. This also suggests that the electrostatic double layer interactions play a very important role in the phenomenon of NOM fouling. Fractal dimension of the cake showed a relationship with permeability. A higher value of FD indicated a densely packed cake layer, and a lower value of FD indicated a loosely packed cake

layer. Thus, we have developed a new combined approach with both macroscopic and microscopic analyses, for the characterization of the humic acid cake layer. Macroscopic parameters like total hydraulic resistance, flux decline with time and modified fouling index and microscopic parameters like scanning electron microscopy and fractal dimension helped us to well characterize the fouling occurred at different pH on a regenerated cellulose UF membranes.

Role of membrane molecular weight cut-off (MWCO) on fouling

Filtration experiments were done using YM series regenerated cellulose membranes provided by Millipore, (France) with MWCO of 10, 30 and 100 kDa. These membranes are having approximate pore sizes of 1.0 ± 0.5 nm, 4 ± 1 nm and 10 ± 3 nm as obtained from the manufacturer, Millipore. Filtration was carried out with a filtration system described in Fig. 8. No stirring was employed in any of the experiments. Humic acid was purchased from Acrôs organics. Humic acid particle sizes and zeta potentials were determined at different pH ranges (Fig. 20) 5mg/L solution of humic acid was prepared in ultra pure water having conductivity less than $1\mu\text{S}/\text{cm}$. Experiments were carried out at solution pH 6.7 at constant pressure of 2 bars. The results obtained for each of the experiments are summarized in Table 8

Table 8 Permeability, resistance values, MFI values obtained during the filtration of Acros humic acid 5 mg/L at pH 6.7 with different MWCO (100 kDa, 30 kDa and 10 kDa) RC membranes

Parameters	YM 10	YM 30	YM 100
L_p clean ($\text{L}\cdot\text{m}^{-2}\cdot\text{h}^{-1}\cdot\text{bar}^{-1}$)	28 ± 3	167 ± 17	597 ± 50
L_p fouled ($\text{L}\cdot\text{m}^{-2}\cdot\text{h}^{-1}\cdot\text{bar}^{-1}$)	20 ± 2	83 ± 8	155 ± 16
Flux decline of at the end of constant pressure filtration (%)	22	59	85
$R_m \times 10^{12} \text{ m}^{-1}$	12.86 ± 0.65	2.15 ± 0.1	0.60 ± 0.03
$R_c \times 10^{12} \text{ m}^{-1}$	5.14 ± 0.25	2.19 ± 0.1	1.72 ± 0.05
$R_t \times 10^{12} \text{ m}^{-1}$	18 ± 0.9	4.34 ± 0.21	2.32 ± 0.12
MFI (s/L^2)	4585 ± 460	997 ± 175	1324 ± 135

Hydraulic permeability (L_p) coefficients are in a decreasing trend with decreasing MWCO because of the decrease in pore size. YM 100 membrane is having a L_p value 597 L.

$\text{m}^{-2} \cdot \text{h}^{-1} \cdot \text{bar}^{-1}$, YM 30 membranes with a L_p of $167 \text{ L} \cdot \text{m}^{-2} \cdot \text{h}^{-1} \cdot \text{bar}^{-1}$ and YM 10 membranes are having a L_p value of $28 \text{ L} \cdot \text{m}^{-2} \cdot \text{h}^{-1} \cdot \text{bar}^{-1}$ in the clean state. Membrane resistance, R_m , found to be increasing with decreasing MWCO.

After filtration with humic acid solution ($[\text{HA}] = 5 \text{ mg/L}$, $\text{pH} = 6.7$) at a constant pressure of 2 bars, the flux decreased 22%, 59% and 85% for 10 kDa, 30 kDa and 100 kDa respectively (Fig. 24). Hydraulic permeability of each membrane was determined with pure water after fouling with humic acid. It was found that the L_p values were decreased drastically due to fouling (Table 8).

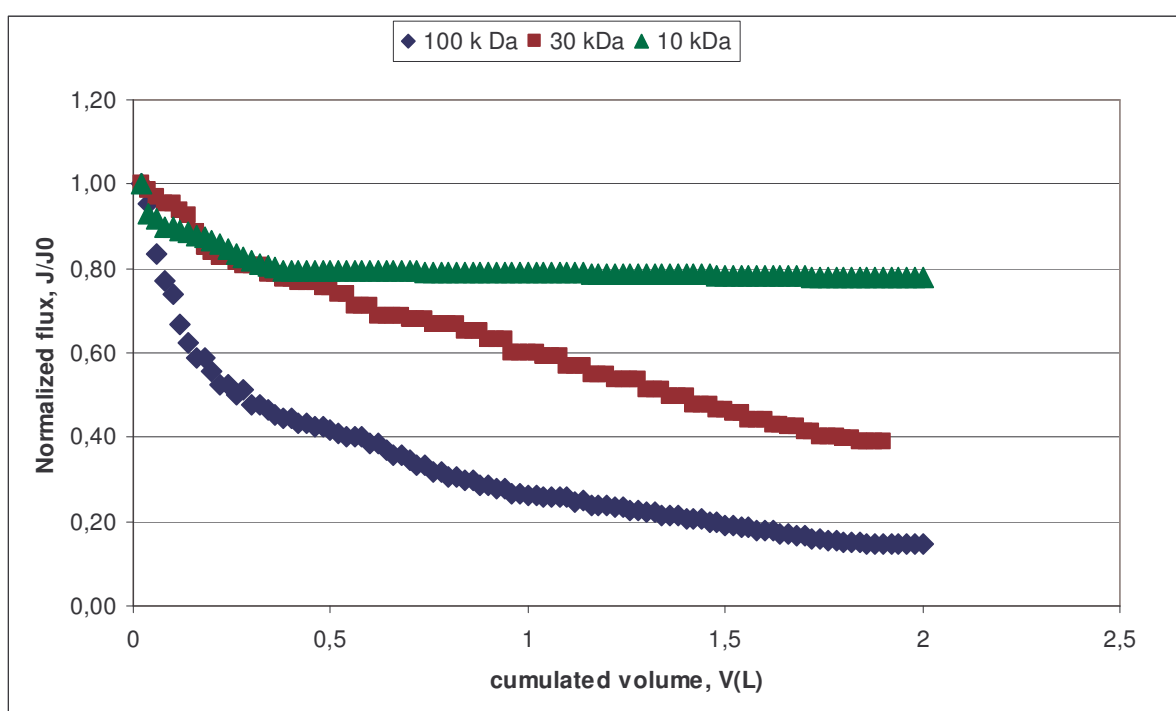


Figure 24 Normalized flux with filtration volume for the filtration of 5 mg/L humic acid solution at pH 6.7, $\Delta P = 2$ bars, $T = 20^\circ \text{C}$ for 100 kDa, 30kDa and 10kDa regenerated cellulose membranes.

After 2L of filtration with humic acid, higher MWCO membrane showed the highest flux decline, i. e, 85% for YM 100, 59% for YM 30 membrane and only 22% for the YM 10 membrane.

Fig 24 demonstrates evolution of flux with time for the three different MWCO membranes. We can see that, even though YM 100 membrane possessed a greater initial flux,

it declined so quickly and severely during the first few minutes, which can be attributed to initial concentration polarization or pore adsorption of the large aggregates to the pores. As the average size of the humic acid particles was determined as ~300 nm (Fig. 20), there is no possibility for the humic acid particles to enter the pores of all the three MWCO membranes. So the only possible mechanism which can increase total hydraulic resistance is cake formation. Researches on humic acid fouling of microfiltration membranes has suggested that the convective transport and deposition of large aggregates on the membrane surface dominated the fouling by humic substances (Yuan and Zydney, 1999 ; Jones and O'Melia, 2000)

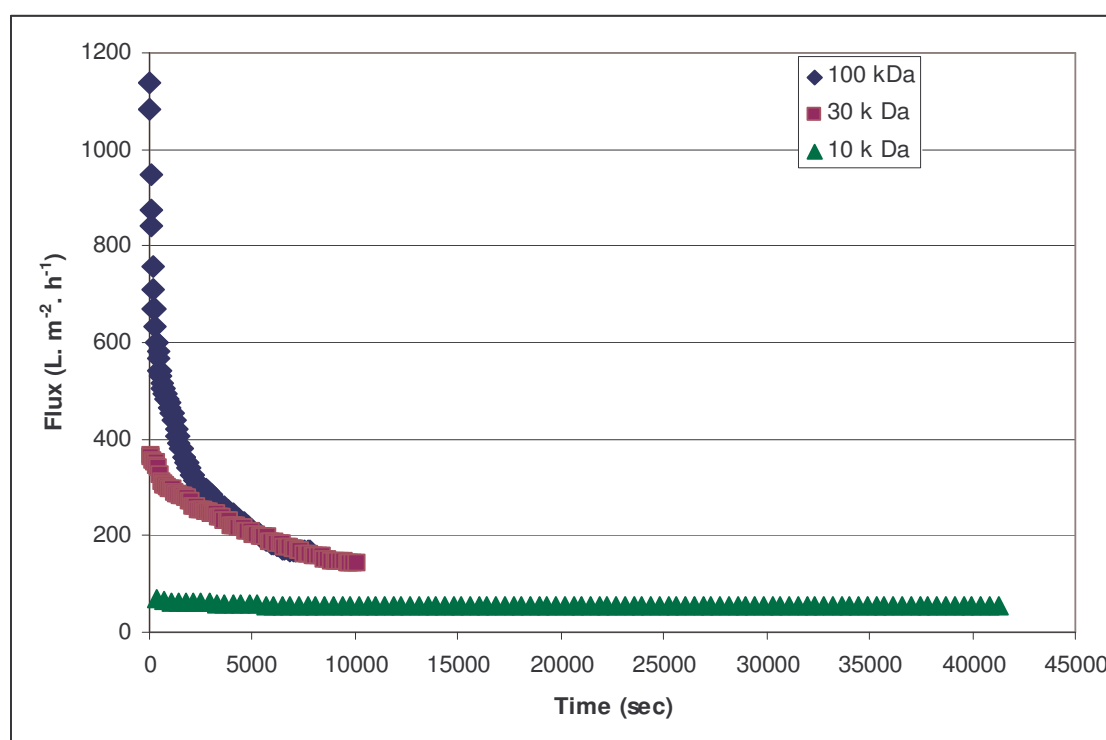


Figure 25 Evolution of flux with time for YM 100, YM 30 and YM 10 membranes during the filtration of Acrôs humic acid in a concentration of 5mg/L at a pH 6.7. $\Delta P = 2$ bars, $T = 20^{\circ}\text{C}$.

It was shown that initial fouling occurred as the result of aggregate deposition, which could catalyze subsequent fouling, even by feed solutions that had been pre-filtered to remove aggregates. (Aoustin *e. al.*, 2001) They also showed that the role of larger aggregates was shown to be less significant for smaller molecular weight cut-off membranes. So for YM 100

membranes, the initial sharp flux decline can be attributed to the deposition of large aggregates by which complete pore blockage, or pore constriction had occurred, followed by cake formation. In our study with the YM 30 membrane, the initial severe flux decline is less significantly observed comparatively to 100 kDa membrane. Flux decline from the initial value at the end of the filtration experiment was 59%. For the 10 kDa membrane, flux decline at the end of the experiment was only 22% which did not show much flux decline comparing with the other membranes.

Membrane resistance value, R_m , was found to be increasing with decreasing MWCO. Total hydraulic resistance was found to increase with decrease in MWCO. For 10 kDa, the R_m value was $12.86 \times 10^{-12} \text{ m}^{-1}$, for 30 kDa it was found to be $2.15 \times 10^{-12} \text{ m}^{-1}$ and for 100 kDa that was $0.60 \times 10^{-12} \text{ m}^{-1}$. Lower the MWCO, lower the hydraulic permeability values become, and that is the reason why we found higher membrane resistance values with lower MWCO. For 10 kDa, we determined R_c as $5.14 \times 10^{-12} \text{ m}^{-1}$, for 30 kDa it was determined as $2.19 \times 10^{-12} \text{ m}^{-1}$ and for 100 kDa it was $1.72 \times 10^{-12} \text{ m}^{-1}$. It is interesting to note that cake resistance contributed 29%, 50% and 74% to the total resistance, R_t , for 10 kDa, 30 kDa and 100 kDa membranes respectively.

From these resistance values, it is clear that fouling due to cake layer was more predominant in 100 kDa. In 30 kDa, both of the two resistance components were having equal importance. In 10 kDa, the membrane resistance was the predominant one. Lower flux indeed decreased the amount of fouling by reducing the possibility pore penetration. As suggested by Aoustin *et al.* (2001), higher flux of 100 kDa membrane could cause severe concentration polarization and membrane solute interaction, resulting in greater amount of fouling. This also demonstrates that flux is a critical parameter in membrane fouling.

To further investigate which fouling mechanism is operative, the charge related modifications on the membrane were also taken into account. Results obtained for streaming potential measurements are summarized in the Table 9.

Table 9 Experimental results of streaming potential measurements of clean and fouled membranes of YM 100, YM30 and YM 10 membranes KCl 10^{-3} M, pH 6.5, $T = 20^{\circ}\text{C}$

Streaming potential, SP (mV/bar) KCl 10^{-3} M, pH 6.5, $T = 20^{\circ}\text{C}$	10 kDa	30 kDa	100 kDa
Clean membrane	-7 ± 0.5	-17 ± 1	-46 ± 5
Fouled membrane	-6.4 ± 0.5	-18 ± 1	-18 ± 3

The results showed (Table 9) that for 10 and 30 kDa membranes there is no practical change in the SP values. For 100 kDa, there was a noticeable difference in the SP measurements between the clean and the fouled states. This further emphasizes on the fact that in 100 kDa membrane, fouling was happened due to pore penetration of lower molecular weight (smaller than the minimum average particle size) particles of humic acid. In 10 kDa and 30 kDa, because of their smaller pore size, particles are retained, which in a long run, resulted in the formation of a cake to decrease the flux.

Modified fouling index (MFI) values at constant pressure were determined from the slope of the t/V vs. V curve. The results show that MFI values increased with MWCO. Boelarge *et al.* (2000) reported that, MFI is independent of MWCO. As a Contradiction, in our results we found that MFI values depend on molecular weight cut-off of the membrane (Table 8). For 10 kDa, MFI was determined as $4585 \pm 460 \text{ s/L}^2$, for 30 kDa as $997 \pm 100 \text{ s/L}^2$ and for 100 kDa as $1324 \pm 135 \text{ s/L}^2$. MFI value also points towards the low fouling potential of the solution on YM 30 membrane. Reason for the increasing tendency of MFI value on YM 10 can be explained in terms of flux. Flux for the tighter YM 10 membrane was so low that it took more time to permeate the same volume. So the YM 10 membrane was in contact with the solution for a higher amount of time, which in turn can cause a higher adsorption of particles.

This could simply increase the cake mass and also the resistance. That is the reason why MFI value is the highest for 10 kDa membranes.

To analyze the microstructure of the humic acid cake we have done the measurement of fractal dimension (FD) of the surface cake. We have determined the fractal dimension of the fouled membranes of YM 10, YM 30 and YM 100. The FD values were determined as 1.81, 1.62 and 1.57 for YM 10, YM 30 and YM 100 membranes respectively. Fouled membranes FD values were in a decreasing trend with increasing MWCO or, in other words, fractal dimension increased with decrease in permeability as shown in Fig. 26.

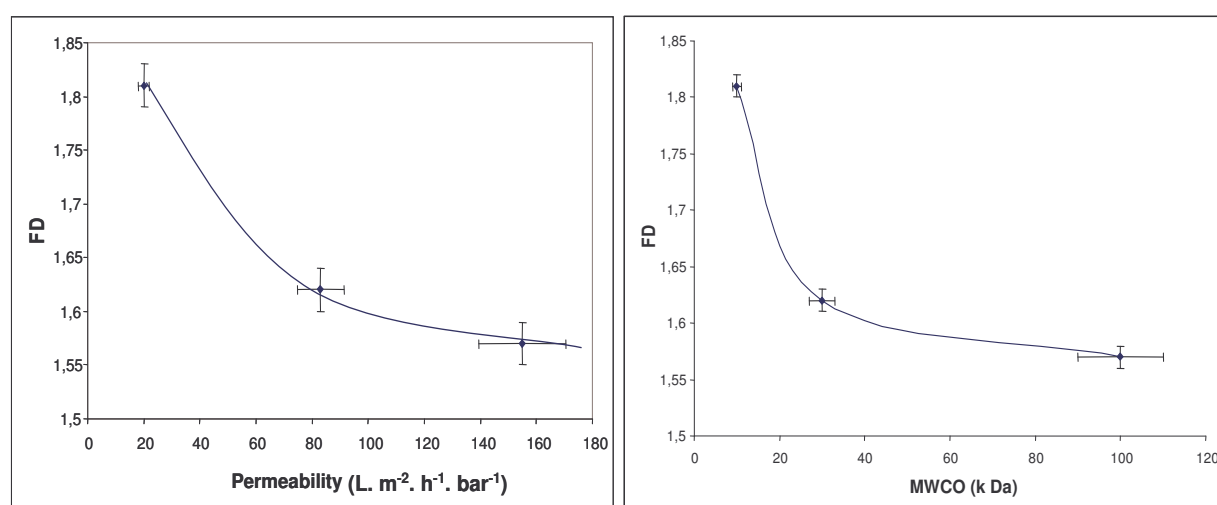


Figure 26 Evolution of fractal dimension values with fouled (membranes fouled by HA 5 mg/L at pH 6.7, $\Delta P = 2$ bars, $T = 20^\circ\text{C}$) membrane permeability values and fractal dimension variation with MWCO.

Fig. 26 shows the variation of permeability with fractal dimension and variation of FD value with MWCO. From these fractal dimension values, it can be correlated that a higher value of fractal dimension corresponds to a lower value of permeability. Meng *et al.* (2005) investigated the fouling of membrane bioreactors (MBR) due to cake formation using fractal theory (Meng *et al.* 2005, Meng *et al.* 2006). They found that fractal dimension has a linear relationship with cake porosity. According to their observations, permeability increased as FD decreased which is also coherent with our results.

To complete the analysis of the cake, SP measurements were done for the virgin and the fouled membranes. SP results showed that there is no practical difference in the global

charge of the membranes of 30 kDa and 10 kDa membranes. 100 kDa membrane showed a significant difference in the surface charge before and after fouling. Before fouling, 100 kDa membrane's charge was -46 mV/bar. Upon fouling, it has changed to -18 mV/bar. At pH 6.7, humic acid particles are closer to their isoelectric point. This can be attributed to the diminution of the total charge of the fouled membranes.

Partial conclusion 3

Humic acid fouling was studied with different MWCO membranes. It was shown that tighter membranes were less fouled compared to larger MWCO membranes. Out of the three MWCO s used in our study, the 100 kDa membrane showed the highest degree of fouling and the 10 kDa membrane showed the lowest degree of fouling. But one of the problems encountered in the 10 kDa membrane filtration was the low permeate flux. Cake resistance and the membrane resistance were equally dominant in the 30 kDa membrane. So applying proper operating conditions like trans-membrane pressure and careful selection of solution pH and ionic strength, we can produce better performance from the YM 30 membrane. Fractal dimension showed a correlation with hydraulic permeability as well as with MWCO. Thus combining macroscopic and microscopic approaches, we have characterized the humic acid cake on the membrane.

Role of trans-membrane pressure on fouling

Trans-membrane pressure is one of the very important factors that affect fouling. Regenerated cellulose 30 kDa (coded as YM 30) membranes were subjected to humic acid filtration at constant pressures of 1 bar, 2 bars and 4 bars. Acrôs humic acid solution, at a concentration of 5 mg/L at a pH 6.7 was used for the experiment. The results obtained are summarized in Table 10.

Table 10 Permeability, resistance values and MFI values obtained during humic acid filtration at different trans-membrane pressures HA Acrôs 5 mg/L, pH 6.7

Parameters	ΔP 1 bar (a)	ΔP 2 bar (b)	ΔP 4 bar (c)
L_p (L.m ⁻² .h ⁻¹ .bar ⁻¹) Clean	140 ± 15	162 ± 15	162± 15
% of flux decline	63	60	83
L_p (L.m ⁻² .h ⁻¹ .bar ⁻¹) Fouled	60 ± 5	83 ± 8	50 ± 5
$R_m \times 10^{12}$ m-1	2.57 ± 0.05	2.23 ± 0.05	2.23 ± 0.05
$R_c \times 10^{12}$ m-1	3.43 ± 0.05	2.12 ± 0.05	4.92 ± 0.05
$R_t \times 10^{12}$ m-1	6 ± 0.05	4.34 ± 0.05	7.15 ± 0.05
MFI (s/L ²)	951 ± 48	1031 ± 52	1882 ± 100

It can be seen that the pure water flux after fouling is the highest for filtration at constant pressure of 2 bars (in column b) and that the lowest for filtration at a constant pressure of 4 bars. For filtration at constant pressure of 1 bar the flux is intermediate. From the table given above, we can see that after filtration at constant pressure of 4 bar, the pure water permeability has decreased from 162 L. m⁻². h⁻¹. bar⁻¹ to 50 L. m⁻². h⁻¹. bar⁻¹. In the study of 2 bars constant pressure filtration, the pure water permeability decreased from 162 L. m⁻². h⁻¹. bar⁻¹ to 83 L. m⁻². h⁻¹. bar⁻¹. For 1 bar constant pressure filtration, it decreased to 60 L. m⁻². h⁻¹. bar⁻¹ from 140 L. m⁻². h⁻¹. bar⁻¹.

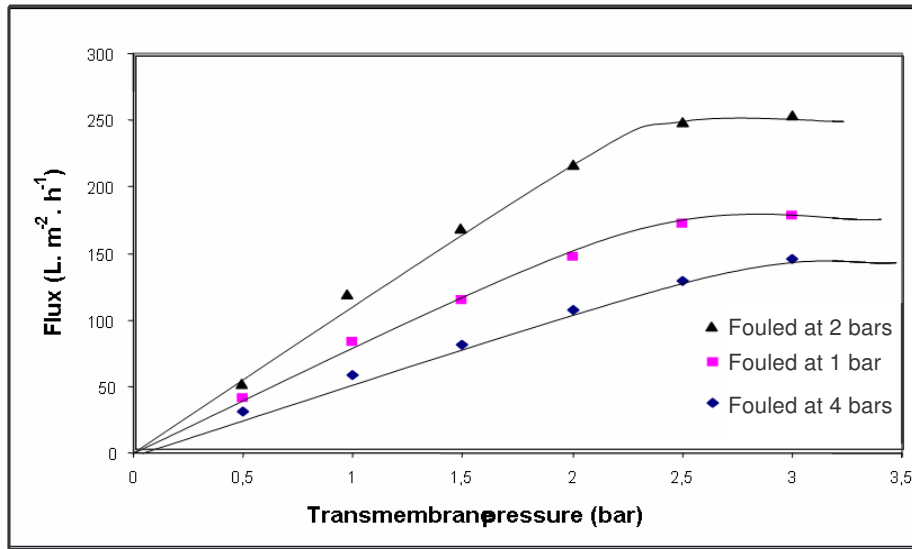


Figure 27 Evolution of pure water flux with trans-membrane pressure for membranes fouled with humic acid Acrôs 5mg/L, at pH 6.7(a) after filtration with HA at constant pressure of 2 bars (b) after filtration with HA at constant pressure of 1 bar (c) after filtration with HA at constant pressure of 4 bar

Fig. 27 shows the measurement of pure water permeability values after fouling. Observing the curves of Fig. 27, we can see that there is a region which is pressure dependent and another region which is independent of pressure. Up to 2.5 bars the flux depends on pressure. Starting from 2.5 bars, the value of flux becomes independent of the trans-membrane pressure. Flux reaches a limiting value known as limiting flux. Limiting flux is the highest for membrane fouled at 2 bars constant pressure and the lowest for membrane fouled at 4 bars constant pressure.

Analyzing the resistance values (Table 10), we can see that, the intrinsic membrane resistance, R_m is similar for all the clean membranes because the pure water permeability values for each membrane were similar. In the case of fouling layer resistance or cake layer resistance, R_c , the value obtained after 4 bar constant pressure filtration is the highest which indicates greatest extent of fouling due to humic acid. The R_c value obtained after 4 bar constant pressure filtration is $4.92 \times 10^{-12} \text{ m}^{-1}$, that for 2 bar constant pressure filtration is $2.12 \times 10^{-12} \text{ m}^{-1}$ and that for 1 bar constant pressure filtration is $2.57 \times 10^{-12} \text{ m}^{-1}$. These values indicate that the fouling caused by humic acid at 4 bars is the highest and that at 2 bars is the

lowest. Moreover, R_c contributed 57%, 49 % and 69% and to the total resistance, R_t in the cases of 1 bar constant pressure filtration, 2 bars constant pressure filtration and 4 bars constant pressure filtration respectively. This also underlines the dominance of cake resistance in 4 bars constant pressure filtration which caused the greatest amount of fouling.

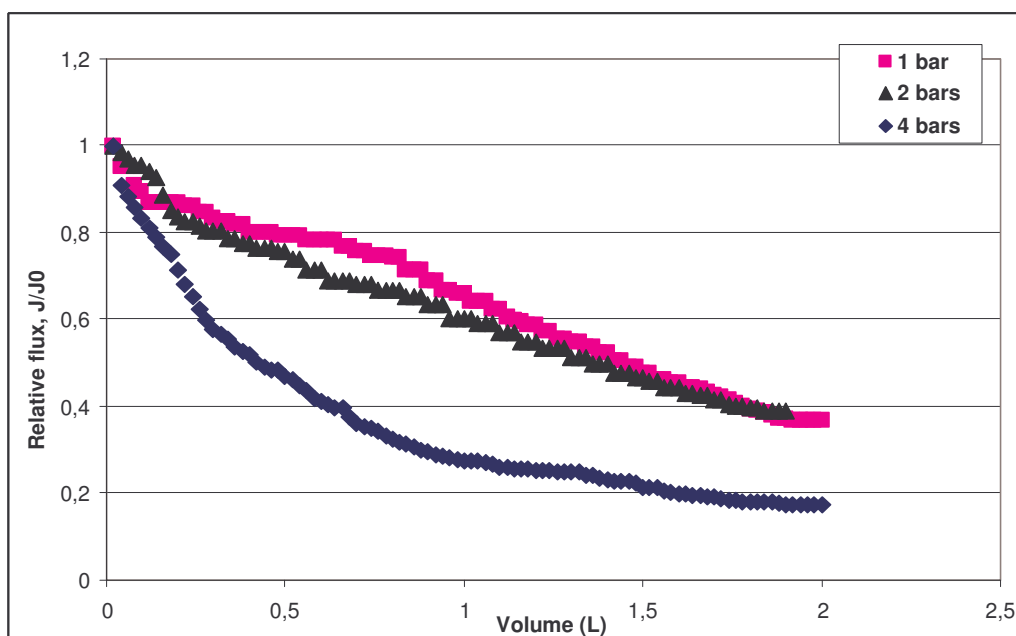


Figure 28 Evolution of normalized flux with filtration volume during humic acid filtration through YM30 membranes at constant pressure of 1bar, 2 bars and 4 bars. $[HA] = 5 \text{ mg/L}$; $pH = 6.7$ $T = 20^\circ \text{ C}$.

Fig. 28 shows the evolution of normalized flux with filtration volume during filtration of Acros humic acid at constant pressures of 1 bar, 2 bars and 4 bars. From the curves, we can observe that the flux decrease is the highest during 4 bar constant pressure filtration. For 2 bars and 1 bar, flux decline at the end of the experiment was practically the same. At the end of 4 bars constant pressure filtration, the flux decreased 83% and at the end of 1 bar and 2 bars it showed a flux decline of 63% and 60% respectively. Combining this fact with the resistance values, we can say that the highest amount of fouling happened at 4 bars constant pressure filtration, and the lowest at 2 bars constant pressure filtration. As the pressure increases, the cake resistance, which is directly connected to the specific cake resistance, α increases, which explains the highest fouling, caused during the filtration of HA solution at a constant pressure

of 4 bars (Eqn 3). An empirical relationship often applied to account for trans-membrane pressure is Eqn 3 which relates specific cake resistance, α to trans-membrane pressure to the power of a compressibility coefficient (n) and a constant α_0 .

Modified fouling index, a parameter which gives information about the particulate fouling potential of the solution was used in our study. From Table 7, it was found that MFI increases with increase in pressure. Boelarge *et al.* (1998) analyzed the pressure dependence of MFI and found that the fouling index, I , in the MFI-UF equation is dependent on pressure. Boelarge *et al.* found that a higher applied pressure gave a higher MFI value, which is also coherent with our results. Thus, a higher MFI-UF value at 4 bar filtration furthermore emphasizes the severe fouling happened during filtration.

In the equation of MFI (Eqn 5 and Eqn. 6), the term fouling index, I is directly proportional to the specific resistance of the cake, α and the particle concentration C_b . So, we have determined the factor of compressibility (n) from MFI (which is directly related to α) and different trans-membrane pressure values. For incompressible cakes, n is zero and the higher the value of n , the more compressible the cake. In our case, the value of n was determined as 0.49 (results not shown), i. e, the cake is compressible.

High pressure indeed increased the possibility of pore penetration. To understand completely the fouling mechanism undergoing, the charge and size of the particles were also taken into account. Foulant sizes may strongly affect fouling mechanisms in membrane filtration systems. If foulants have comparable or smaller sizes than the membrane pores, pore blocking may occur. However, if the foulants are generally much larger than that of the membrane pores, they cannot enter the pores and a cake layer may be formed on the membrane surface. In our case, the YM30 membrane is having a pore diameter ~ 4 nm and the particles of humic acid in solution is having an average size of 300 nm at pH 6.7. Conventionally, a particle cannot pass through the pores of 30 kDa membrane at this specific pH. From that we assume

that the only mechanism that can induce fouling could be cake layer formation. But to understand it completely the charge related modifications should also be taken into account. To understand the charge related modifications, we have carried out the streaming potential measurements.

Table 11 Experimental results of streaming potential measurements of clean and fouled membranes of YM30 membranes

Streaming potential, SP (mV/bar) KCl 10^{-3} M, pH 6.5, T = 20° C	ΔP 1 bar	ΔP 2 bars	ΔP 4 bars
Clean YM 30	-15 ± 1	-17 ± 1	-18 ± 1
Fouled YM 30	-14 ± 0.5	-18 ± 1	-13 ± 0.5

Streaming potential measurement was carried out in the trans-membrane pressure range of 0.5 to 3 bars, with 0.001 M KCl at a pH of 6.5. Streaming potential coefficients, determined from $\Delta\phi$ versus ΔP curves are summarized in Table 11. For fouled membranes after 1 and 2 bars constant pressure filtration, no practical difference in SP values was observed. But after 4 bars constant pressure filtration, the SP values of the membrane has changed from -17 mV/bar to -13 mV/bar in between the clean and the fouled states. The humic acid particles at pH 6.7 are having a zeta potential of -20 mV (Figure 20) and the resulting charge on the membrane should be more negative. But the global charge of the membrane has become less negative. This can be explained by the fact that at 50 mg/L, due to the fact that the dense cake layer formed on the membrane, itself acted as another membrane and totally screened the potential exerted by the electrical double layer. Thus the total charge appeared less negative.

SEM images of the fouled surface cake were analyzed using an image analyzer called *Image J*. From the original image, a threshold (binary) image is generated with the help of the software. Fractal box count method is applied to calculate the two dimensional fractal

dimension (FD). The FD values for 1 bar, 2 bars and 4 bars constant pressure filtration were determined as 1.70, 1.62 and 1.84 respectively. Aimar *et al.* (2005) reported that in dead end filtration, a higher value of fractal dimension corresponds to a lower value of permeability or higher value of hydraulic resistance.

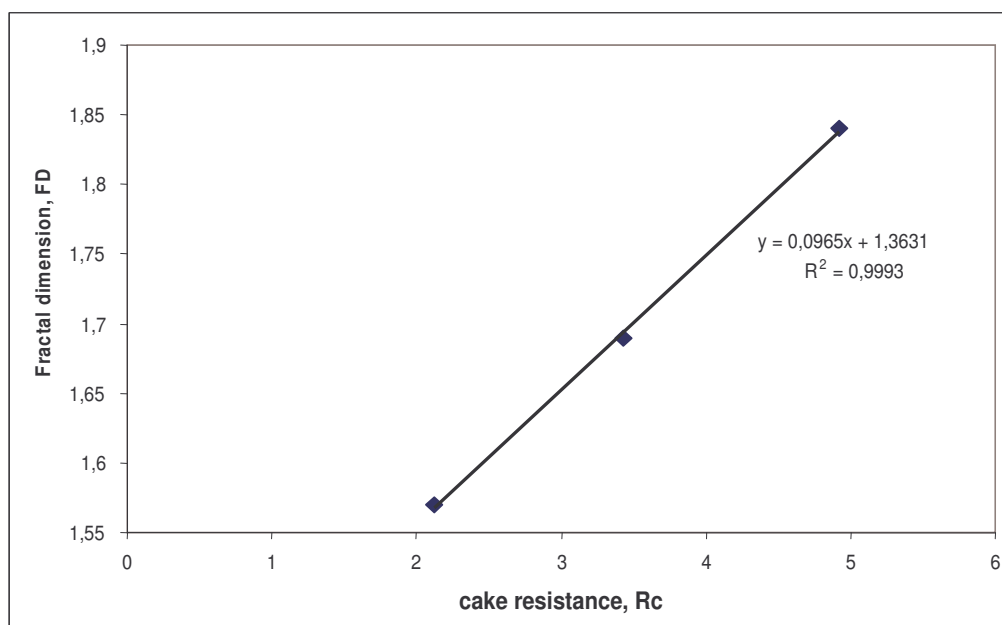


Figure 29 Evolution of fractal dimension with cake layer resistance. Membranes fouled with 5 mg/L solution of Acrôs humic acid at pH 6.7. Filtration was carried out in three different trans-membrane pressure, 1 bar, 2 bar and 4 bar at 20 °C.

Figure 29 shows linearity of resistance values with fractal dimension. Thus fractal dimension can be used as a new approach to analyze fouling and cake formation. A higher value of fractal dimension represents a lower value of permeability for a humic acid cake.

Partial conclusion 4

Fouling experiments with Acrôs humic acid at different trans-membrane pressures were carried out. It was found that the highest degree of fouling was happened at 4 bars and the lowest degree of fouling was caused at 2 bars. In all the three trans-membrane pressures, cake formation was the dominant fouling mechanism. But in the case of 4 bar constant pressure filtration, some extend of pore penetration was also happened which is confirmed from the SP

values. MFI values were found to be increasing with trans-membrane pressure which also confirmed the higher extent of fouling occurred at 4 bar. FD values of fouled cake surfaces showed a linear relation with cake resistance, R_c .

Role of humic acid concentration on fouling

Filtration of humic acid was carried out in three different concentrations, 5mg/L, 10 mg/L and 50 mg/L. Membranes used was regenerated cellulose flat-sheet type having a molecular weight 30 k Da (YM30). Humic acid solutions (Acrôs) were prepared in ultra pure water with concentrations of 5 mg/L, 10 mg/L and 50 mg/L at a pH 6.7. Filtrations were carried in Non-stirred mode in an Amicon 8200 model cell which has a capacity of 200 ml and a diameter of 63.5 mm. All experiments were done at room temperature (20° C). The results are reported in the Table 12.

Table 12 Permeability, resistance values and MFI values obtained during the filtration of humic acid solutions at pH 6.7, different concentrations, 5 mg/L, 10 mg/L and 50 mg/L. $\Delta P = 2$ bars, 30k Da Regenerated cellulose membranes (YM 30)

Parameters	5 mg/L	10 mg/L	50 mg/L
Lp clean ($\text{L.m}^{-2}.\text{h}^{-1}.\text{bar}^{-1}$)	167 \pm 17	167 \pm 17	167 \pm 17
Lp fouled ($\text{L.m}^{-2}.\text{h}^{-1}.\text{bar}^{-1}$)	83 \pm 8	35 \pm 3	27 \pm 3
Flux decline at the end of constant pressure filtration (%)	59	76	94
$R_m \times 10^{12} \text{ m}^{-1}$	2.15 \pm 0.1	2.15 \pm 0.1	2.15 \pm 0.1
$R_c \times 10^{12} \text{ m}^{-1}$	2.19 \pm 0.1	8.44 \pm 0.43	11.19 \pm 0.56
$R_t \times 10^{12} \text{ m}^{-1}$	4.34 \pm 0.2	10.59 \pm 0.59	13.34 \pm 0.67
MFI (s/L^2)	997 \pm 100	2749 \pm 300	4086 \pm 400

Hydraulic permeability values were found to be the same (167 $\text{L.m}^{-2}.\text{h}^{-1}.\text{bar}^{-1}$) for all the YM 30 membranes and hence the same membrane resistance ($2.15 \times 10^{-12} \text{ m}^{-1}$) values. Cake resistance values were in an increasing trend with increasing concentration of humic acid. As the concentration of humic acid increases, the total mass of the cake on the membrane

increases. Thus the specific resistance of the cake increases which depends on the concentration of particles. Increase in the fouling layer resistance can be attributed to increase in the concentration of humic acid particles. For 5mg/L the cake layer resistance, R_c was only $2.19 \times 10^{-12} \text{ m}^{-1}$ (50% total hydraulic resistance, R_t) and when the concentration was increased to 10 mg/L, R_c increased to $8.44 \times 10^{-12} \text{ m}^{-1}$ (79% of R_t). When the concentration was again increased to 50 mg/L, cake resistance increased to $11.19 \times 10^{-12} \text{ m}^{-1}$ (84% of R_t). Clearly, it demonstrates that the cake layer resistance is dependant on particle concentration.

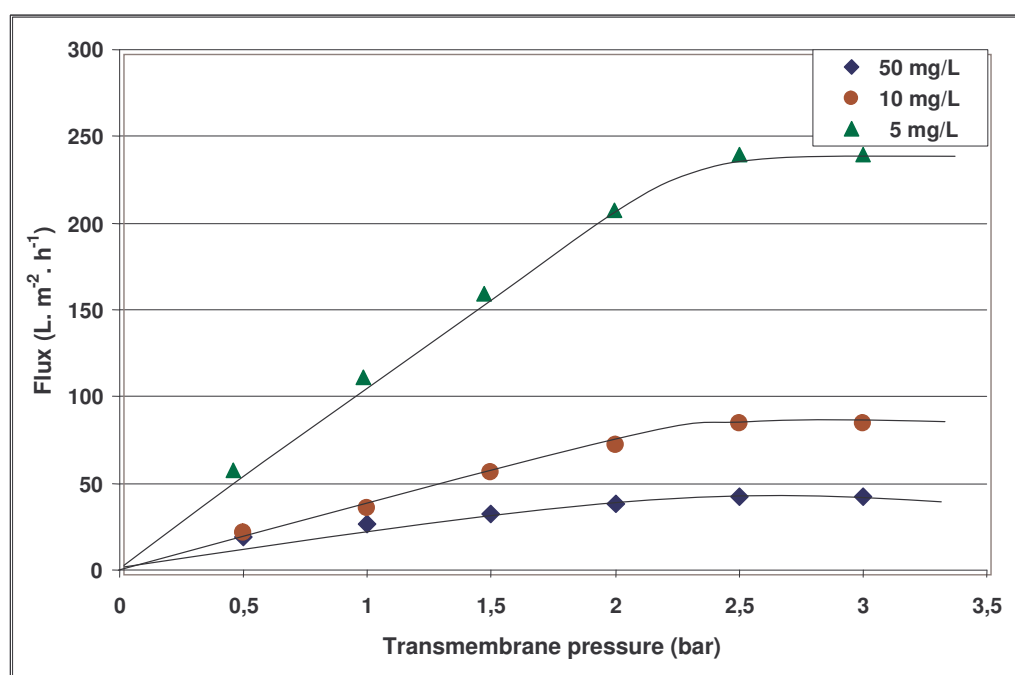


Figure 30 Variation of pure water flux with trans-membrane pressure for 30 kDa YM 30 membranes, after filtration with different concentration of Acros humic acid (5 mg/L, 10 mg/L, 50 mg/L) at pH 6.7, $\Delta P = 2 \text{ bar}$, $T = 20^\circ \text{C}$

Fig 30 shows the pure water flux after fouling for each concentration of humic acid. Regarding the limiting flux (value of flux from which permeation is independent of trans-membrane pressure) values, it can be seen that up to, $\Delta P = 2.5 \text{ bar}$, flux depends on pressure. From 2.5 bars onwards, even on an increment of pressure, flux remained the same. The flux was limited because of the formation of the cake and fouling. Limiting flux for fouled membrane after 5 mg/L solution filtration was found to be $240 \text{ L.m}^{-2}.\text{h}^{-1}$, that for membrane fouled with 10 mg/L solution was found to be $85 \text{ L.m}^{-2}.\text{h}^{-1}$ and that for membrane fouled with

50 mg/L solution was determined as $42 \text{ L} \cdot \text{m}^{-2} \cdot \text{h}^{-1}$. This underlines the fact that increase in concentration of particles will increase fouling.

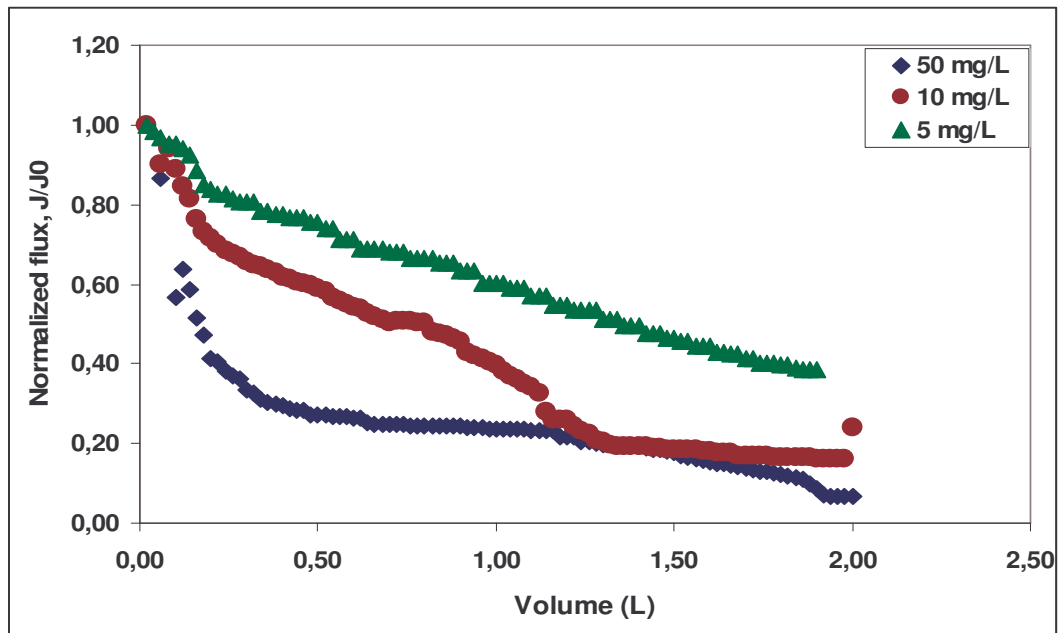


Figure 31 Normalized flux with filtration volume during the filtration of 5 mg/L, 10 mg/L and 50 mg/L concentrations of Acros humic acid solutions at pH 6.7, $\Delta P = 2$ bars, $T = 20^\circ \text{C}$ for 30kDa regenerated cellulose membranes.

Fig 31 shows the normalized fluxes with cumulated volume during the filtration of humic acid in three different concentrations. Flux reduction was the highest for 50 mg/L solution, followed by 10 mg/L solution and the least flux reduction was found for 5 mg/L solution of humic acid. At the end of 50 mg/L humic acid filtration, flux reduction was 94%, which can be attributed to a dense humic acid cake layer. After 10 mg/L filtration, the flux declined to 76% from the initial value. After filtration with 5mg/L solution, flux reduced to 59% from the initial value. Each time, same volume of solution was filtered through each membrane.

As the concentration of the solution increases, the specific cake resistance of the cake, which depends on the total mass of the cake, is also increased. Fractal dimension of the surface of the membrane after fouling with 50 mg/L humic acid was determined as 1.90. A higher value of fractal dimension points towards a thick and dense cake layer with very less porosity. Fractal dimension for 10 mg/L was determined as 1.72 which is also a dense cake,

but more porous than the cake formed after filtration with 50 mg/L solution. For 5 mg/L, FD value was found to be 1.62 which is comparatively lower than the above mentioned FD values. This means that the cake formed after filtration with 5 mg/L was comparatively more permeable. Meng *et al.* (2005) reported similar results for membrane bio reactors (MBR). The authors reported that cake formed on the surface of a membrane is having fractal nature with a fractal dimension in the range of 1.975 to 1.995. The authors explained that as the fractal dimension value increases it indicates a less permeable or less porous cake. They have also correlated cake resistance with fractal dimension. In our study, we found that cake resistance increases with increase in fractal dimension which also corresponds to decrease in permeability. Thus it also shows that fractal dimension may be a useful parameter to describe cake permeability.

Modified fouling index is a parameter which depends purely on cake formation mechanism (Schipper *et al.*, 1980). It is determined from the slope of the linear portion of t/V with V curve as shown in the following figure.

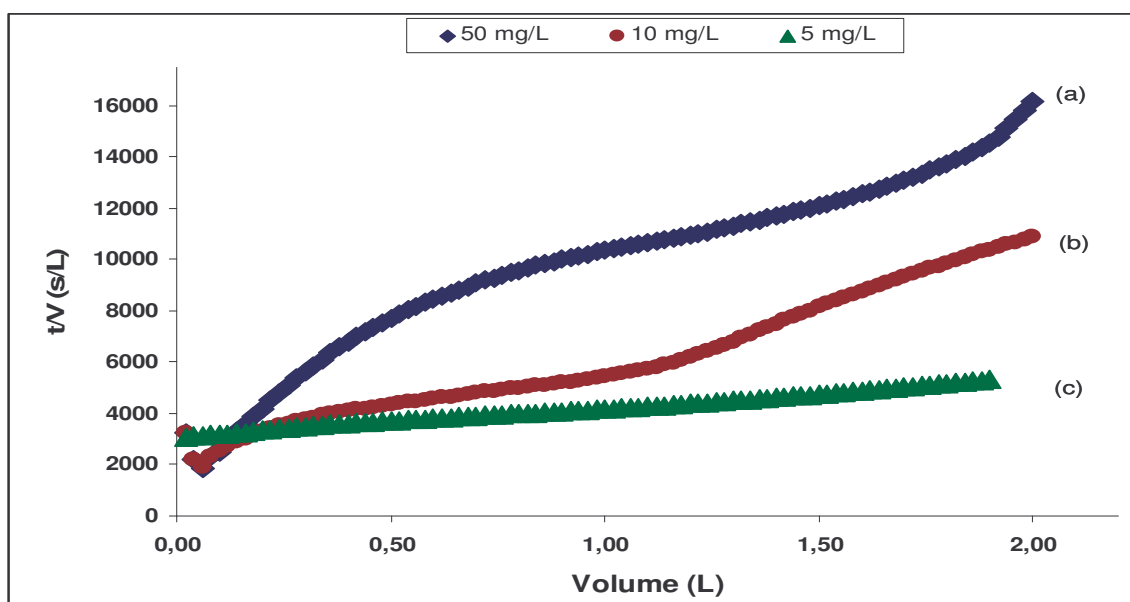


Figure 32 Evolution of t/V with V during the filtration of Acros humic acid solutions at pH 6.7 in different concentrations (a) 50 mg/L, (b) 10 mg/L and (c) 5 mg/L ; $\Delta P = 2$ bar, $T = 20^\circ$

Observing the curves Fig 32, we can see that for (a) 50 mg/L, there are three distinct portions, of which the first one corresponds to adsorption of particles to the membrane surface, the second one to cake formation and the third one to cake compaction or cake clogging. Boelarge *et al.* (S. F. E. Boelarge *et al.*, 1998) reported that MFI-UF value has a linear relationship with particle concentration. The MFI value determined for 50 mg/L was 4086 s/L². For 10 mg/L, the MFI value obtained was 2479 s/L² and for 5 mg/L, it was 997 s/L². The lower value of MFI for 5 mg/L indicates the lower fouling potential of the solution and the higher value of MFI for 50 mg/L, indicates the highest fouling potential of the solution.

Streaming potential measurements helped us to analyze the charge related modifications of the cake (Table 13). Clean membrane had a SP of -17 mV/bar. When it was fouled by 5 mg/L, the charge remained practically the same. But when it was fouled by 10 mg/L solution of HA and 50 mg/L solution of HA, the SP values had changed to -10mV/bar and -11 mV/bar respectively. This can be attributed to the dense cake formed on the membrane surface. The cake itself acted as another membrane due to the high rejection of organic matter, and screened the charge exerted by the electrical double layer on the shear plane.

Table 13 Streaming potential values for clean and fouled (by 5 mg/L, 10 mg/L and 50 mg/L solutions of Ha at pH 6.7) YM 30 membranes. KCl = 0.001 M, pH 6.5, T = 20 ° C.

Membrane	SP (mV/bar) KCl = 0.001 M, pH 6.5, T =20 ° C
Clean YM 30	-17 ± 2
Fouled by 5 mg/L HA	-17.5 ± 2
Fouled by 10 mg/L HA	-10 ± 1
Fouled by 50 mg/L HA	-11 ± 1

Partial conclusion 5

From this study with different concentration of humic acid solution, we have found that as the concentration of the solute increased, membrane solute interactions were also increased, or in other words fouling was also intensified. Flux decline with time, cake resistance and modified fouling index found to increase with increase in solute concentration. Fractal dimension values were also in an increasing trend with increase in solute concentration, which indicated a dense humic acid cake. Thus, in this study we have combined macroscopic parameters like hydraulic permeability or hydraulic resistance, modified fouling index and microscopic parameters like fractal dimension to characterize the humic acid cake formed on a membrane of ultrafiltration. Streaming potential measurement which is an in-situ parameter helped us to study the membrane-solute interactions more effectively. Thus our work provides a new approach to study cake properties and cake formation mechanism.

D- PERSPECTIVES

Pre-treatment to minimize NOM fouling

To minimize the effect of humic acid fouling we have done adsorption with a naturally occurring clay, namely montmorillonite (or bentonite). Membrane used was 100 kDa RC (YM 100). To 5 mg/L solution of bentonite, 2g/L concentration of modified bentonite (mont-Al-CTAB) (Zermane *et al.* 2005, Naceur *et al.* 2004) was added and stirred for 3 hrs to reach equilibrium. To compare the effect of adsorption, flux vs. time graph was plotted as shown in Fig.28.

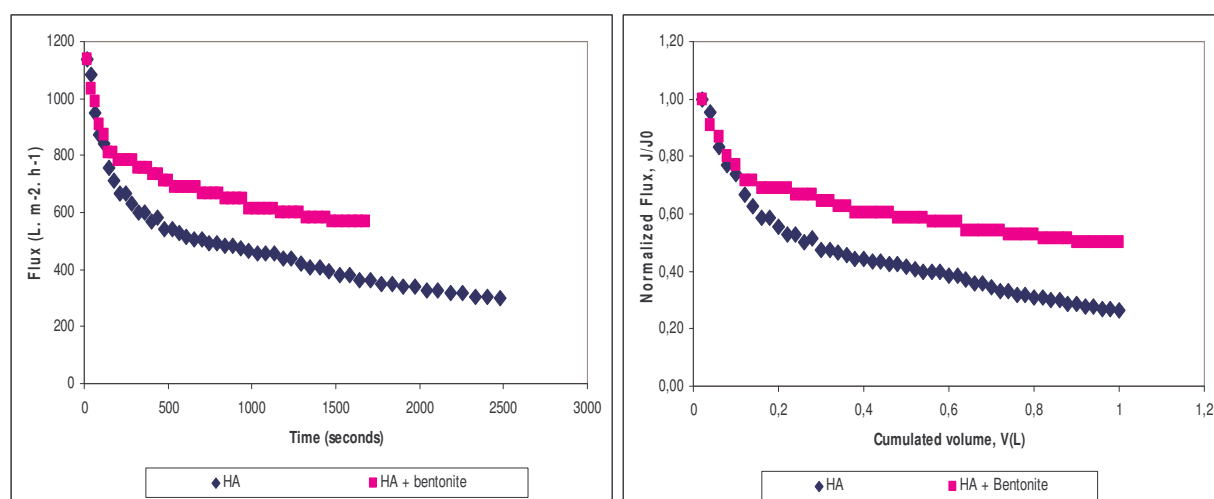


Figure 33 Evolution of flux with time and normalized flux with filtration volume during the filtration of humic acid and humic acid + bentonite suspension. pH of humic acid 6.7, $\Delta P = 2$ bar, $T = 20$ °C.

Fig. 33 shows the normalized flux with time and normalized flux with filtration volume both for HA alone and HA+bentonite. It can be seen that, solution of humic acid alone has caused more flux decline than HA+bentonite suspension. This can be attributed to the formation of complexes by humic acid particles with the inorganic groups (metal ions) present in bentonite. With humic acid alone, the flux decline was 75%. But with HA+bentonite suspension, the flux decline was found to be 50%. The 50% flux decline occurred during the filtration of HA +bentonite can be attributed to metal ion -HA complex adsorption to the membrane surface (Naceur *et al.* 2004, Cheknane *et al.* 2006)).

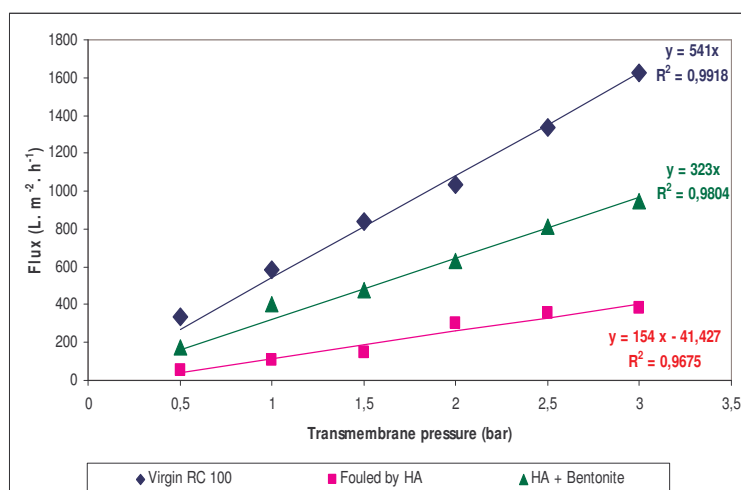


Figure 34 Evolution of pure water flux with trans-membrane pressure for virgin RC 100 membrane, membrane fouled by HA (Acros 5mg/L, pH 6.7, $\Delta P = 2$ bar $T = 20^{\circ}\text{C}$) and HA+bentonite(mont-Al-CTAB 2g/L) suspension.

The hydraulic permeability values obtained after filtration with HA + bentonite was found to be greater than that obtained for HA alone (Fig. 34). From this, following the resistance model, the resistances were calculated. R_m was found to be $0.67 \times 10^{12} \text{ m}^{-1}$ and after R_c for humic acid cake alone was found to be $1.67 \times 10^{12} \text{ m}^{-1}$. But the value of $R_{\text{bentonite}}$ was found to be $0.45 \times 10^{12} \text{ m}^{-1}$. Thus in HA+ bentonite filtration, the total hydraulic resistance was found to be lower than that due to HA alone, $R_{\text{bentonite}}$ was found even lower than the membrane resistance.

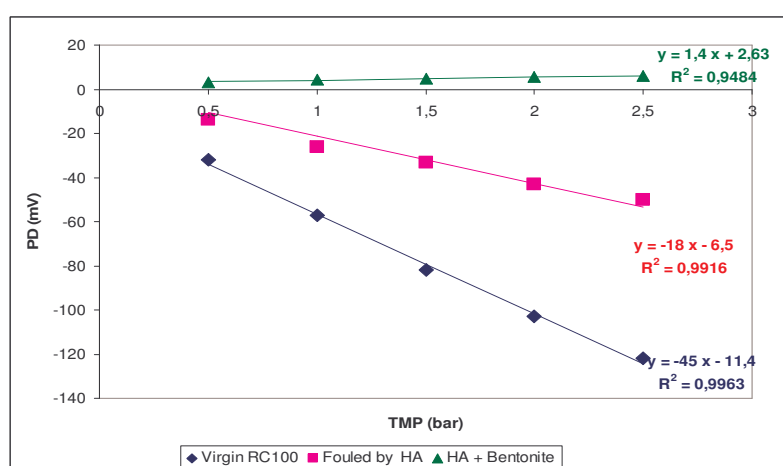


Figure 35 Evolution of potential difference (mV) with trans-membrane pressure (bar) for virgin membrane, membrane fouled by HA (Acros 5 mg/L, pH - .7, $\Delta P = 2$ bar, $T = 20^{\circ}\text{C}$) and HA+ bentonite (mont-Al₁₃-CTAB 2g/L) Electrolyte KCL 0.001M, pH 6.5.

Charge related modifications were analysed with the help of SP as shown in Fig 35. For the virgin membrane, the charge was determined as -45 mV/bar. When it was fouled by HA, the charge was changed to -18 mV/bar. But when it was filtered with HA+ bentonite, the global charge of the membrane has become positive. This can be attributed to the inorganic groups present in bentonite (Al^{3+} , Ca^{2+} , Mg^{2+} , SiO_2 etc) which formed complexes with HA particles and changed the total charge carried by the membrane.

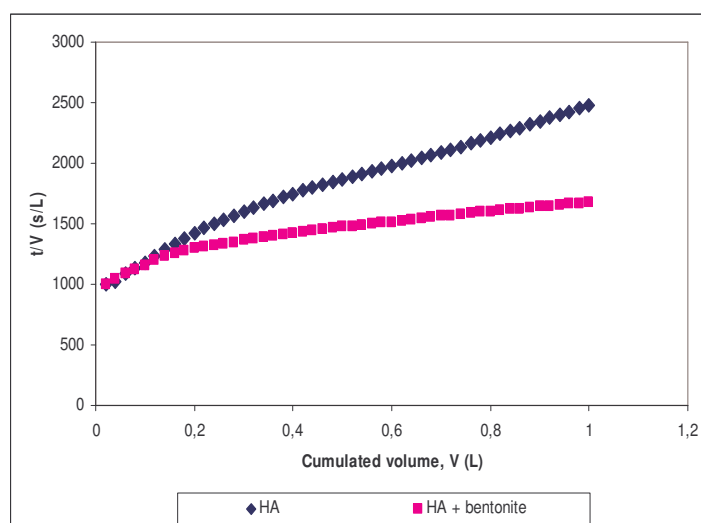


Figure 36 Evolution of t/V with V for the determination of MFI-UF. $[\text{HA}] = 5\text{mg/L}$, $\text{pH} = 6.7$, $\Delta P = 2$ bar, $[\text{mont-Al}_{13} \text{ CTAB}] = 2\text{g/L}$

Modified fouling index (MFI-UF) was determined with HA alone and with HA+bentonite (Fig 36). The value of MFI-UF for HA alone was found to be $1358 \pm 140 \text{ s/L}^2$ for HA alone and that for HA+bentonite was found to be $594 \pm 60 \text{ s/L}^2$. This indicated that for HA+bentonite system, the particulate fouling potential of the feed was lowered. This can be attributed to the lowering of specific resistance of the cake, α , which was further confirmed by a lowering of R_c in presence of bentonite.

Partial conclusion 6

Filtration of humic acid alone and HA+ bentonite suspension at a constant trans-membrane pressure of 2 bar was conducted in order to study the pre-treatment efficiency of bentonite. It was shown that in presence of bentonite, the cake resistance have considerably reduced comparing to the value of cake resistance inpresence of HA alone. In the case of HA, cake resistance was the dominant factor of the total resistance, but with HA + bentonite, cake resistance was found to be even lower than the membrane resistance, R_m . This result opens interesting perspectives to the utilization of UF coupled with bentonite for the elimination of NOM from sea water before passing to RO desalination.

AWWARF project (CONFIDENTIAL RESULTS)

The second part of the perspectives of our work deals with “Natural Organic Matter Fouling of Low Pressure Membrane Systems”. This work was included in a project (RFP n° 2952) of the AWWARF (American Water Work Association and Research Foundation), with the Principal Investigator: James C. Lozier (P.E. CH2M HILL) and the Co-Principal Investigators were Gary Amy, (University of Colorado, USA) and J.P. Croué (Poitiers University, France) and M. Pontié (Angers university, France).

In this study we analyzed three UF membranes in the form of hollow fibers : A, hydronautics Polyethersulfone (PES) UF membrane; B, Zenon Polyvinylidene fluoride (PVDF) UF membrane; C, Norit (PES) UF membrane. We conducted SEM, contact angle, and SP experiments before and after fouling with natural water in order to determine morphology aspects of the surface, FD, hydrophilicity of the surface and the charge and the IEP of the membranes before and after fouling.

FESEM analysis results

Hollow fibres were cut into three different pieces in order to observe external surface, internal surface and the transverse section as shown in Fig. 37.

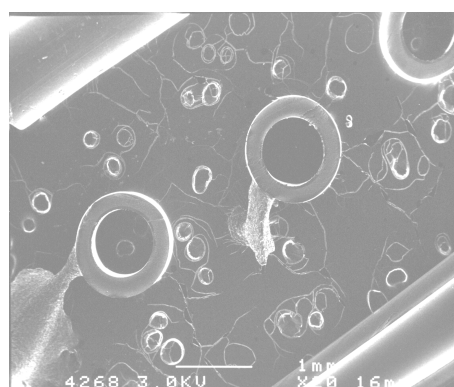


Figure 37 Pieces of one fibre cut in order to see the exterior and interior surfaces and the circular transverse section of the membranes inside SEM chamber

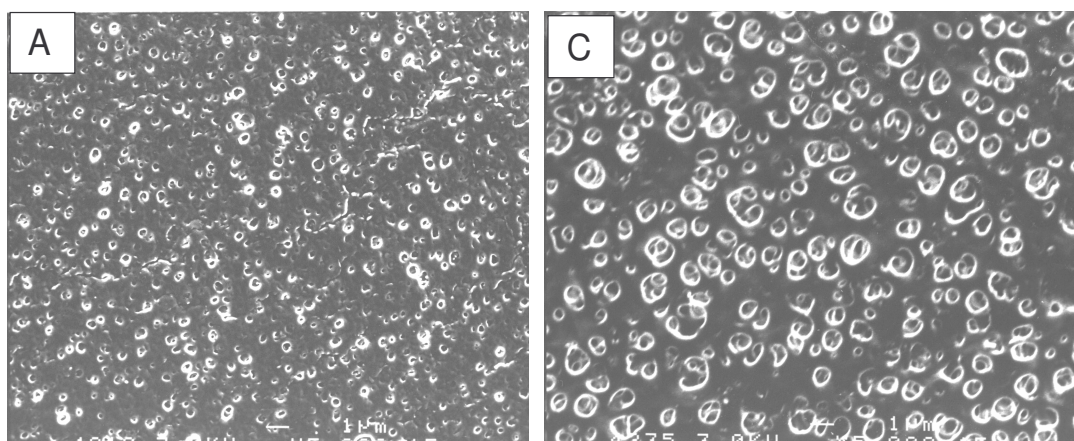


Figure 38 External surface of A- Hydranautics (PES) and C- Norit (PES) membrane in a magnification of 5000 in the clean state.

As shown in Fig. 38 pores of membrane A appear to be smaller than that of membrane C. To analyze them more precisely, the FD values were calculated. For membrane A, the FD value was determined as 1.35 and for membrane C, it was determined as 1.52. Thus the difference in morphology was made clearer with FD determination. These membranes are PES ultrafiltration (UF) membranes with In-Out configurations. FESEM analysis of the interior surface of these membranes are also performed which is indicated in Fig. 39.

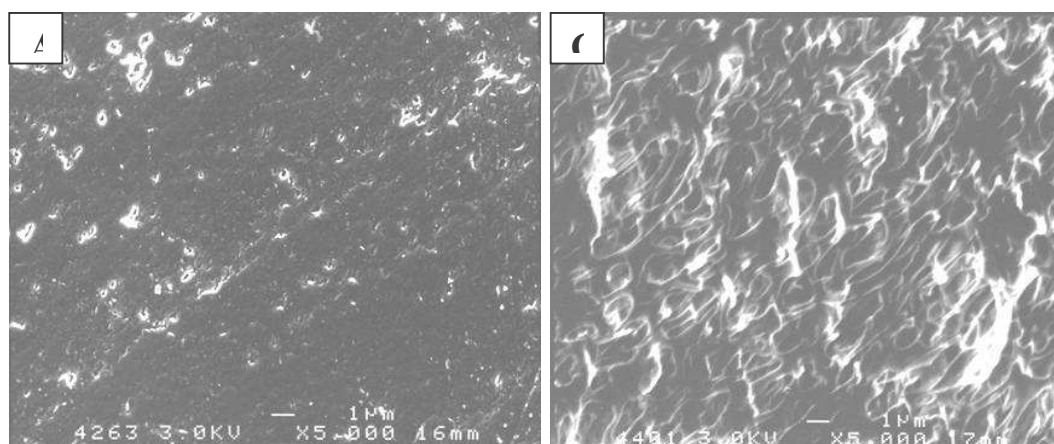


Figure 39 Internal surfaces of both A-Hydranautics and C-Norit membranes in a magnification of 5000
The interior morphology of these fibers did not appear to be similar. For interior surface of membrane A, FD value was determined as 1.31 and that for membrane C was determined as 1.52. Thus fractal dimension can be used as a new tool to analyze the morphologies of membranes along with SEM analysis.

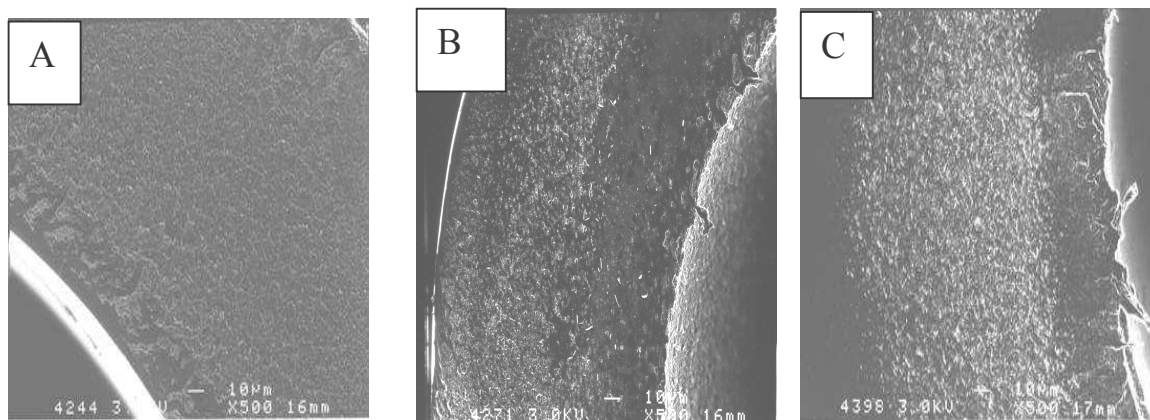


Figure 40 FESEM image of cross section of membranes A, B & C in a magnification of 500

Fig 40 shows the cross section of the hollow fibres. Membrane B appeared to be lower in thickness than that of the other two PES membranes. Membrane characteristics obtained from FESEM observations are listed in Table 14. It has been observed that both the PES membranes are having the similar inner diameter values and slightly different outer diameter values. The thickness values varied from 130 to 200.

Table 14 Membrane characteristics from FESEM observations

Membrane	Material	Outer Diameter (μm)	Inner Diameter (μm)	Thickness (μm)
Hydranautics A	PES	1050	725	200
Zenon B	PVDF	821	479	131
Norit C	PES	1172	735	158

AFM results

AFM characterisations have been performed in order to understand the difference in topography of the membranes. The resulting roughness for 1 scan (10x10 μm²), is reported in Table 15. The roughness parameter (Ra) was automatically calculated by the AFM apparatus itself. The mean roughness is the mean value of surface related to the central plane and that of the plane for which the volume enclosed by the image above and below is equal.

Table 15 Average roughness (Ra) of samples A, B and C

Membrane	A	B	C
Field analyzed	10x10 μm^2	10x10 μm^2	10x10 μm^2
Ra (nm)	49	18	40

Concerning the virgin UF membranes, the lower roughness is observed for the membrane B which is made of PVDF. Furthermore, membranes A and C are very similar due to the fact that they are made of the same material, PES.

SP and IEP determination

Streaming potential measurement is a powerful tool which helps to characterize the active layer of the membrane. It helps us to determine the charge related modifications of the membranes. The system used for the determination of Streaming potential is shown on Fig. 37. Streaming potential measurements were carried out both for clean membranes and fouled membranes. Following the SP values for different pH, we determined the isoelectric point (IEP) of the membrane. On IEP, SP or membrane charge vanishes.

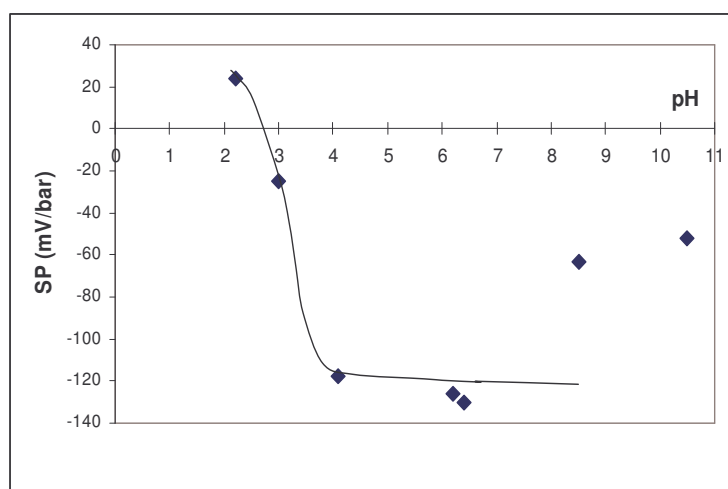


Figure 41 Evolution of SP with pH for the determination of IEP of clean Hydranautics PES membrane.[KCl]

The IEP values obtained for clean PES membranes were similar (2.8 ± 0.5) as indicated in Fig. 41 and Table 16. Both the membranes A and D are made of the same material and exhibited the same value of IEP. Even though both the membranes are having the same IEP, the membrane charges determined at normal pH were not the same.

Table 16 IEP/Membrane charge values for clean membranes

Membrane	Material	SP (mV/bar) KCl = $2 \cdot 10^{-4}$ M pH 6.5, T = 20°C	IEP
Hydranautics A	PES	- 190 \pm 5	2.8 \pm 0.5
Zenon B	PVDF	- 80 \pm 5	No iep
Norit C	PES	- 126 \pm 5	2.8 \pm 0.5

For Hydranautics (PES) membrane, the charge obtained was -190 mV/bar and for Norit (PES) membrane the charge obtained was -126 mV/bar. For PVDF membrane we could not determine the IEP. In all the range of pH values, the membrane was negatively charged.

Pyrolysis Results (GC/MS at 400° C)

Pyrolysis of clean membranes was realized using Gas chromatography/mass spectrometry at 400° C.

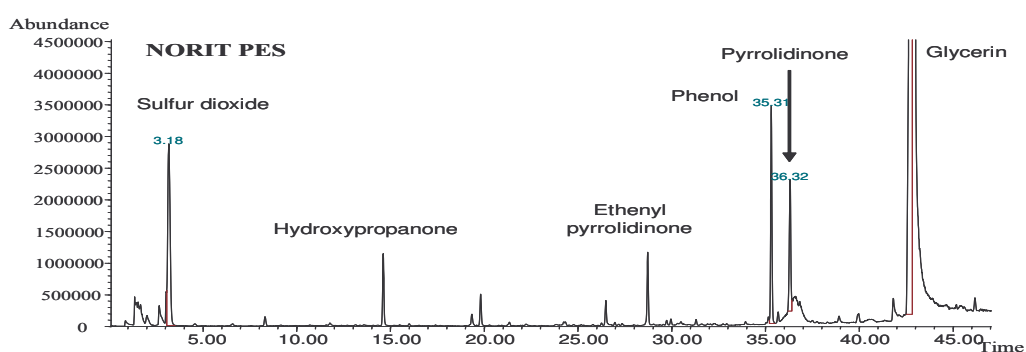


Figure 42 Pyrochromatogram of virgin membrane Norit PES

Fig. 42 shows the pyrochromatogram of PES membrane, D-Norit. SO₂ and phenol are produced from the thermal degradation of the polymer. Pyrrolidinone is a product added by the manufacturer to make the membrane more hydrophilic. Hydroxypropanaone is produced from the thermal degradation of glycerine which is a preservative, to prevent drying during transportation.

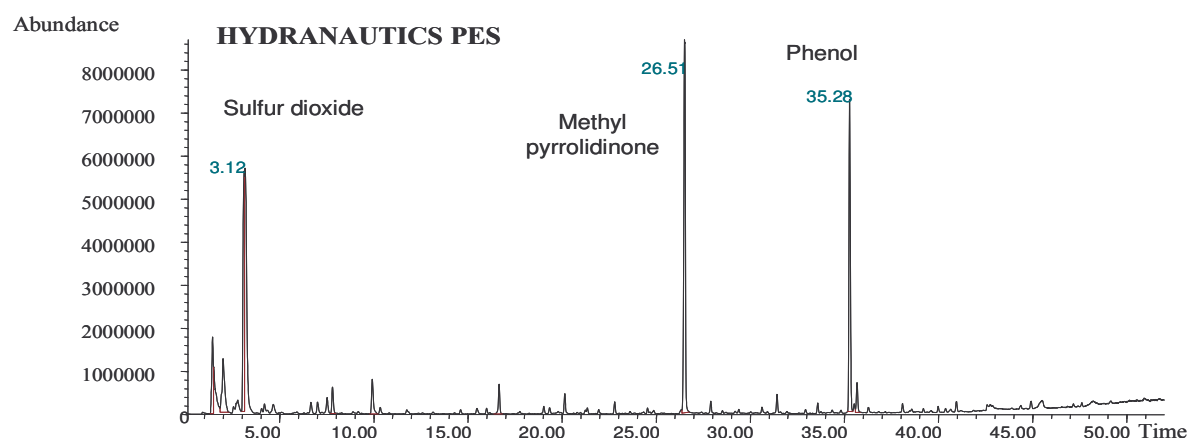


Figure 43 Pyrochromatogram of virgin Hydranautics PES membrane.

As shown in Fig. 43, Hydranautics is similar to Norit except in the fact that it contains lower amount of glycerine. All other groups like phenol, sulphur dioxide are found in Norit also which is generated from the membrane material, polyethersulfone.

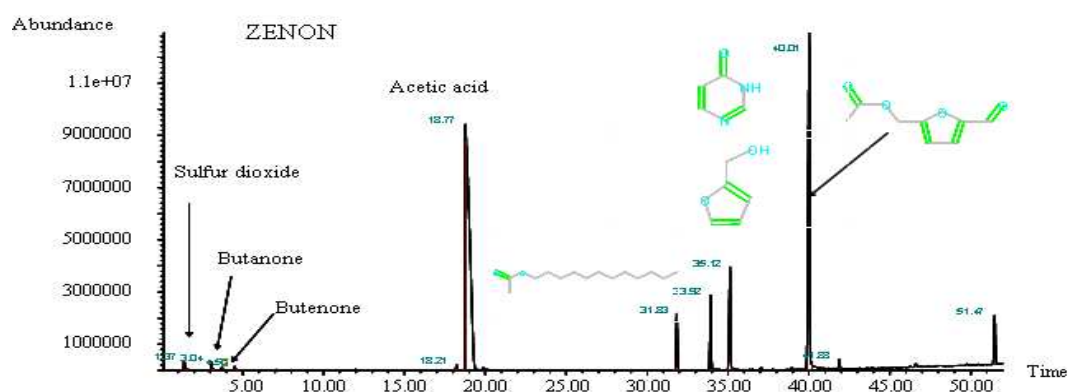


Figure 44 Pyrochromatogram of virgin Zenon PVDF membrane.

This pyrochromatogram (Fig. 44) showed the presence of highly hydrophilic products in the membrane. Presence of carbohydrates should also be considered.

Results for contact angle measurements.

Contact angle measurement helped us to analyze the hydrophilicity/hydrophobicity. Total wetting of Hydranautics (A) and Norit (C) membranes didn't allow the measurement of the contact angle. Zenon clean membrane showed contact angles 63° .

Fouled fibre autopsies

FESEM Analysis

We analysed one fouled fibre (Zenon PVDF) which is fouled by Tampa bay water NOM. Fig. 45 shows the clean fibre the deposit of NOM on the fibre, which also shows the external surface of the membrane in a magnification of 5000.

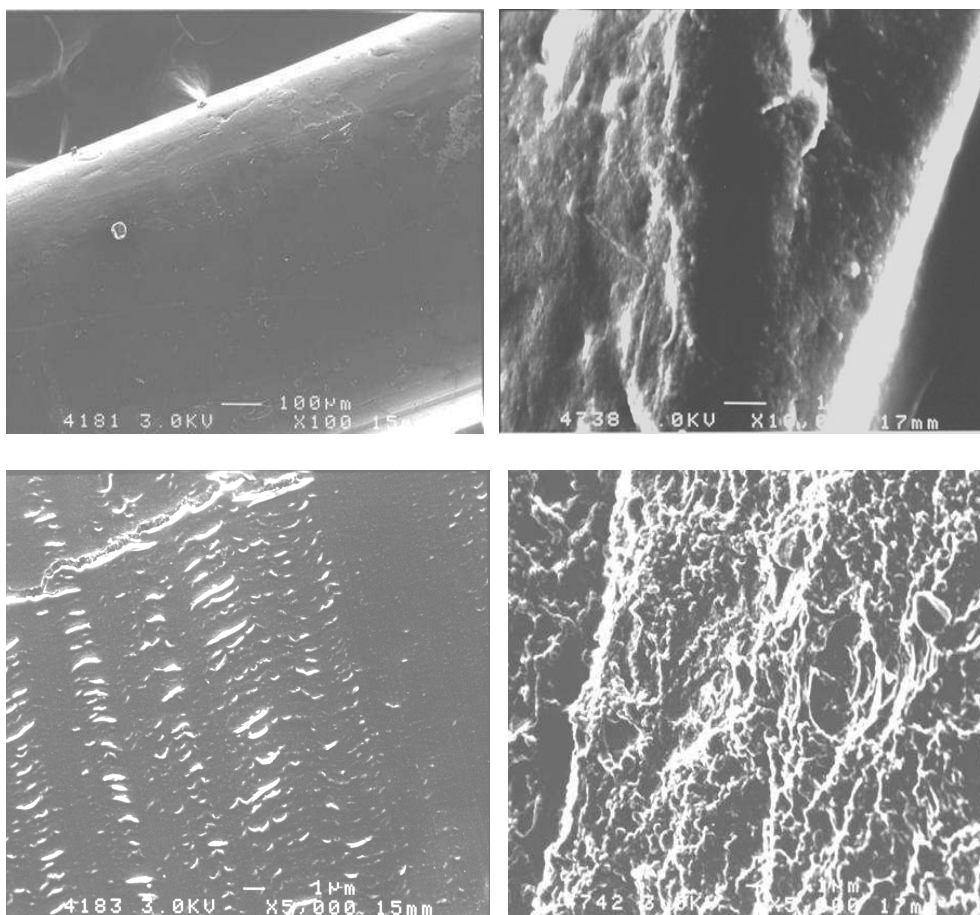


Figure 45 External surfaces of clean and fouled of Zenon PVDF showing the NOM in a magnification of 500 and 5000

Fig. 45 shows the SEM images of virgin and fouled fibres of Zenon PVDF. SEM images showed the presence of NOM on fouled fibers. To understand the morphological differences more accurately, we have determined the fractal dimension of the virgin and fouled surfaces (x5000). The virgin membrane surface FD was determined as 1.33 and that for fouled membrane surface was determined as 1.52. Thus the structural changes are made clearer with the help of FD.

We have also analysed the inner side of the fibre B (Fig.46). We could not see any fouling inside the membrane, which confirmed the “out-in” configuration of the membrane.

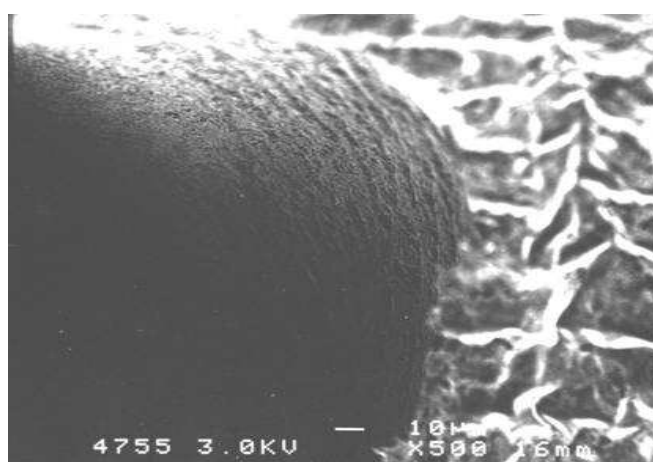


Figure 46 FESEM image of the Inner side of the fouled Zenon PVDF membrane x 500

FESEM analysis is a very useful analytical tool, which helped us to diagnose the changes in morphology caused by fouling.

Contact angle measurements

After fouling, the contact angle increased from 84° (virgin) to 90° (fouled) which indicated the hydrophobic nature of the NOM

SP measurements and IEP determinations for Fouled fibres

Fig.47 shows the IEP values before and after fouling. In the clean state the membrane was negatively charged in all the pH ranges. But in the fouled state, there was an apparition of IEP. The value obtained was 5 ± 0.5 . This can be explained by the modification of the global charge of the membrane due to the deposition of NOM on the surface/inside the pores.

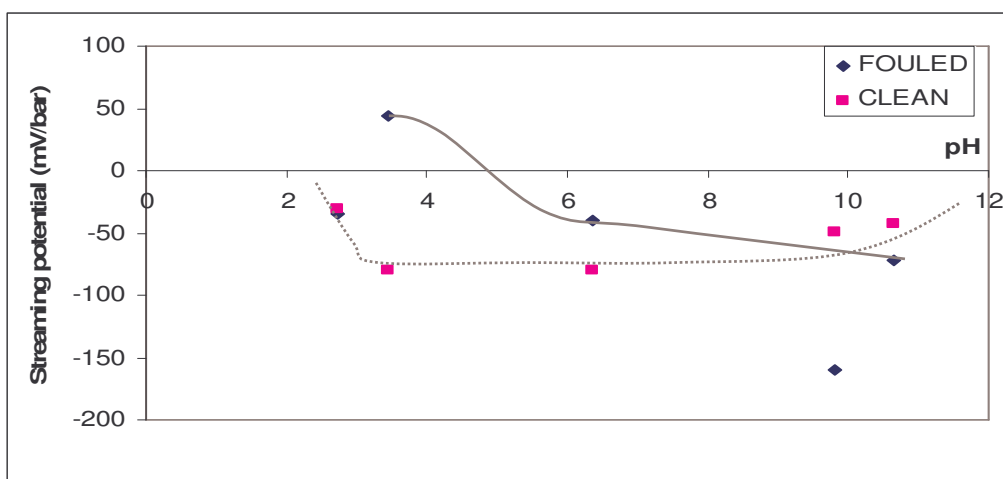


Figure 47 Evolution of SP with pH for Zenon PVDF membrane before and after fouling.

The IEP displacement (Fig. 47) can be attributable to the presence of positively /neutrally charged groups of NOM deposited inside the fibre, as reported elsewhere (Violleau *et al.* 2005). Further experiments were conducted in order to determine the chemical nature of those foulants (results not shown).

Partial Conclusion 7

Membrane Autopsy of clean and one fouled membranes were done. SEM, AFM, streaming potential and IEP measurements and contact angle measurements were performed. SEM analysis of clean membranes showed that the PES membranes are having similar morphology and PVDF membrane is having a different morphology. We analysed one fouled fibre of Zenon PVDF and it showed the NOM deposits on the exterior surface and not in the interior which confirms the out-in configuration of the fibre. AFM analysis of clean membranes was done to understand the topography. It also confirmed the similarity between Hydranautics and Norit membranes as observed in SEM (both are PES membranes). Zenon PVDF membrane posses lower roughness in the clean state. From contact angle measurements, all the clean membranes are having hydrophobic character (63-84°). Contact angle measurements of Zenon PVDF showed a contact angle of 90° after fouling, which showed the hydrophobic nature of the NOM (fouled by Tampa bay water). SP and IEP measurements showed the charge related

modifications on the clean membranes and fouled membranes. All the clean membranes were negatively charged. Apparition of IEP on the fouled Zenon membrane showed the presence of neutral or positively charged groups in NOM.

E-ABSTRACTS OF THE FOLLOWING PUBLISHED WORKS :

- a. **Anju Thekkedath**, Wahib M. Naceur, Karima Kecili, Mohammed Sbair, Audrey Elana, Laurent Auret, Hervé Suty, Claire Machinal, Maxime Pontié; *Macroscopic and microscopic characterizations of a cellulosic ultrafiltration (UF) membrane fouled by a humic acid cake deposit: First step for intensification of reverse osmosis (RO) pre-treatments*, Comptes Rendus Chimie 10 (2007) 803-812
- b. Maxime Pontie, **Anju Thekkedath**, Karima Kecili, Helana Habarou, Hervé Suty, Jean-philippe Croue, *Membrane autopsy as a sustainable management of fouling phenomena occurring in MF, UF and NF processes* Desalination, 204 (1) (2007) 155-169
- c. Maxime Pontié, Sophie Rappene, **Anju Thekkedath**, Jean Duchesne, Valérie Jacquemet, Jerome Leparc, Hervé Suty; *Tools for membrane autopsies and antifouling strategies for seawater feeds: a review*, Desalination 181(2005) 75-90

In the **first publication (a)** presented a preliminary study of fouling due to humic acid on a flat sheet regenerated cellulose 100 kDa membrane used for ultrafiltration (UF). Humic acid used was Aldrich in a concentration of 5 mg/L at a pH 6.7. It is reported that humic acid fouling is mainly governed by cake formation. The originality of the work lies in a double approach on cake analysis at both microscopic and macroscopic scales. Extend of fouling was analyzed in terms of percentage of flux decline with time, resistance in series, modified fouling index for ultrafiltration (MFI-UF) etc. We obtained that the cake resistance contributed 52% to the total resistance, which was higher than that of the membrane resistance. Adsorption resistance (membrane in contact with the solution for 2 hrs) contributed only 2% to the total resistance. From FESEM images, it was found that the humic acid cake is well organized, and particularly in *fractal* forms. The fractal dimension (FD) of the cake was determined using fractal box counting method. The value of fractal dimension in three dimensions for clean and fouled humic acid cake for 100 kDa membrane was determined as 2.52 in three dimensions. Theoretically a FD value of 2.51 corresponds to particle-cluster aggregation coming under diffusion - limited aggregation (DLA). The classical slit density index (SDI) and the new modified fouling index (MFI-UF) were obtained also proved the presence of the cake. Trans-membrane streaming potential measurement (SP) was carried out to complete this approach which helped us to differentiate pore penetration from cake formation. Thus an original approach combining macroscopic and microscopic parameters for the analysis of humic acid cake formed on membrane was developed, for a better understanding of membrane fouling due to NOM in drinking water treatment.

The **second publication (b)** was focused on membrane autopsies conducted on hollow fibre membranes with which real raw surface water was filtered. Another study was a characterization of two different humic acid fractions, hydrophobic (denoted as HPOA) and transphilic or non-humic (TPIA) which were isolated from Blavet river (France) using a

polyamide flat sheet nanofiltration membrane (commercial name NF -55). A large panel of analytical tools, including scanning SEM, AFM, contact angle measurements, electron spectroscopy for chemical analysis (ESCA) and pyrolysis by gas chromatography/mass spectrometry (GC/MS) was used in this study. Complementary information was obtained from the analyses feed water, permeate and backwashed water solutions (DOC, UV 254, HPSEC, total amino acids, total amino sugar, hardness and alkalinity). Results showed a severe flux decline for MF membranes comparing with UF membranes. Also, out of the MF membranes, PVDF membrane (appeared rougher more hydrophobic than PS, appeared more negatively charged) showed higher flux decline than MF PS. GC/MS showed more light to the suspicion (from SEM and AFM) that there was bio-fouling in MF PVDF. Analysis of backwash water also confirmed the presence of bacteria. The comparison of the affinity of both the NOM fractions were verified with polyamide membrane using hydraulic permeability measurements, contact angle measurements, streaming potential measurements and NaCl permeation measurements. HPOA was retained inside the pores compared to TPIA which was adsorbed on the surface. Furthermore, membrane acidic-basic properties were amplified after deposition of foulants because of the sorption of monovalent and divalent ions.

Third publication (c) is a review which reports all the analytical tools used for membrane autopsies in sea water feeds. We have given a detailed account of different types of new pre-treatment possibilities before seawater reverse osmosis (RO) such as ultrafiltration (UF), microfiltration (MF), nanofiltration (NF) and membrane bioreactors (MBR). The last part gives an account of brine disposal, reuse of RO modules and a discussion about fresh water price is also presented.

F-GENERAL CONCLUSION

Our objective was to characterize the humic acid cake formed on flat sheet ultrafiltration membranes to understand the fouling phenomena occurring during drinking water treatment.

As a preliminary study, regenerated cellulose 100 kDa membranes were subjected to humic acid fouling and the results showed that the cake resistance is the dominant part in total hydraulic resistance which confirmed the fouling mechanism of cake formation. Moreover, SEM images of the humic acid cake revealed well organized fractal structures. Thus as we have used this microscopic parameter along with the macroscopic parameters like percentage of flux decline with time, hydraulic permeability (before and after fouling), resistance of the cake and modified fouling index for a better analysis of fouling. Furthermore, trans-membrane streaming potential measurements were also done (before and after fouling) to analyze the charge related modifications on the membrane due to fouling.

We have carried out different fouling experiments with varying operating parameters like pH of the solution, MWCO of the membrane, trans-membrane pressure and humic acid concentrations.

The results of different pH experiments showed that the highest degree of fouling happened at neutral pH (pH 6.7) and the lowest degree of fouling happened at basic pH (pH 9.5). The results were explained in terms of particle size, charge and conformation of the humic acid particles in different solution pH. At neutral pH, the humic acid particles were very close to their isoelectric point (IEP for Acrôs humic acid 6.99) and the presence of neutrally charged particles in solution intensified the fouling process because of a lack of electrostatic repulsion. At higher pH, the humic acid macromolecules were having a smaller macromolecular configuration because of the reduced inter chain electrostatic repulsion. Smaller particles can form a more thickly packed cake, which was confirmed from the highest fractal dimension value at acidic pH. A lowest value of fractal dimension was observed at basic pH, which

further indicated a thin and loosely packed cake (confirmed from lower FD values), which was the cause of the lowest fouling at pH 9.5.

Fouling studies with three different MWCO (100 kDa, 30 kDa and 10 kDa) of regenerated cellulose membranes were carried out in order to understand the role of MWCO in fouling. It was shown that the tighter membranes were less fouled comparing with the higher MWCO membranes. Out of the three MWCOs used in our study, the 100 kDa membrane showed the highest degree of fouling and the 10 kDa membrane showed the lowest degree of fouling. But one of the problems encountered in the 10 kDa membrane filtration was the low permeate flux. Cake resistance and the membrane resistance were equally dominant in the 30 kDa membrane. So applying proper operating conditions like trans-membrane pressure and a careful selection of solution pH and ionic strength, we can produce better performance from the 30 kDa membrane. Fractal dimension showed a correlation with hydraulic permeability as well as with MWCO. It was found that, fractal dimension decreased with decrease in permeability.

Trans-membrane pressure is one of the very important factors affecting fouling. Fouling experiments with 5 mg/L Acrôs humic acid showed that the highest degree of fouling was happened at 4 bars constant pressure filtration and the lowest degree of fouling was caused at 2 bars constant pressure filtration. In all the three trans-membrane pressures, cake formation was the dominant fouling mechanism. But in the case of 4 bars constant pressure filtration, some extend of pore penetration was also happened which is confirmed from the SP values. MFI values were found to be increasing with trans-membrane pressures which also confirmed the higher extent of fouling occurred at 4 bars. FD values of fouled cake surfaces showed a linear relation with cake resistance, R_c .

Fouling studies with humic acid Acrôs in three different concentrations (5 mg/L, 10 mg/L and 50 mg/L) were conducted. We have found that as the concentration of the solute increased, membrane solute interactions were also increased, or in other words fouling was also intensified. Flux decline with time, cake resistance and modified fouling index were found to

increase with increase in solute concentration. Fractal dimension values were also in an increasing trend with increase in humic acid concentration.

Thus we have developed a new approach in humic acid cake analysis combining both macroscopic and microscopic parameters. The originality of our work lies in the combination of macroscopic and microscopic parameters for a better understanding of humic acid cake formation and a better understanding of membrane fouling in drinking water treatment. Macroscopic parameters like percentage of flux decline with time, MFI-UF, resistance in series were applied along with microscopic parameters like fractal dimension and SEM images. To complete this approach, trans-membrane SP measurements (*in situ* tool) were also conducted with a newly developed SP apparatus, which worked with software *profluid 3.0*, helped us to better understand the fouling phenomena, due to humic acid cake formation.

As an extension of this study, effectiveness of a pre-treatment method was studied. Pre-treatment was done with a naturally occurring clay namely bentonite. It was found that in presence of bentonite, the cake resistance as well as the total hydraulic resistance were considerably decreased comparing to the filtration with humic acid alone. Thus, the pre-treatment was effective and can be employed to sea water before passing to RO desalination to remove NOM.

This method was extended to hollow fibre membranes coupled with membrane autopsy. The fibres were fouled with real water NOM (Tampa bay water, USA). SEM, AFM, streaming potential and IEP measurements and contact angle measurements were performed. Fractal dimension determination of clean and fouled external surfaces of the fibre helped us to analyze the morphological changes due to NOM deposition more precisely.

An original approach combining macroscopic, microscopic and *in situ* tools helped us to better characterize the humic acid cake formed on UF membranes. Thus our study gives a new insight into NOM fouling in low-pressure membrane processes dedicated to drinking water treatment.

G- REFERENCES

- Aoustin E., Schafer A. I., Fane A. G, Waite T. D., Sep. Purif. Tech. 22-23 (2001) 63
- Aptel P., Wiesner M. R., Water Treatment Membrane Processes, (1996) McGraw-Hill. USA
- Averett R.C., Leenheer J.A., McKnight D.M., Thorn K.A., U.S. Geological Survey Water-Supply paper, 2373 (1994) 224.
- Baker, A., Environ. Sci. Tech., (2001), 35, 948.
- Belfer, S., Fainchtein, R., Purinson, Y. and Kedem, O., J. Membr. Sci. 172 (2000), 113
- Bian, R., Watanabe Y., Tambo, N., Ozawa, G., (1999), Wat. Sci. Tech. 40(9), 121.
- Boerlage S. F. E., Kennedy M. D., Aniye M. P., Abogrean E., Tarawneh Z. S., Schippers J. C., J. Membr. Sci. 211 (2003) 271 and references there in.
- Boelarge S. F. E., Kennedy M. D, Aniye M. P, Aboregan E. M., Galjaard. G, Schippers J. C., Desalination 118 (1998) 131-142
- Boelarge S. F. E., Kennedy M. D, Aniye M. P, Aboregan E. M., Desalination 131 (2000) 201
- Bowen W., Calvo, J., and Hernandez, A., J. Membr. Sci.(1995) 101 , 153.
- Bowen, W. R., Hilal, N., Lovitt, R. W., Williams, P. M., J. Coll. Inter. Sci., 180 (1996), 350.
- Braghetta, A., DiGiano, F. A., and Ball, W. P., 1997, J. Environ. Engg., 628-641
- Carroll T., King S., Gray S. R., Balto B.A., Booker N. A., Wat. Res. 34 No. 11 (2000) 2868
- Costa A. R., Pinho M., J. Membr. Sci. 255 (2005) 49
- Cheryan M., Ultrafiltration and Microfiltration Handbook (1998) Technomic publishing Co.
- Cho, J., Amy, G., Pellegrino, J. Membr. Sci., 164 (2000) 89.
- Cho, J., Amy, G., Pellegrino, J., Yoon, Y., , Desalination, 118, (1998) 101.
- Cho, J., Ph.D Thesis, (1999), University of Colorado at Boulder USA.
- Combe, C., Molis, E., Lucas, P., Riley, R., and Clark, M., J. Membr. Sci., 154 (1999) , 73
- Crozes G. F., Jacangelo J. G., Anselme C., Lainé J. M., J. Membr. Sci. 124 (1997) 63.
- Dietz P., Hansman P. K., Inacker, O., Lehmann, H.D., and Herrmann, K. H., J Membr. Sci., 65 (1992), 101.
- Esparza-Soto, M., Westerhoff, P.K., Wat. Sci. Tech. 43(6), (2001), 87.
- Fan, L., Harris, J., Roddick, F., and Booker, N., Wat. Res., 35(18), (2001), 4455.

- Ghosh K., Schnitzer M, Macromolecular structure of humic substances. Soil. Sci. 129 (1980) 266
- Habarou H. PhD Thesis, University of Poitiers, France..
- Her, N., Amy, G., Jarusutthirak, C., Desalination, 132 (2000), 143.
- Her, N., Amy, G., Foss, D., Cho, J., Yoon, Y., and Kosenka, P., Environ. Sci. Tech. 36. (2002), 1069
- Ho, C., Zydney, A. L., J Coll. Inter. Sci., 232, (2000) 389
- Hong S, .Elimlech M, J. Membr. Sci. 132 (1997) 152
- Huber, S.A., Gluschke, M, Ultraputer water, 15(3) (1998,), 48.
- Jacangelo, J.G. and Buckley, C.A., Water treatment membrane processes, McGraw-Hill. (1996) USA
- Jarusutthirak C., Amy G., Wat. Res. 41 (2007) 2787-2793
- Jones K., O'Melia, C., J. Membr. Sci., 165 (2000), 31
- Jonsson, A. and Jonsson ,B., , Sep. Sci. Tech., 30(2) (1995) 301.
- Kecili K., PhD Thesis (2006),University of Pierre and Marie Curie, Paris VI, France.
- Kim, J. Y., Lee, H. K., and Kim, S. C., J. Membr. Sci., 163 (1999), ,159
- Koros W. J., Ma Y. H., Shimidzu T., J. Membr. Sci. 120 (1996) 149
- Lee N., Amy G., Croué J.P., Buisson H Water Res. 38 (2004) 4511
- Lee, N., Amy, G., Habarou H., Schrotter J C., 2002, Proceeding–IWA, Membranes in Drinking and Industrial Water Production (MDIW), 677.
- Lee N. , Amy G., Croué J.P Wat. Res. 40 (2006) 2357
- Lee, N., Amy G., Makdissy G, Croué, J-P, Buisson, H., and Schrotter, J-C, 2003, Proceeding-AWWA Mem. Tech. Conf. (MTC), T3.
- Lee N., Amy G., Croué J P., Buisson H., J. membr. Sci. 261 (2005) 7
- Lee S., Cho J., Elimelech M., J. Membr. Sci. 262 (2005) 27
- Li C. W, Chen Y. S., Desalination 170 (2004) 59
- Li J., Yang F., Li Y., Wong F S., Chua F C., Desalination 225 (2008) 356
- Lin C.F., Lin T. Y., and Hao, O.J., Wat. Res., 34(4) (2000), 1097.

- Lin C. F., Huang Y. J., Hao O. J., Wat. Res. No. 5 (1999) 1252
- Mandelbrot B B., The Fractal Geometry of Nature, Freeman, San Francisco, (1982) USA.
- Maartense A., Swart P., Jacobs E. P., Desalination 115 (1998) 215
- Maartens A., Swart P., Jacobs E.P., Wat. Sci. Tech40, (9), (1999), 113
- Maartense A., Swart P, Jacobs E. P., J. Membr. Sci. 163 (1999) 51
- Madaeni, S. S., J Por. Mat, (1997), 4, 239.
- Meakin P., Phys. Rev. B, 27 (5), (1983) 2616
- Meng F., Yang F. , Xiao J., Zhang H., Gong Z., J. Membr. Sci. 285 (2006) 159
- Meng F.G., Zhang H.M., Li Y.S., Zhang X.W., YangF.L, Xiao J.N, . Sep. Purif. Tech. 44 (2005), 250
- Nyström M., Ruohomaki K., Kaipia L, Desalination 106 (1996) 179
- Naceur M. W., Messaouedne N. A., Megatli S., Khelifa A., Desalination 168 (2004) 253
- O'Melia, C. R., Becker, W. , Au, K. (1999), Wat. Sci. Tech., Vol. 40(9), 47.
- Pontié M., J. Membr.. Sci. 154 (1999) 213
- Pontié M., Desalination 181 (2005) 75 and references there in.
- Pontié M. Chasseray X. Lemordant. D, Lainé J. M., J. Membr. Sci. 129 (1997) 125
- Peng X., Luan Z., Chen F., Tian BJia., Z., Desalination 174(2005) 135
- Ruohomaki. K, Vaisanen, Metsamuuronen. S, Kulovaara. M, Nyström M, Desalination (1998) 273
- Schäfer, A.I., Fane, A.G., Waite, T.D., Desalination, 2000, 131, 215-224.
- Schäffer A. I., Fane A. G., Waite T. D., Wat. Res. No. 6 (2001) 1509.
- Schippers J. C., Verdouw J., Desalination 32 (1980) 137
- Schnitzer M., Humic substances: Chemistry and Reactions, Soil organic matter, 1978 pp1 Elsevier, Amsterdam,
- Senesi N., Rizzi F.R., Dellino P, Acquafredda P.; Coll. Surf. A: Physicochem. Eng.. Asp. 127 (1997) 57
- Singer P. C., Wat. Sci. Tech., 40(9) (1999), 25.
- Sridang P. C, Wisniewski C, Ognier S., Grasmick A. Desalination 191 (2006) 71

Stevenson F. J., Humus Chemistry, Genesis, composition, Reactions; Wiley, New York NY USA (1982) 443

Stern, O. Z. *Electrochem*, 30 (1924) 508

Svinko V. I., Knyazkova T. V., Kulsky. L. A, *Chem. Water Technol.* 9 (1987) 126

Thurman E M., Malcom R, Aiken G R., *Analytical Chemistry* 50 (6) (1978) 775

Thurman, E. M., *Organic Geochemistry of Natural Waters* (1985), Martinus Nijhoff/Dr W. Junk, publishers

Thekkedath A., Naceur W. M., Kecili K., Sbai M., Elana A., Auret L., Suty H., Machinal C., Pontié M., *Compt. Rend. Chim.* 10 (2007) 1

Violleau D., Essis-Tomé H., Habarou H., Croué J.P., Pontié M., *Desalination* 173 (2005) 223

Waite T. D., Schäfer, A. I., Fane, A. G., Heuer, A., , *J. Coll. Inter. Sci.* 212 (1999), 264

Weisner M. R. and Lainé J. M., *Coagulation and Membrane Separation in Water Treatment Membrane Processes* (1996) , eds. J. Malleviale, P. E. Odennal and M. R. Weisner, Mc Graw Hill USA pp 16.1- 16. 12;.

Witten T. A., Sander L. M., *Phys. Rev. B*, 27, (9) (1983) 5686

Xi. W, Rong. W, Fane. A. G, Fook-Sin. W, *Water Sci. Tech: Water Supply* (2004) 4 (No. 4) 197

Yuan, W., Zydney, A., *J. Membr. Sci.*, 157 (1999), 1.

Zeman L., Zydney A., *Microfiltration and Ultrafiltration: Principles and Applications* (1996) Marcel Dekker, Inc.

Zermane F., Naceur M. W., Cheknane B., Messaoudene N. A, *Desalination* 179 (2005) 375

Zeng Y., Wang Z, Wan L., Shi Y., Chen G., Bai, C., *J Appl. Poly. Sci.* 88 (2003) 1328

Zhang M., Li C., Benjamin M. M., Chang Y., *Env.. Sci. Techn.* 37 (2003) 1663

Zydney A L., Yuan W., *J. Membr. Sci.* 157 (1999) 1

Zydney. A. L, Yuan W, *Environ. Sci. Technol* (2000) 34, 5043

APPENDIXES

PUBLICATIONS

1. **Anju Thekkedath**, Wahib M. Naceur, Karima Kecili, Mohammed Sbair, Audrey Elana, Laurent Auret, Hervé Suty, Claire Machinal, Maxime Pontié; *Macroscopic and microscopic characterizations of a cellulosic ultrafiltration (UF) membrane fouled by a humic acid cake deposit: First step for intensification of reverse osmosis (RO) pre-treatments*, Comptes Rendus Chimie 10 (2007) 803-812
2. Maxime Pontie, **Anju Thekkedath**, Karima Kecili, Helana Habarou, Hervé Suty, Jean-philippe Croue, *Membrane autopsy as a sustainable management of fouling phenomena occurring in MF, UF and NF processes* Desalination, 204 (1) (2007) 155-169
3. Maxime Pontié, Sophie Rappene, **Anju Thekkedath**, Jean Duchesne, Valérie Jacquemet, Jerome Leparc, Hervé Suty; *Tools for membrane autopsies and antifouling strategies for seawater feeds: a review*, Desalination 181(2005) 75-90
4. Karima Kécili, **Anju Thekkedath**, Hervé Suty, Maxime Pontié, *Characterization of a polysulfone ultrafiltration low pressure hollow fiber membrane: intensification of cleaning operations*, J. Membr. Sci., **in preparation**

PROCEEDINGS AND ORAL COMMUNICATIONS

Proceedings

Maxime Pontié, Zouhiar Qafas, Karima Kécili, Anju Thekkedath, David Violleau, Hortense Essis-Tome, Pierre Miquel, Courfia Diawara, *Premières études sur la purification de H₃PO₄ industriel issu de la voie humide par un procédé intégré de précipitation-ultrafiltration (PUF)*, Récents Progrès en Génie des procédés, SFGP, 2005 (**proceeding+poster presentation**)

Anju Thekkedath, Maxime Pontié, Karima Kecili, Jean Duchesne; *Adhesion and Fractal Organization of humic acids on a regenerated cellulose ultrafiltration membrane*; 13^e Journée d'études sur l'adhésion, 25-30 September 2005 Bollwiller, France (**proceeding + poster presentation**)

Anju Thekkedath, Wahib naceur, Maxime Pontié; *Macroscopic and microscopic characterizations of a humic acid cake deposit on a cellulosic UF membrane*, 17^{èmes} Journées Information Eaux, 25-28 September 2006 (**proceeding + poster presentation**)

Oral communications

Anju Thekkedath, Maxime Pontié, Jean Duchesne, *Membrane, fouling and fractals*, conference on Membranes et Sustainable Développement, Meeting of Club Français des Membranes (CFM), 29 March 2006, Angers (**Oral presentation**)

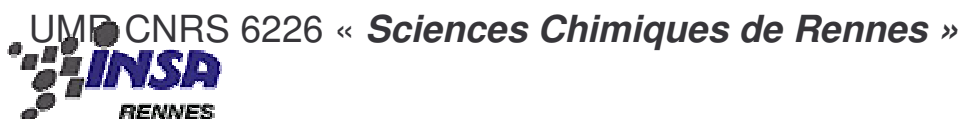
Anju Thekkedath, Wahib Naceur, Hervé Suty, Laurent Auret, Maxime Pontié; *Intensification of reverse osmosis (RO) pre-treatments: characterization of a humic acid cake on ultrafiltration (UF) membrane*; EDS Conference on Desalination and the Environment, Halkidiki, Greece, 22-25 April 2007(**Oral presentation**)

Maxime Pontié, **Anju Thekkedath**, Karima Kecili; *Streaming potential and new fouling indices determination for low pressure MF/UF submerged membranes for the intensification of cleaning procedures*; AFS Topical conference, March 27-31 2007, Orlando, USA (**Invited conference**)

Maxime Pontié, **Anju Thekkedath**, Karima Kecili, Hélène Habarou, Hervé Suty, J-P. Croué, *Membrane autopsy as a sustainable tool to increase the management of fouling phenomena occurring in MF, UF and NF processes*, Euromed 22-24, May 2006, Montpellier, France (**Oral presentation**)

Referees REPORTS

Chimie et Ingénierie des Procédés



Rapport sur le mémoire de thèse de Anju THEKKEDATH

ETUDE DU COLMATAGE DE MEMBRANES D' ULTRAFILTRATION PAR LES MATIERES ORGANIQUES NATURELLES/ INTENSIFICATION DE LA PRODUCTION D' EAU DESTINEE A LA CONSOMMATION HUMAINE

Université d'Angers, Spécialité Chimie Analytique, Ecole doctorale d'Angers

Rapporteur: Murielle RABILLER-BAUDRY, Professeur, Université Rennes 1
murielle.rabiller-baudry@univ-rennes1.fr

Le travail de thèse de M^{elle} Anju Thekkedath a été réalisé sous la direction du Professeur Maxime Pontié, au sein du Groupe Analyse et Procédés de l'université d'Angers. Le mémoire est rédigé en anglais selon un plan assez original : 78 pages exposent le travail réalisé, elles sont suivies de 14 pages de perspectives qui constituent un projet AWWARF confidentiel, puis 3 publications issues de ce travail et parues dans des revues internationales à comité de lecture, une conclusion générale de 3 pages et enfin 95 références bibliographiques.

Le mémoire est organisé en 4 parties

A- Introduction (5 pages)

B- Etude bibliographique (16 pages)

C- Etudes fondamentales avec des membranes planes utilisées en filtration frontale (40 pages)

D- Perspectives (14 pages)

Introduction : Les objectifs scientifiques et techniques de la thèse sont clairement exposés dès l'introduction. Il s'agit de contribuer à la compréhension du colmatage de membranes d'ultrafiltration en cellulose régénérée (RC) par la matière organique naturelle (NOM) présente dans des eaux naturelles à potabiliser, qui est un verrou scientifique et technique du procédé considéré.

Les membranes en cellulose régénérée, avec les membranes en polysulfone, sont les plus utilisées à l'échelle industrielle pour ces applications, d'où l'intérêt de l'étude proposée. Les membranes choisies sont sous forme plane et utilisées en cellule non agitée alors que l'on utilise des membranes fibres creuses, généralement immergées, à l'échelle industrielle. L'auteur aurait avantageusement pu évoquer les difficultés qui pourraient être rencontrées pour la transposition d'une géométrie à l'autre et discuter également du rôle possible de l'agitation.

La complexité de la NOM fait que, comme toujours dans les milieux complexes, la modélisation du colmatage *a priori* n'est pas possible et par suite la prédiction des flux en cours de production non plus. De nombreux travaux existent dans ce domaine, qui n'ont pas encore permis la totale compréhension des phénomènes fondamentaux qui régissent le colmatage ce qui manque pour une meilleure maîtrise des opérations industrielles. La démarche méthodologique proposée est fondée sur la filtration de solutions modèles d'acides humiques dans l'eau ultrapure, qui sont une partie identifiée de la NOM responsable du colmatage des membranes.

L'approche proposée ici s'inscrit dans une démarche moderne et multi-échelles ou analyses macroscopiques et microscopiques se complètent, en ayant recours à différentes techniques d'analyses sophistiquées telles que l'AFM et la mesure de potentiel d'écoulement (utilisant un pilote et un logiciel ? mis au point au laboratoire). L'analyse des dimensions fractales du dépôt à partir des clichés de microscopie électronique à balayage (MEB) est originale et pertinente. Selon une démarche désormais devenue classique, l'auteur cherche à tirer partie des autopsies destructives de membranes colmatées. Elle utilise les techniques citées ci-dessus ainsi que la mesure d'angle de contact pour suivre l'évolution de la balance polaire/apolaire de la surface membranaire avant et après colmatage.

La partie B introduit les notions utiles à l'étude qui va suivre :

- les équations nécessaires pour décrire le colmatage des membranes (modèle des résistances en série, modèles de blocage des pores, index de colmatage modifié (MFI))
- le potentiel d'écoulement pour caractériser les charges de surface des membranes. Il est introduit avec précision et je suppose qu'au plan expérimental ce seront des mesures à travers les pores des membranes et non pas en surface car ce n'est pas clairement explicité ici.
- la NOM. Il est plusieurs fois indiqué que la composition de la NOM est complexe, mais aucune des formules (pourtant utiles à la compréhension des interactions physico-chimiques) des acides humiques, fulviques n'est proposée. De même l'auteur fait référence à une large gamme de taille des constituants de la NOM sans précision sur les valeurs limites qui permettraient de comprendre le choix de l'UF.
- les procédés à membranes sont très brièvement décrits. Par contre la bibliographie sur les applications UF/MF (et un peu NF) au traitement de l'eau à potabiliser est bien documentée.

L'auteur insiste également sur les prétraitements physico-chimiques possibles de l'eau avant ultrafiltration et leurs impacts sur le colmatage. Elle souligne les résultats antagonistes publiés en particulier dans le cas des ajouts de charbon actif (sans effet sur le colmatage quand ils sont seuls en suspension), mais sans donner son analyse personnelle de ces résultats (on sait par exemple que le Procédé Cristal est développé à grande échelle, mais il n'est pas mentionné...).

- la théorie sur les dimensions fractales est présentée. J'aurai aimé comprendre ici comment l'auteur envisage de l'utiliser dans son travail, car il n'est présenté aucun lien avec la filtration, bien que de la bibliographie sur ce point apparaisse succinctement dans la discussion de la partie C. Il m'a finalement semblé au fil de la lecture du manuscrit que plus 2D- FD est élevée plus le dépôt est compact (page 74) mais j'ai parfois cru comprendre le contraire (page 44) ou lorsque l'on compare FD d'une membrane neuve ($FD = 1.33$) que je suppose plus « dense » que le dépôt à la même membrane, mais colmatée ($FD = 1.52$) (page 91). Un effort de clarification est nécessaire pour la version définitive du manuscrit.

- les techniques analytiques, principalement macroscopiques, pour réaliser les autopsies sont citées mais sans détails utiles qui permettraient au lecteur de comprendre ce que l'on peut en attendre ; introduction aux techniques généralement bien venues dans des chapitres de thèse. Finalement, je considère que la plupart des notions nécessaires à la compréhension de l'étude sont introduites selon une démarche classique dans une publication, mais d'une façon trop brève à mon goût pour un manuscrit de thèse. Ce chapitre nécessiterait, à mon avis, des compléments dans une version définitive.

Il n'y a pas de chapitre Matériels et Méthodes dans ce manuscrit ce qui constitue un manque important à mon avis. Par exemple il faut attendre la page 49 pour savoir que la membrane RC est une YM100 et la page 58 pour savoir qu'elle est fabriquée par Millipore et avoir ses caractéristiques...

L'auteur renvoie le lecteur à la littérature sans lui donner les clefs de ses expériences (dont les incertitudes sur certaines mesures qui sont pourtant décisives pour les commentaires ultérieurs). Il semble qu'une partie de cette thèse ait été concernée par la mise au point d'un pilote de mesure de potentiel d'écoulement. Sachant la difficulté que ce type de travail représente, il est dommage que ce ne soit pas mentionné de façon plus détaillée dans le manuscrit. Finalement, je considère comme un manque important, l'absence d'un chapitre expérimental qui aurait rendu le manuscrit auto-suffisant au lieu de renvoyer à des publications qui, certes, explicitent certains points, mais ne permettent pas de juger du recul de la candidate sur ces différents aspects qui, à mon sens, sont fondamentaux pour un expérimentateur.

La partie C constitue le cœur du travail de la thèse, elle fait l'objet de 5 sous-parties.

La première partie résume les expériences préliminaires réalisées en filtration frontale sans agitation sur une membrane de 29 cm² en cellulose régénérée de seuil de coupure 100 kDa. La solution modèle est constituée d'acides humiques (Aldrich) à 5 ppm dans de l'eau pure (pH 6.7). Le modèle des résistances en série permet de montrer que le colmatage de la membrane est principalement dû à la formation d'un gâteau et que le colmatage par adsorption des HA est assez faible ce qui était escompté en raison de la forte hydrophobicité des HA et de l'hydrophilie de la membrane. La description du colmatage est ensuite approfondie par l'utilisation de 2 techniques :

- la mesure du potentiel d'écoulement (SP) révèle la diminution de la charge des pores de la membrane, variation occasionnée par le colmatage en profondeur par les HA (-27 mV bar⁻¹ à -13 mV bar⁻¹, KCl 1 mM, pH 6.7). La mesure de la taille des HA conduit à des valeurs entre 220 et 290 nm et ne permettrait pas d'expliquer ce colmatage en profondeur. Je me demande si ces mesures de taille correspondent à des HA libres ou à des agrégats solubles, ce dernier cas permettant alors de comprendre le transfert de HA à travers les pores de la membrane.

- la caractérisation du dépôt par ses dimensions fractales conduit à une proposition de type DLCA, c'est-à-dire une couche compacte obtenue par agrégation de particules sous une forme dite « cluster de particules » par-dessus laquelle s'agrègent des particules sous une forme moins compacte (ou plus poreuse) dite « agrégation sous forme de cluster de particules limitée par la diffusion ». Cette description est intuitivement satisfaisante et en accord avec d'autres propositions de la littérature.

La seconde partie étudie le rôle du pH de la solution modèle de HA sur le colmatage de la membrane RC. Le colmatage de la membrane est fonction du pH : il est plus important à pH 6.7 (réduction du flux -88%) qu'à pH 3.0 (-68%) ou pH 9.5 (-53%). Afin de mieux analyser le phénomène, au plan fondamental, les potentiels d'écoulement des membranes colmatées ont été déterminés ainsi que la taille des HA.

- Les figures 12, 15 et 16 proposent des valeurs de SP qui ne me semblent pas toujours être les mêmes, et ce point devrait être clarifié pour faciliter la compréhension de la discussion (Par exemple SP# 0 mV bar⁻¹ à pH 6.7 fig. 12 et SP # -30 mV bar⁻¹, fig 15, peut être ne s'agit il

pas de la même membrane... ? De même les tailles oscillent entre 220 et 300 nm fig 12 et 250 et 2500 nm fig 15... Y a-t-il eu une filtration 0.45 μ m dans le premier cas et pas le second... ?).

- La dimension fractale 2D-FD a été déterminée à partir des clichés MEB des dépôts aux différents pH. FD # 1.6 dans les trois cas (1.57, 1.62, 1.52 pour pH 3.0, 6.7, 9.5, respectivement). D'après le Tableau 4, les MFI à pH 3.0 et 9.5 me semblent concordants (544 et 490 s L⁻², \pm 50(55), respectivement) et par suite je suppose que les FD pourraient l'être également. La soutenance orale pourra être l'occasion de discuter ce point.

La troisième partie étudie le rôle du seuil de coupure de la membrane RC sur le colmatage par les HA. Trois membranes en RC ont été utilisées YM10, YM30 et YM100, de seuil de coupure MWCO 10, 30 et 100 kg mol⁻¹, respectivement. Je suis surprise de la petite taille de pores annoncée en particulier pour la YM10 (1 nm) qui n'est manifestement pas une membrane de NF, de même que la YM100 (10 nm) sachant que des membranes minérales M1-Orelis de MWCO 150 kDa ont des pores de 100 nm... L'étude est réalisée à 2 bar et pH 6.5-6.7 qui correspond au pH pour lequel le colmatage par les HA est le plus sévère et également au cas réel du traitement d'eau de surface.

- Bien qu'à base de RC les 3 membranes neuves ont des caractéristiques différentes : elles sont toutes chargées négativement mais les valeurs de SP varient : -7, -17 et -46 mV bar⁻¹, la charge étant d'autant plus forte que MWCO est élevé. Après colmatage les membranes 30 et 100 kDa présentent les mêmes SP (-18 mV bar⁻¹) mais les membranes 10 kDa et 30 kDa ont conservé leur charge initiale.

- Les résultats montrent que la perte de flux, due au colmatage par les HA, est d'autant plus importante que le MWCO est élevé. (-85%, -48%, -22%). Il est intéressant de souligner que la perméabilité des membranes en fonctionnement varie entre 20 et 155 L h⁻¹ m⁻² bar⁻¹ alors que les perméabilités initiales étaient beaucoup plus éloignées (de 28 à 597 L h⁻¹ m⁻² bar⁻¹). Ces mesures montrent bien que ce sont les HA qui imposent la perméabilité plus que le MWCO de la membrane elle-même.

- La dimension fractale FD du dépôt diminue (de façon non linéaire) avec MWCO. Cela signifie-t-il que le dépôt est plus compact avec une membrane de faible taille de pores, dans lesquels les HA ne pénètrent pas, qu'avec des membranes plus ouvertes ou les HA sont (peut être) susceptibles de pénétrer ?

La quatrième partie étudie le rôle de la pression transmembranaire (PTM de 1 à 4 bar) sur le colmatage d'une membrane RC 30 kDa par une solution modèle de HA à 5 ppm à pH 6.7. Les résultats montrent que le colmatage irréversible est plus important après UF à 4 bar. Cependant l'ordre relatif des résultats après UF à 1 et 2 bar est troublant (colmatage irréversible plus important à 1 bar qu'à 2 bar) et mériterait d'être commenté plus en détail. Dans la mesure où SP (avant et après colmatage, respectivement) est identique pour les 3 essais les variations sont discutées en terme de compression possible du dépôt, mais les valeurs de α (résistance spécifique du gâteau) et celles du facteur de compressibilité (n) ne sont pas fournies ce qui est dommage puisqu'il est écrit qu'elles ont été calculées.

Finalement une relation empirique linéaire est alors proposée entre FD et la résistance de colmatage due au dépôt : la résistance est d'autant plus importante que FD est petite et on aimerait connaître la variation de FD avec n .

La cinquième partie étudie le rôle de la concentration en HA (5, 10 et 50 ppm) sur le colmatage de la membrane RC 30 kDa à pH 6.7. Le colmatage irréversible de la membrane par les HA est mis en évidence par la mesure de SP pour les concentrations élevées en HA (SP # -10 mV bar⁻¹) mais pas avec la solution à 5 ppm, ce qui laisse supposer que dans ce cas la surface des pores n'est pas encore totalement saturée par HA au contraire des solutions plus concentrées.

Le colmatage global ainsi que le colmatage irréversible sont d'autant plus importants que la concentration en HA est élevée. Le MFI et FD augmentent avec la concentration en HA.

L'application du modèle du gel qui est tentée ici me semble discutable, compte-tenu de la faible corrélation obtenue (figure 28).

La partie D décrit les perspectives de ce travail sous la forme d'un projet de l'AWWARF (American Water Work Association and Research Foundation) traitant de différentes membranes fibres creuses et utilisant des HA ou parfois une eau réelle (Tampa Bay water, USA). Je ne commente pas de façon détaillée cette partie compte tenu de sa confidentialité, mais elle est clairement orientée vers la valorisation des résultats décrits ci-dessus et implique plusieurs partenaires internationaux.

Ce projet utilise des analyses complémentaires comme l'AFM, l'évaluation de l'hydrophobicité de surface par mesure d'angle de contact et l'analyse des composés issus de la pyrolyse de la membrane neuve, par chromatographie en phase gazeuse couplée à un détecteur spectromètre de masse (GC-MS) qui est le seul détecteur structural permettant d'identifier, sans ambiguïté, les différents constituants. Cette dernière analyse serait probablement intéressante si elle était réalisée sur membrane colmatée pour identifier les HA responsables du colmatage irréversible.

La conclusion dresse en 3 pages un bilan succinct du travail effectué et des conclusions et qui s'en dégage, les perspectives ayant été largement détaillées dans la partie D.

En conclusion, ce travail de thèse constitue un apport à la compréhension du colmatage des membranes en cellulose régénérée par des substances humiques lors de la filtration d'eaux de surface. Le choix méthodologique d'utiliser des membranes planes permet la mise en œuvre de techniques d'analyses multiples et adaptées qui seraient d'un emploi plus délicat avec une géométrie fibre creuse. La mise au point d'analyse en ligne demeure cependant un enjeu important pour une production durable et on peut espérer y parvenir avec les mesures du potentiel d'écoulement bien qu'elles soient particulièrement délicates à maîtriser et nécessitent encore probablement de la mise au point. Au plan fondamental, l'utilisation de dimensions fractales pour décrire des dépôts plus ou moins denses et compressibles est originale et pertinente. Les relations empiriques proposées sont une première étape dans l'utilisation de FD qui pourra sans doute être encore développée dans le futur.

Certains passages du manuscrit devront être clarifiés dans une version définitive pour en faciliter la lecture et la soutenance orale sera l'occasion de les préciser.

Les résultats de ces travaux ont été valorisés sous la forme de plusieurs publications parues dans des journaux internationaux à comité de lecture, jointes au corps du manuscrit. **J'émet donc un avis favorable à la soutenance de thèse de doctorat de M^{elle} Anju THEKKEDATH.**

Rennes, le 15 novembre

Murielle Rabiller-Baudry



Muscat, November 15, 2007

Université d'Angers – Ecole Doctorale
40 rue de Rennes BP 73532
49035 Angers Cedex 01
Fax : +33-241962367

*Rapport de Pré-soutenance de la Thèse de Mme Marie Anju
THEKKEDATH*

Mrs. Marie Anju THEKKEDATH's PhD Pre-Defense Report

Mrs. Marie Anju THEKKEDATH submitted her PhD thesis in English on "*Etude de colmatage de membranes d'ultrafiltration par les matières organiques naturelles: Intensification de la production d'eau destinée à la consommation humaine*" for reviewing and approval to present her research work to obtain the PhD Degree from Angers University, *Ecole Doctorale d'Angers, Spécialité: Chimie Analytique*. The Thesis was prepared under the supervision of Professor Maxime PONTIE, Angers University, France.

The aim of this work was to investigate the fouling problem in ultrafiltration membranes in drinking water treatment applications and test their resistance to natural organic matter (NOM) fouling especially humic acid (HA) foulants and its control.

The thesis consists of three main parts. After an overview and state of the art of membrane fouling due to NOM and the different methods to characterize and analyze the foulants, the experimental results and their discussion were clearly presented in the main part of the document. Finally, a pretreatment method was used to minimize NOM fouling and some important results from American Water Work Association and Research Foundation (AWWARF) project were presented in perspectives. The Author included two papers published in Desalination and one paper in Chimie Journals of Elsevier before presenting the conclusions.

The Thesis is of good quality and presented very interesting results but it is poorly written with a lot of grammar and typing mistakes except introduction and conclusion which are acceptable. Furthermore, different formats are used in the different figures, tables, titles and most of the paper contents. Mme THEKKEDATH should be more careful in presenting her results. For example, in figure 22, the flux is plotted versus transmembrane pressure for different pressures! The fact that English is not the author's

MIDDLE EAST DESALINATION RESEARCH CENTER

P.O. Box 21, Al Khuwair, P.C. 133, Sultanate of Oman Tel: (968) 24695 351 Fax: (968) 24697 107
Website : www.medrc.org E-mail: info@medrc.org.om



native language may not be a good excuse for the poor quality of presentation especially in discussion and interpretation. Mme Marie Anju should extensively revise the entire thesis before providing the final version to the University library.

The bibliography part could be improved by presenting some information and details on different types of fouling and foulants, especially particulate fouling due to NOM.

The influence of the different operational parameters mainly pH of solution, membrane molecular weight cut-off (MWCO), transmembrane pressure and HA concentration, on the transient filtration rate were presented. However, it is not mentioned why feed temperature was always kept constant. It might be one of the most important parameters which influence the flux.

The double approach on surface analysis at both macroscopic and microscopic scales is very interesting. The physico-chemical approach strengthens the filtration mechanisms explanation since HA particles might change their charge by changing some operating parameters.

Fractal dimension of the cake and streaming potential measurements conducted with in-situ apparatus gave an excellent and additional approach to the interpretation. However, the author did not take this opportunity to correct the contradiction between the results of the two approaches. In the text, sometimes it is stated that there is no penetration of HA particles within the membrane pores (standard fouling) because the mean particle size is much bigger than the membrane pore size and sometimes it is stated that there is an internal blocking. This contradiction could be avoided by the author since she got an extensive results supported by SEM images. The main reason of this contradiction is that the author is comparing the mean particle size with the membrane pore size which, in my opinion, has no meaning. The pore size should be compared to the smallest particle size of HA; hence, the mean particle size represented in figures 12 and 15 should be replaced by the particulate and NOM size distribution to compare and understand the flux decline due to irreversible fouling of the membrane pores and reversible fouling with cake deposition formation protecting the internal texture of the membrane. Then, most probably there is penetration of the smallest HA particles in the membrane pores since earlier works showed HA pass through the pores even in NF membranes. The analysis of the permeate quality can confirm this result. It is also interesting to check the HA particle size variation with pH because it might be the reason for the obtained lowest flux at pH 6.7.

The different fouling phenomena were well explained by investigating the deposit formed on the membrane surface and the calculations of the specific cake resistance. The use of the modified fouling index (MFI-UF) also helped to understand the flux decline. But, it is regrettable for not correlating it with silt density index which is widely used in the industry and it is a standard for most of the membrane manufacturers.

Other specific and general comments will be sent to Mme THEKKEDATH to incorporate them in the final version of the thesis.

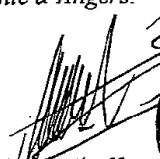
MIDDLE EAST DESALINATION RESEARCH CENTER

P.O. Box 21, Al Khuwair, P.C. 133, Sultanate of Oman Tel: (968) 24695 351 Fax: (968) 24697 107
Website : www.medrc.org E-mail: info@medrc.org.om



In conclusion, due to the interesting results presented in this thesis and the originality of the approaches used in the interpretation, I do recommend to present this work as PhD thesis of Angers University.

Compte tenu de l'intérêt du travail et de son originalité à utiliser plusieurs outils d'autopsie à l'échelle macroscopique et microscopique, je suis très favorable à la tenue de la soutenance de Mme Marie Anju pour l'obtention du grade de Docteur de l'Université d'Angers.


Dr. Noredine Ghaffour
R&D Project Manager
Middle East Desalination Research Center,
An international institution, headquarter: Muscat
Sultanate of Oman



MIDDLE EAST DESALINATION RESEARCH CENTER

P.O. Box 21, Al Khuwair, P.C. 133, Sultanate of Oman Tel: (968) 24695 351 Fax: (968) 24697 107
Website : www.medrc.org E-mail: info@medrc.org.om